



# Efficient RNA Interference in *C. Elegans* Requires the Putative RNA Helicase RDE-12 and Early Exposure to Double-Stranded RNA

## Permanent link

<http://nrs.harvard.edu/urn-3:HUL.InstRepos:40046482>

## Terms of Use

This article was downloaded from Harvard University's DASH repository, and is made available under the terms and conditions applicable to Other Posted Material, as set forth at <http://nrs.harvard.edu/urn-3:HUL.InstRepos:dash.current.terms-of-use#LAA>

## Share Your Story

The Harvard community has made this article openly available. Please share how this access benefits you. [Submit a story](#).

[Accessibility](#)

**Efficient RNA interference in *C. elegans* requires the putative RNA helicase  
RDE-12 and early exposure to double-stranded RNA**

A dissertation presented

by

Philip Shiu

to

The Department of Molecular and Cellular Biology

in partial fulfillment of the requirements

for the degree of

Doctor of Philosophy

in the subject of

Biochemistry

Harvard University

Cambridge, Massachusetts

April 2017

© 2017 Philip Shiu

**Efficient RNA interference in *C. elegans* requires the putative RNA helicase  
RDE-12 and early exposure to double-stranded RNA**

**Abstract**

RNA interference (RNAi) is a phenomenon in which double stranded RNA (dsRNA) triggers silencing of cognate genes. In the nematode *C. elegans*, RNAi involves an amplification step in which abundant secondary short-interfering RNAs (secondary siRNA) are produced, as well as nuclear processes, in which genes are transcriptionally silenced in a process involving histone modifications. In this thesis, I describe my research on RDE-12, a protein essential for the secondary siRNA amplification step, as well as my discovery that nuclear RNAi has a critical period.

I identified and characterized the gene *rde-12*. Although originally found in a screen for genes required for dsRNA movement, I show that RDE-12 functions cell-autonomously. *rde-12* encodes a putative DEAD-box helicase, and I found that the ATPase domain of RDE-12 is required for its function. Furthermore, I found that RDE-12 is required for amplification or maintenance of secondary siRNA.

Investigating why we found *rde-12* in a screen for dsRNA transport mutants, I found that secondary siRNA amplification is not required for RNAi in the pharyngeal muscle. I found that the pharyngeal muscle is resistant to RNAi when first exposed to dsRNA, but is sensitive when exposed to dsRNA for two generations. Investigating this further, I found that pharyngeal RNAi requires nuclear RNAi genes, and that there is a

critical period for nuclear RNAi, with early exposure to dsRNA triggering stronger silencing than late exposure.

Finally, I found that genes in the Rb pathway extend this critical period. Rb pathway genes encode transcriptional repressors and chromatin modifying enzymes. I find that the known enhanced RNAi phenotype of Rb pathway mutants requires nuclear RNAi. Furthermore, by examining a pharynx::GFP transgene integrated at different loci, I found that local chromatin may influence silencing efficiency. I hypothesize that loss of Rb in humans, which promotes tumor progression, may do so by affecting chromatin compaction and thereby facilitate stochastic gene silencing.

# **Chapter 1: Efficient RNA interference in *C. elegans* requires the putative RNA helicase RDE-12 and early exposure to double-stranded RNA**

## **Introduction**

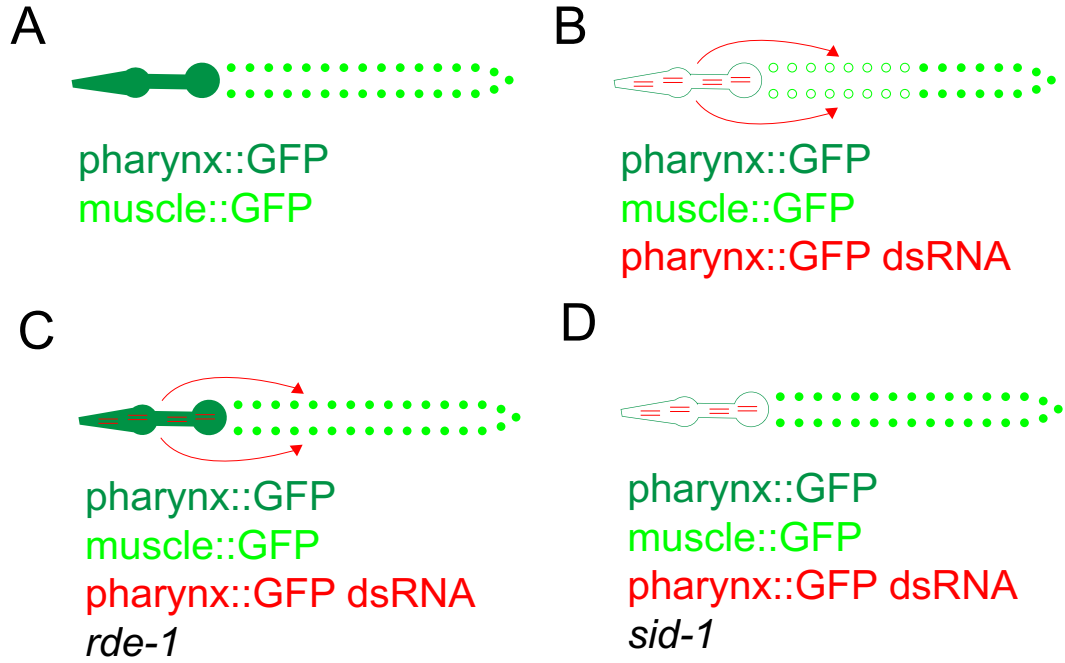
RNA interference (RNAi) is a phenomenon in which double-stranded RNA (dsRNA) triggers silencing of cognate genes (Fire et al., 1998). RNAi is a particularly powerful research tool for studying the nematode *C. elegans* because simply feeding worms bacteria engineered to express gene-specific dsRNA can trigger RNAi, a process known as environmental RNAi (eRNAi) (Timmons and Fire, 1998). In *C. elegans*, RNAi silencing is associated with transcriptional gene silencing mechanisms (nuclear silencing) and post-transcriptional gene silencing mechanisms (cytoplasmic silencing) (Yigit et al., 2006, Guang et al., 2008).

My research focused on the mechanisms through which RNAi in *C. elegans* is robustly generated. I characterized the novel protein RDE-12, which I showed to be a putative RNA helicase involved in the amplification of the RNAi response (Yang et al., 2014; Shiu et al., 2014). Additionally, I found that nuclear RNAi is most potent when worms are exposed to dsRNA early in development (Shiu and Hunter, 2017). Exploring this finding, I found that loss of Rb pathway proteins, which causes cells to adopt a more naïve and germline-like gene expression pattern (Wang et al., 2005, Lehner et al., 2006), enhances silencing through nuclear RNAi. Finally, I found that different locations in the genome are more sensitive to nuclear RNAi than others, indicating that local chromatin affects how readily a particular gene gets silenced.

## **Introduction to *C. elegans* RNAi**

A remarkably property of *C. elegans* RNAi is that it can be triggered by double-stranded RNA (dsRNA) uptaken from its environment, a process called environmental RNAi (eRNAi). For example, simply feeding worms bacteria expressing dsRNA is sufficient to trigger silencing of the targeted gene (Timmons and Fire, 1998). To identify genes essential for movement of dsRNA, the Hunter lab conducted a screen for systemic RNAi mutants (Winston et al., 2002). For this screen, Winston, Molodowitch and Hunter constructed a strain intended to easily distinguish between cell-autonomous and systemic RNAi mutants. GFP was expressed in the pharynx and body-wall muscle (Winston et al. 2002, Figure 1.1A). In addition to these two transgenes, a GFP-hairpin was also expressed in the pharynx (Figure 1.1B). This transgene silenced not only the pharynx, but also adjacent body-wall muscle cells (Winston et al., 2002, Figure 1.1B). Cell-autonomous RNAi mutants, such as *rde-1*, displayed both a bright pharynx and bright body-wall muscle. In contrast, systemic RNAi mutants were predicted to have a dim pharynx, but bright body-wall muscle, indicating that dsRNA failed to be transported to the body-wall muscle. To mutagenize the worms, synchronized hermaphrodites were exposed to 25 mM ethyl methanesulfonate (EMS). F2 animals were placed on bacteria expressing GFP dsRNA, and animals with dim body-wall muscle were selected. In this original screen, at least 106 systemic RNAi mutants were isolated. These mutants defined three major complementation groups, *sid-1*, *sid-2* and *sid-3*. These mutants were cloned and the function of the genes mutated were characterized. In the intestinal lumen of the worm, ingested dsRNA import is mediated by the systemic RNAi defective protein, SID-2. SID-2 is a 311 amino acid

Figure 1.1

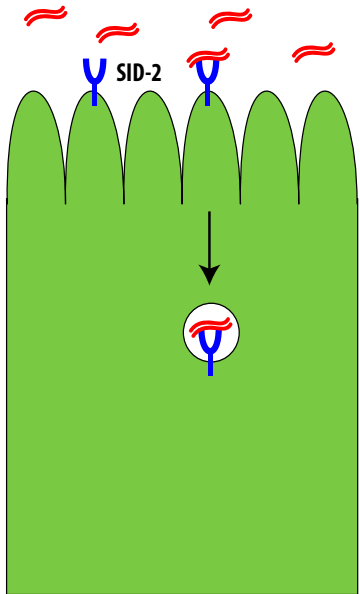




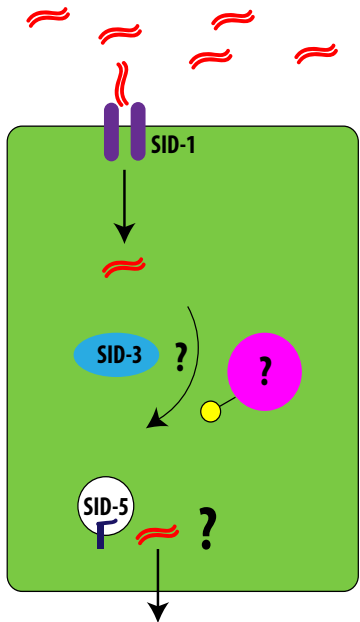
**Figure 1.1 (continued). A screen for systemic RNAi genes.** A. GFP is expressed in the pharynx and in the body-wall muscle. B. Introduction of a GFP-hairpin, which expresses GFP dsRNA under the control of the *myo-2* promoter, which is expressed in the pharyngeal muscle. The GFP dsRNA not only silences the pharynx, but also adjacent body-wall muscle. C. Cell-autonomous RNAi mutants, such as *rde-1*, have bright GFP expressed in the pharynx and body-wall muscle. D. Systemic RNAi mutants, such as *sid-1*, have bright body-wall muscle, but dim pharyngeal muscle.

Figure 1.2

A



B



**Figure 1.2 (continued). Systemic RNAi genes.** A. The transmembrane protein SID-2 binds dsRNA in the intestinal lumen, and is required for dsRNA import. B. The dsRNA channel SID-1 is required for dsRNA import into cells. Additionally, the tyrosine kinase SID-3 is also required for dsRNA entry, although the role it plays and its potential substrates, if any, are not known. The endosome-associated protein SID-5 may be important in dsRNA export.

transmembrane protein. It localizes to the apical membrane of the intestine (Winston et al., 2007), and is sufficient for uptake of dsRNA in *Drosophila S2* cells, indicating that it likely directly binds dsRNA and facilitates its import (McEwan et al., 2012).

Ingested dsRNA may be directly transcytosed into the pseudocoelomic fluid, or it may be first imported into intestinal cells, then exported into the pseudocoelom. A major question in the field of systemic RNAi is what factors are required for the export of dsRNA. However, it is known that after export to the pseudocoelom, import of dsRNA into cells requires the dsRNA channel SID-1 (Winston et al., 2002; Figure 1.2). SID-1 is predicted to have 11 transmembrane domains, and a *sid-1* transcriptional fusion indicates that SID-1 is broadly expressed throughout the worm, except for in neurons (Winston et al., 2002). Consistent with this expression pattern, neurons are resistant to environmental RNAi, however, if SID-1 is transgenically expressed in neurons, they become sensitive to environmental RNAi (Calixto et al., 2010). Although export of dsRNA does not require *sid-1*, *sid-1* is essential for import of dsRNA (Jose et al., 2009). Furthermore, expression of SID-1 in *Drosophila S2* cells, which do not typically import dsRNA, is sufficient to allow for passive import of dsRNA. This indicates that SID-1 may be a dsRNA channel.

Additional proteins required for systemic RNAi include SID-3 and SID-5. SID-3 is a tyrosine kinase required for import of dsRNA (Jose et al., 2012). SID-3 is a homolog of activated cdc-42-associated kinase (ACK), which is known to regulate

endocytosis in mammalian cells. The kinase domain of SID-3 is required for dsRNA import, however, no SID-3 substrates have been identified.

SID-5 is an endosome-associated protein that colocalizes with the late endosomal proteins RAB-7 and LMP-1 (Hinas et al., 2012). SID-5 is a broadly expressed 67 amino-acid transmembrane protein. Interestingly, rescue of SID-5 in the intestine is sufficient to restore silencing in the body-wall muscle, possibly suggesting that SID-5 may be important in export.

Upon entry to a cell, long dsRNA is bound by the Dicer complex, which includes DCR-1 and RDE-4 (Zamore et al., 2000, Knight and Bass, 2001; Figure 1.2). DCR-1, a RNase III endoribonuclease, cleaved the long dsRNA into short (~22 nucleotide) short interfering RNA (siRNA). After this, the Argonaute (Ago) protein RDE-1 binds Dicer products and removes the passenger strand, resulting in single-stranded siRNA (Parrish and Fire, 2001, Tomari et al., 2004, Steiner et al., 2009). In other species, a primary Argonaute protein would bind this primary siRNA and use it as a guide to identify mRNA, which would be degraded by primary Ago protein's RNase H activity. In contrast, in *C. elegans*, primary siRNA guide an RNA-dependent RNA polymerase (RdRP) to cognate mRNA, which is then used to generate abundant secondary siRNA (Alder et al., 2003, Pak and Fire, 2007; Figure 1.3). The high abundance of these secondary siRNA are thought to explain why RNAi is so potent in *C. elegans*. When I began my research, how primary siRNAs guide RdRPs to the mRNA was unknown.

Figure 1.3

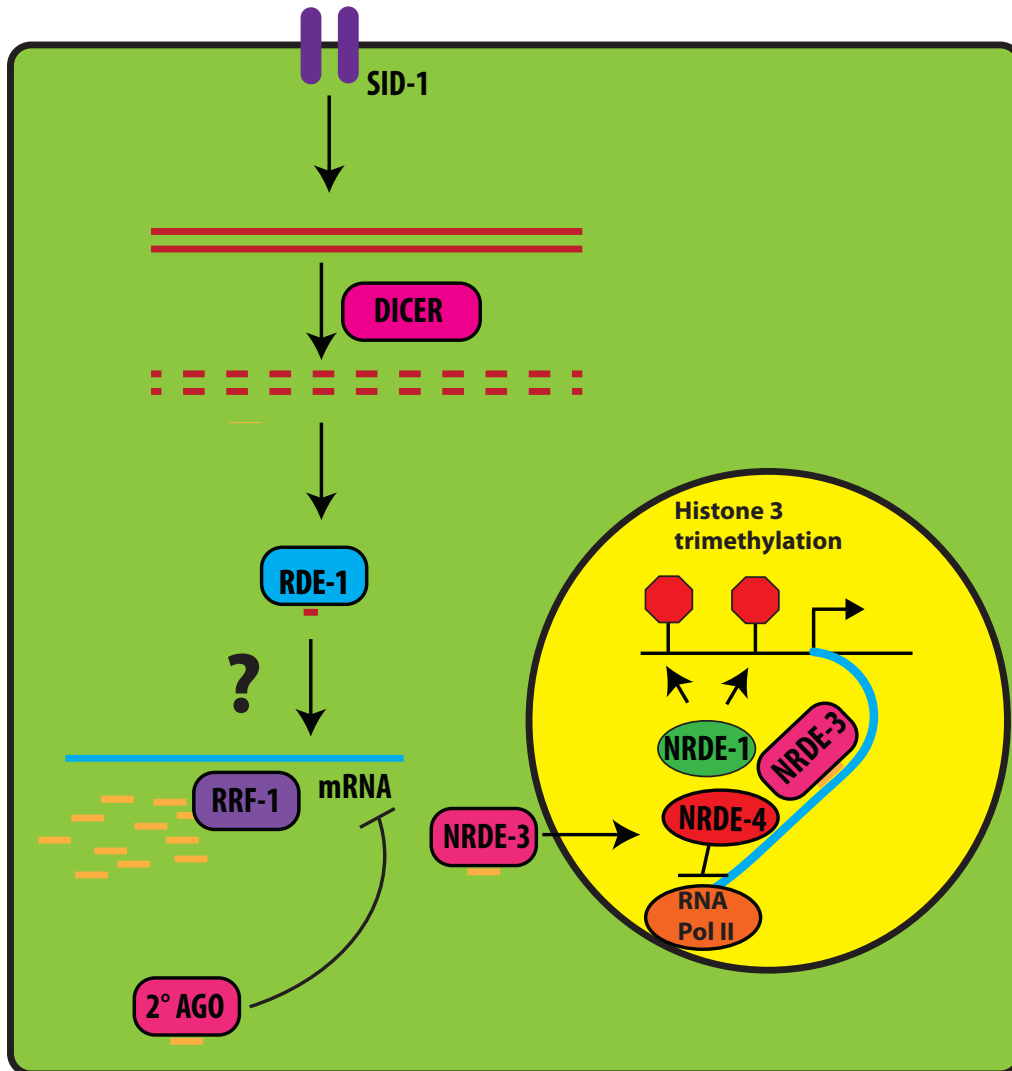


**Figure 1.3 (continued). A model for *C. elegans* cell-autonomous RNAi.** See text for details. Question mark represents the unknown link between *rde-1* and secondary siRNA amplification. 2° Ago: Secondary argonautes, such as SAGO and WAGOs.

After secondary siRNAs are produced, they complex with proteins named secondary argonautes and worm-specific secondary argonautes (SAGOs and WAGOs). These secondary argonautes bind cognate mRNA, and are essential for efficient silencing, for example, of the muscle-expressed gene, *unc-22* (Yigit et al., 2007). The absence of SAGOs results in strong defects in silencing, suggesting that they are responsible for a large portion of silencing ability in *C. elegans*.

Most of the argonautes in *C. elegans*, such as RDE-1, localize to the cytoplasm of the cell. However, in addition to these cytoplasmic RNAi proteins, there are nuclear RNAi proteins. In somatic tissues, NRDE-3, a nuclear argonaute, binds siRNAs and shuttles them into the nucleus from the cytoplasm (Guang et al., 2008; Figure 1.3). Then NRDE-3 complexes with other proteins, including NRDE-1, NRDE-2 and NRDE-4 (Guang et al., 2010), which act to impede RNA polymerase II, and direct histone H3 lysine 9 (H3K9) and H3K27 trimethylation (Mao et al., 2015) to the gene being silenced. Interestingly, silencing of genes in *C. elegans* can be transgenerational, with genes being silenced for multiple generations, even after the silencing trigger is removed. Consistent with this, the H3K9 and H3K27 trimethylation state can be inherited for multiple generations (Mao et al., 2015). Furthermore, nuclear RNAi is considerably more potent in the F1 progeny of worms exposed to dsRNA than the PO generation themselves (Burton et al., 2011), raising the possibility that germline transmission of silencing signals might potentiate silencing ability.



## Enhanced RNAi mutants

In addition to mutants required for RNAi, mutants with an enhanced RNAi (Eri) phenotype have been found. Many of these Eri genes encode proteins that are required for the production of endogenous siRNAs, indicating that these endo-siRNAs likely compete with exogenous siRNAs for limited silencing factors. Thus, reductions in endo-siRNA levels enable exo-siRNAs to elicit stronger silencing. For example, the Eri mutant *eri-1* encodes a 3'-5' exoribonuclease of the DEDDh family that binds Dicer (Kennedy et al., 2004). Loss of *eri-1* causes a specific loss in a particular class of endogenous siRNA. Likewise, loss of the RNA-dependent RNA polymerase RRF-3 causes enhanced RNAi and loss of accumulation of 26G endo-siRNAs (Simmer et al., 2003). These siRNAs regulate, among other processes, spermatogenesis and zygotic development (Han et al., 2009). A significant fraction (~30%) of genes display no phenotype when knocked-down in a wild type background, but do show a phenotype in an *rrf-3* strain (Simmer et al. 2003).

In contrast to these enhanced RNAi mutants, which display a clear loss of production of endo-siRNAs, are the synthetic multivulvae Class B (SynMuv B) mutants, also known as Rb tumor suppressor pathway (Wang et al., 2005). Loss of these genes are not known to cause obvious endo-siRNA misregulation, indicating that the Eri phenotype must arise in a different mechanism. Rb pathway mutants, such as *lin-35*, a Rb homolog, are chromatin factors that function in the repression of cell cycle genes, as well as other genes (Wu et al., 2012). Loss of Rb pathway genes such as *lin-35*, *lin-15b* or *hpl-2* causes misexpression of germline genes in the soma. Included in these misregulated genes are the RNAi factors *C04F12.1*, *sago-2* and *rrf-*

2. Wu et al. have hypothesized that misexpression of these genes in the germline may contribute to the enhanced RNAi phenotype displayed in Rb pathway mutants.

### **Significance**

Understanding the mechanisms through which RNAi is elicited has critical implications for human health, scientific research and biotechnology and agricultural implications. First, RNAi is conserved broadly throughout eukaryotes, including humans. Moreover, given the unique ability of RNAi to knock-down particular genes, it is easy to envision therapeutic possibilities for RNAi, such as knock-down of particular cancer promoting genes. Although delivery of silencing factors such as siRNAs or long dsRNA has proven challenging, an understanding of how animals naturally package, transport and process these factors may provide clues as to how these factors should be delivered.

RNAi has proven to be an extremely useful tool for researchers, especially those in the *C. elegans* community, since simply feeding worms dsRNA can trigger silencing. Indeed, libraries containing bacteria that express dsRNA targeting approximately 90% of *C. elegans* genes have been built (Kamath et al., 2003, Rual et al., 2004). These libraries have been used to understand processes as diverse as aging, nonsense-mediated decay and RNAi itself (Jorgensen and Mango, 2002; Boutros and Ahringer, 2008, Longman et al., 2008). Conveniently, these RNAi screens do not require toxic mutagens and the genes knocked down are immediately known. Furthermore, identifying lethal genes is easier since these strains do not need to be maintained.

Given its usefulness, it is obvious that a full understanding of RNAi must be obtained in order to unlock its full potential as a research tool. For example, identification of enhanced RNAi mutants has help uncover new RNAi phenotypes. Additionally, understanding when RNAi might fail is also critical to understanding how to use RNAi as a research tool. In this thesis, I show that the *C. elegans* pharynx is resistant to first-generation exposure to dsRNA. Additionally, I show that particular loci are more susceptible to nuclear RNAi than others. These observations may help other researchers design their RNAi screens and assays.

In addition to its usefulness to research potential, the power of RNAi is being exploited for biotechnology and agricultural purposes. For example, feeding honey bees dsRNA may be a promising defense against colony collapse disorder, while spraying tobacco with a dsRNA mixture prevents against viral infection for at least three weeks (Brustcher and Flenniken, 2015, Mitter et al., 2017). As anti-pest RNAi treatments in agriculture expand, it will be essential to understand the mechanisms of RNAi to ensure efficient silencing and to understand the potential for resistance to RNAi.

Finally, understanding RNAi is important because it may provide an avenue for understanding other mechanisms in which gene expression is turned off. In particular, nuclear RNAi may be a good model for directed H3K9 and H3K27 trimethylation, and the silenced chromatin with which it is associated. Currently, directing histone modifications to a particular locus to understand its effects, as well as its requirements, is a challenge. Although dCas9 directed histone modifications may prove to be a powerful tool to study this problem, these tools are still under development. Therefore, use of RNAi to direct H3K9 and H3K27 trimethylation may

prove to a convenient tool to understand the efficiency of this histone methylation in particular circumstances.

### **Brief Summary of the Dissertation**

In Chapter 2, I describe the RNAi defective gene, *rde-12*. I show that *rde-12* encodes a conserved phenylalanine-glycine (FG) domain-containing DEAD box helicase.

Although we originally found *rde-12* in a screen for export mutants, I show that RDE-12 is required for cell-autonomous RNAi. In particular, I show that RDE-12 localizes to cytoplasmic puncta, that the RDE-12 helicase domain is required for RNAi processing activity, and that RDE-12 is essential for secondary siRNA, but not primary, accumulation.

In Chapter 3, I show that RDE-12, like other factors required for secondary siRNA production, is not required for pharyngeal muscle silencing in the presence of a strong dsRNA trigger. Exploring this finding, I show that the pharyngeal muscle has a particular requirement for nuclear RNAi. In contrast to a model positing that germline RNAi activity may be required for efficient nuclear RNAi in the progeny, I show that nuclear RNAi in the pharynx does not require maternal germline RNAi activity. Instead, pharyngeal muscle silencing displays a critical period for silencing, with early exposure to dsRNA triggering the strongest silencing.

In Chapter 4, I explore how Rb pathway mutants enhance silencing. I show that Rb pathway mutants significantly extend the critical period, consistent with a model in which loss of Rb pathway genes causes germline-like gene expression and possible de-differentiation. Furthermore, I show that particular loci are more susceptible to nuclear RNAi, indicating that local chromatin state affects sensitivity

to silencing. Finally, I show that the Eri phenotype of Rb pathway mutants requires nuclear RNAi.

In Chapter 5, I conclude the thesis by summarizing my results and proposing future research avenues. Additionally, I speculate that loss of Rb causes de-differentiation and sensitivity to epigenetic changes in systems other than *C. elegans*, in particular in the context of cancer. It has been noted that pediatric retinoblastoma tumors often only have Rb mutated; this implies that the other oncogenic changes must be epigenetic. I speculate that mutation of Rb, among other effects, facilitates the ease at which epigenetic changes may be made.

## Literature Cited

- [1] Alder MN, Dames S, Gaudet J, Mango SE. Gene silencing in *Caenorhabditis elegans* by transitive RNA interference. *RNA* 2003;9:25–32.
- [2] Boutros M, Ahringer J. The art and design of genetic screens: RNA interference. *Nat Rev Genet* 2008;9:554–66. doi:10.1038/nrg2364.
- [3] Brutscher LM, Flenniken ML. RNAi and Antiviral Defense in the Honey Bee. *J Immunol Res* 2015;2015:941897. doi:10.1155/2015/941897.
- [4] Burton NO, Burkhart KB, Kennedy S. Nuclear RNAi maintains heritable gene silencing in *Caenorhabditis elegans*. *Proc Natl Acad Sci* 2011;108:19683–8. doi:10.1073/pnas.1113310108.
- [5] Calixto A, Chelur D, Topalidou I, Chen X, Chalfie M. Enhanced neuronal RNAi in *C. elegans* using SID-1. *Nat Methods* 2010;7:554–9. doi:10.1038/nmeth.1463.
- [6] Feinberg EH, Hunter CP. Transport of dsRNA into cells by the transmembrane protein SID-1. *Science* (80- ) 2003;301:1545–7. doi:10.1126/science.1087117 301/5639/1545 [pii].
- [7] Fire A, Xu S, Montgomery MK, Kostas SA, Driver SE, Mello CC. Potent and specific genetic interference by double-stranded RNA in *Caenorhabditis elegans*. *Nature* 1998;391:806–11. doi:10.1038/35888.
- [8] Guang S, Bochner AF, Burkhart KB, Burton N, Pavelec DM, Kennedy S. Small regulatory RNAs inhibit RNA polymerase II during the elongation phase of transcription. *Nature* 2010;465:1097–101. doi:10.1038/nature09095.
- [9] Guang S, Bochner AF, Pavelec DM, Burkhart KB, Harding S, Lachowiec J, et al. An Argonaute transports siRNAs from the cytoplasm to the nucleus. *Science* 2008;321:537–41. doi:10.1126/science.1157647.
- [10] Han T, Manoharan AP, Harkins TT, Bouffard P, Fitzpatrick C, Chu DS, et al. 26G endo-siRNAs regulate spermatogenic and zygotic gene expression in *Caenorhabditis elegans*. *Proc Natl Acad Sci U S A* 2009;106:18674–9. doi:10.1073/pnas.0906378106.
- [11] Jorgensen EM, Mango SE. The art and design of genetic screens: *caenorhabditis elegans*. *Nat Rev Genet* 2002;3:356–69. doi:10.1038/nrg794.
- [12] Jose a. M, Kim Y a., Leal-Ekman S, Hunter CP. Conserved tyrosine kinase promotes the import of silencing RNA into *Caenorhabditis elegans* cells. *Proc Natl Acad Sci* 2012;109:14520–5. doi:10.1073/pnas.1201153109.

- [13] Kamath RS, Ahringer J. Genome-wide RNAi screening in *Caenorhabditis elegans*. *Methods* 2003;30:313–21. doi:10.1016/S1046-2023(03)00050-1.
- [14] Kennedy S, Wang D, Ruvkun G. A conserved siRNA-degrading RNase negatively regulates RNA interference in *C. elegans*. *Nature* 2004;427:645–9. doi:10.1038/nature02302.
- [15] Knight SW, Bass BL. A role for the RNase III enzyme DCR-1 in RNA interference and germ line development in *Caenorhabditis elegans*. *Science* 2001;293:2269–71. doi:10.1126/science.1062039.
- [16] Lehner B, Calixto A, Crombie C, Tischler J, Fortunato A, Chalfie M, et al. Loss of LIN-35, the *Caenorhabditis elegans* ortholog of the tumor suppressor p105Rb, results in enhanced RNA interference. *Genome Biol* 2006;7:R4. doi:10.1186/gb-2006-7-1-r4.
- [17] Longman D, Plasterk RHA, Johnstone IL, Cáceres JF. Mechanistic insights and identification of two novel factors in the *C. elegans* NMD pathway. *Genes Dev* 2007;21:1075–85. doi:10.1101/gad.417707.
- [18] Mao H, Zhu C, Zong D, Weng C, Yang X, Huang H, et al. The Nrde Pathway Mediates Small-RNA-Directed Histone H3 Lysine 27 Trimethylation in *Caenorhabditis elegans*. *Curr Biol* 2015;25:2398–403. doi:10.1016/j.cub.2015.07.051.
- [19] McEwan DL, Weisman AS, Hunter CP. Uptake of Extracellular Double-Stranded RNA by SID-2. *Mol Cell* 2012;47:746–54. doi:10.1016/j.molcel.2012.07.014.
- [20] Mitter N, Worrall EA, Robinson KE, Li P, Jain RG, Taochy C, et al. Clay nanosheets for topical delivery of RNAi for sustained protection against plant viruses. *Nat Plants* 2017;3:16207. doi:10.1038/nplants.2016.207.
- [21] Pak J, Fire A. Distinct populations of primary and secondary effectors during RNAi in *C. elegans*. *Science* 2007;315:241–4. doi:10.1126/science.1132839.
- [22] Parrish S, Fire A. Distinct roles for RDE-1 and RDE-4 during RNA interference in *Caenorhabditis elegans*. *RNA* 2001;7:1397–402.
- [23] Rual J-F, Ceron J, Koreth J, Hao T, Nicot A-S, Hirozane-Kishikawa T, et al. Toward improving *Caenorhabditis elegans* phenome mapping with an ORFeome-based RNAi library. *Genome Res* 2004;14:2162–8. doi:10.1101/gr.2505604.
- [24] Shiu PK, Zhuang JJ, Hunter CP. *Animal Endo-SiRNAs* 2014;1173:71–87. doi:10.1007/978-1-4939-0931-5.

- [25] Simmer F, Tijsterman M, Parrish S, Koushika SP, Nonet ML, Fire A, et al. Loss of the putative RNA-directed RNA polymerase RRF-3 makes *C. elegans* hypersensitive to RNAi. *Curr Biol* 2002;12:1317–9. doi:10.1016/S0960-9822(02)01041-2.
- [26] Steiner F a, Okihara KL, Hoogstrate SW, Sijen T, Ketting RF. RDE-1 slicer activity is required only for passenger-strand cleavage during RNAi in *Caenorhabditis elegans*. *Nat Struct Mol Biol* 2009;16:207–11. doi:10.1038/nsmb.1541.
- [27] Timmons L, Fire a. Specific interference by ingested dsRNA. *Nature* 1998;395:854. doi:10.1038/27579.
- [28] Tomari Y, Du T, Haley B, Schwarz DS, Bennett R, Cook HA, et al. RISC assembly defects in the *Drosophila* RNAi mutant armitage. *Cell* 2004;116:831–41. doi:10.1016/S0092-8674(04)00218-1.
- [29] Wang D, Kennedy S, Conte D, Kim JK, Gabel HW, Kamath RS, et al. Somatic misexpression of germline P granules and enhanced RNA interference in retinoblastoma pathway mutants. *Nature* 2005;436:593–7. doi:10.1038/nature04010.
- [30] Winston WM, Molodowitch C, Hunter CP. Systemic RNAi in *C. elegans* requires the putative transmembrane protein SID-1. *Science* (80- ) 2002;295:2456–9. doi:10.1126/science.1068836 1068836 [pii].
- [31] Winston WM, Sutherlin M, Wright AJ, Feinberg EH, Hunter CP. *Caenorhabditis elegans* SID-2 is required for environmental RNA interference. *Proc Natl Acad Sci U S A* 2007;104:10565–70. doi:0611282104 [pii] 10.1073/pnas.0611282104.
- [32] Wu X, Shi Z, Cui M, Han M, Ruvkun G. Repression of germline RNAi pathways in somatic cells by retinoblastoma pathway chromatin complexes. *PLoS Genet* 2012;8:e1002542. doi:10.1371/journal.pgen.1002542.
- [33] Yang H, Vallandingham J, Shiu P, Li H, Hunter CP, Mak HY. The DEAD box helicase RDE-12 promotes amplification of RNAi in cytoplasmic foci in *C. Elegans*. *Curr Biol* 2014;24:832–8.
- [34] Yigit E, Batista PJ, Bei Y, Pang KM, Chen CCG, Tolia NH, et al. Analysis of the *C. elegans* Argonaute Family Reveals that Distinct Argonautes Act Sequentially during RNAi. *Cell* 2006;127:747–57. doi:10.1016/j.cell.2006.09.033.
- [35] Zamore PD, Tuschl T, Sharp P a, Bartel DP. RNAi: double-stranded RNA directs the ATP-dependent cleavage of mRNA at 21 to 23 nucleotide intervals. *Cell* 2000;101:25–33. doi:10.1016/S0092-8674(00)80620.



## Chapter 2: RDE-12 is a DEAD-box RNA helicase essential for accumulation of secondary siRNA

**Introduction:** RNA interference, a process in which double stranded RNA triggers silencing of cognate genes, was first discovered in the nematode *C. elegans*. In this process, double-stranded RNA triggers sequence-specific destruction of mRNA. Due to the strong response of *C. elegans* to exogenous dsRNA, RNAi has proven to be a powerful tool for *C. elegans* geneticists. Two elements of *C. elegans* RNAi make the response of the nematode to exogenous dsRNA especially potent: systemic RNAi machinery that transports silencing signals from tissue to tissue, and an amplification process that produces abundant secondary siRNAs (Zhuang and Hunter, 2012).

RNAi in *C. elegans* is systemic: silencing signals spread for tissue to tissue. Upon digestion of dsRNA, the transport of long dsRNA across the intestinal lumen is facilitated by SID-2 (Winston et al., 2007, McEwan et al., 2012). After import of dsRNA by SID-2, dsRNA is exported into the pseudocoelom. Later, long dsRNA and short double-stranded intermediates are imported across cellular membranes by the dsRNA channel SID-1 (Winston et al., 2002, Jose et al., 2009).

Imported dsRNA is processed by the dicer complex to produce short (~22 nt) double-stranded RNA molecules called primary siRNA (Tabara et al, 2002). The primary siRNA are processed by the argonaute RDE-1 to produce single-stranded siRNA that engage with the RNA-dependent RNA polymerases RRF-1 (soma) or EGO-1 (germline) and target mRNA to produce abundant secondary siRNA (Pak and Fire, 2007). Secondary siRNA have 5' triphosphates and are antisense to the mRNA targeting, suggesting that RdRPs catalyze the unprimed synthesis of secondary siRNA using the mRNA as template. These secondary

siRNAs then trigger destruction of cognate mRNA. For most genes, the production of secondary siRNA is required for silencing. Secondary siRNA bind to secondary argonautes (SAGOs: secondary argonaute and WAGOs: worm-specific argonaute) to promote transcriptional repression and destruction of mRNA or are imported into the nucleus by the argonaute NRDE-3 to effect transcriptional silencing (Yigit et al., 2006, Guang et al., 2008).

Despite the clear importance of secondary siRNAs in *C. elegans* RNAi, major questions remain regarding the production and function of siRNA. How secondary siRNAs are produced via unprimed synthesis from an mRNA target is not well understood. Additionally, the genetic requirements for the accumulation of siRNA are not fully known.

Here we identify RDE-12, a DEAD-box RNA helicase. We demonstrate that *rde-12* is resistant to a variety of exogenous dsRNA. *rde-12* is expressed broadly throughout the worm. Although we initially found *rde-12* in a screen for systemic RNAi mutants, we show that *rde-12* functions cell-autonomously (RNAi defective: Rde) and is not systemic RNAi defective (Sid). The *rde-12* RNAi defect is dosage sensitive and can be overcome by large amounts of dsRNA delivered by injection, expression or feeding. Investigating this dosage effect lead to the discovery that RDE-12 is required for the amplification and or stability of secondary siRNAs. Finally, we demonstrate that RDE-12 requires its ATPase domain to function.

**Results:** The original aim of our screen was to identify systemic RNAi export mutants. To distinguish between cell-autonomous RNAi defective mutants and systemic RNAi mutants, we used a strain that expresses GFP in the pharynx and body-wall muscle, and a GFP-hairpin in the pharynx. The GFP-hairpin in the pharynx not only silences GFP in

**Figure 2.1**

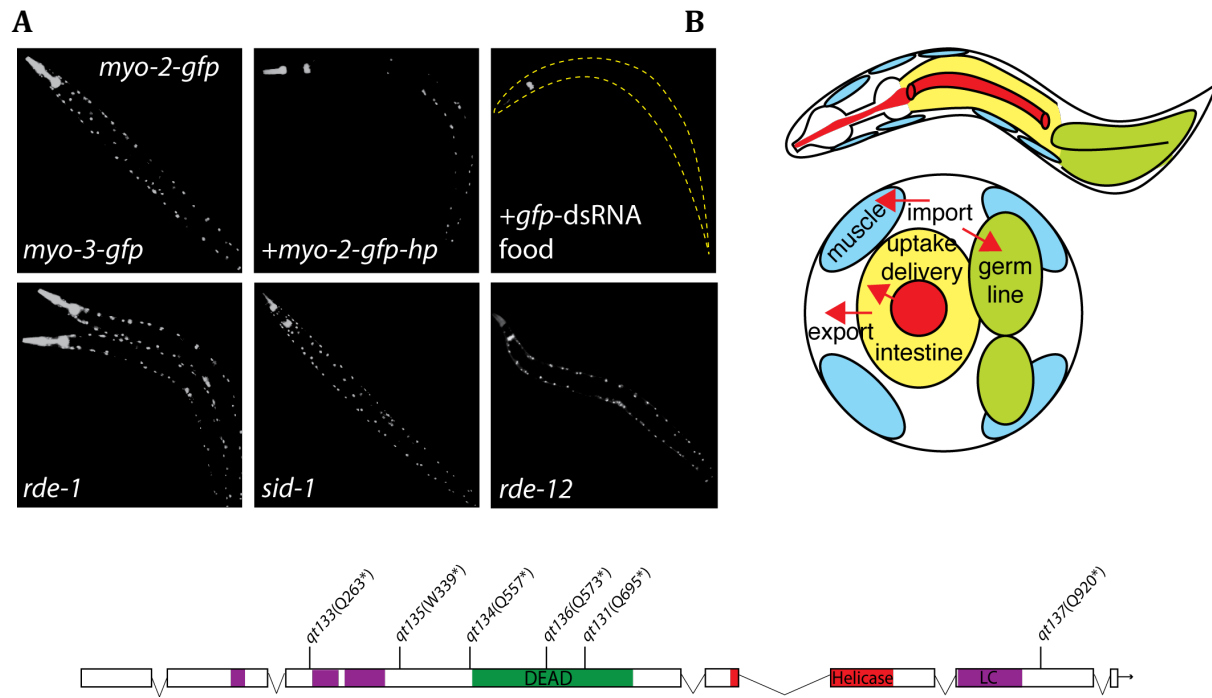


**Figure 2.1 (continued) A Screen for RNA export deficient mutants identifies DEAD-box helicase RDE-12.**

- A) Worms expressing *myo-2p::gfp* (pharynx), *myo-3p::nls\_gfp* (bodywall muscle nuclei [bwm]) and *myo-2p::gfp-pfg* (gfp hairpin dsRNA) grown on OP50 or gfp-dsRNA bacteria (top three panels). The gfp-pfg hairpin causes incomplete autonomous silencing in the pharynx and non-autonomous silencing of anterior bwm cells. The remaining bwm cells are silenced in response to ingested gfp dsRNA. All GFP silencing is dependent on RDE-1, while SID-1 and RDE-12 are important for non-autonomous silencing in bwm cells.
- B) To identify export mutants animals resistant to silencing in muscle and germline in response to ingested dsRNA were selected. These animals were then tested for sensitivity to intestinal cell marker, which requires uptake and cytoplasmic delivery. Such animals should be enriched for mutants defective in export of ingested dsRNA from the intestine.
- C) The location of six recovered RDE-12 alleles.

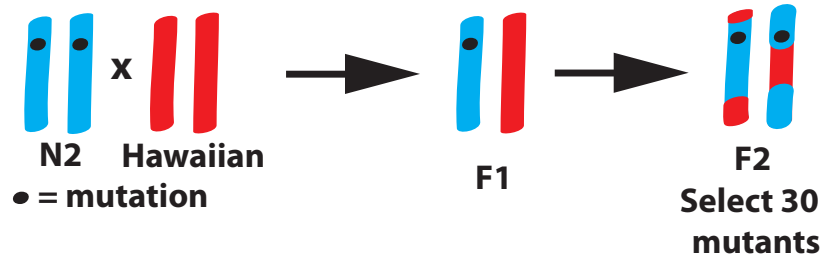
the pharynx, but also nearby body-wall muscle cells (Winston et al, 2002; Figure 2.1A). Cell-autonomous RNAi mutants will have a bright pharynx and bright body-wall muscle. However, systemic RNAi mutants will have a silenced pharynx, but bright body-wall muscle, even when exposed to environmental GFP RNAi. To enrich for export mutants, we

selected first for mutants resistant to feeding RNAi targeting a gene required for fertility (*unc-45*). Mutants were then subsequently tested for sensitivity to feeding RNAi targeting an intestinal gene (*act-5*) required for viability (Figure 2.1b). Genes identified in this manner would be potential RNAi export mutants: they can elicit an RNAi response in the intestine (a tissue presumably directly exposed to the ingested dsRNA), but cannot export silencing signals to the rest of the worm. We found no strains that were fully resistant to *unc-45* and fully sensitive to *act-5*. However, we did find a strain that we named *rde-12* (*qt131*), that was fully resistant to *unc-45* and partially sensitive to *act-5* RNAi. Subsequently, we found five additional *rde-12* alleles in an independent screen for systemic RNAi mutants. Like other previous systemic RNAi mutants, *rde-12* has a silenced pharynx, but bright body-wall muscle, even when exposed to GFP dsRNA (Figure 2.1A).

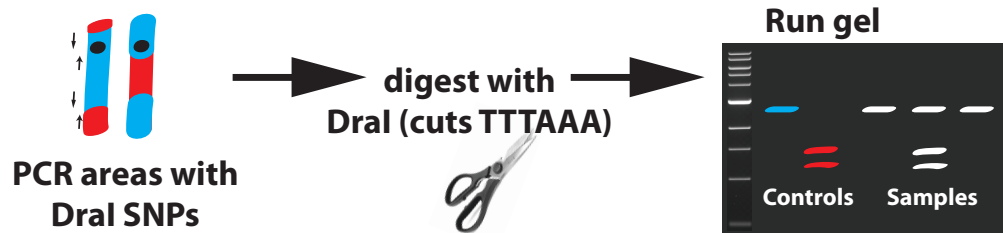
**The open reading frame F58G11.2 encodes RDE-12.** We initially mapped *rde-12* using a “SNP-snip” method developed by Davis et al. In this method, mutants in the N2 Bristol background are crossed to the Hawaiian strain CB4856 (Figure 2.2). F1 progeny are allowed to self-fertilize, and I selected mutant F2 animals by selecting worms resistant to *act-5* RNAi. Locations linked to the *rde-12* locus will have predominantly N2 single nucleotide polymorphisms (SNPs). These SNPs were

PCR amplified, then to distinguish between N2 and CB4856, digested by the restriction endonuclease DraI. I ran these DNA fragments on an agarose gel, allowing me to distinguish between N2 and CB4856 SNPs.

### Step 1: Cross N2 and Hawaiian strains



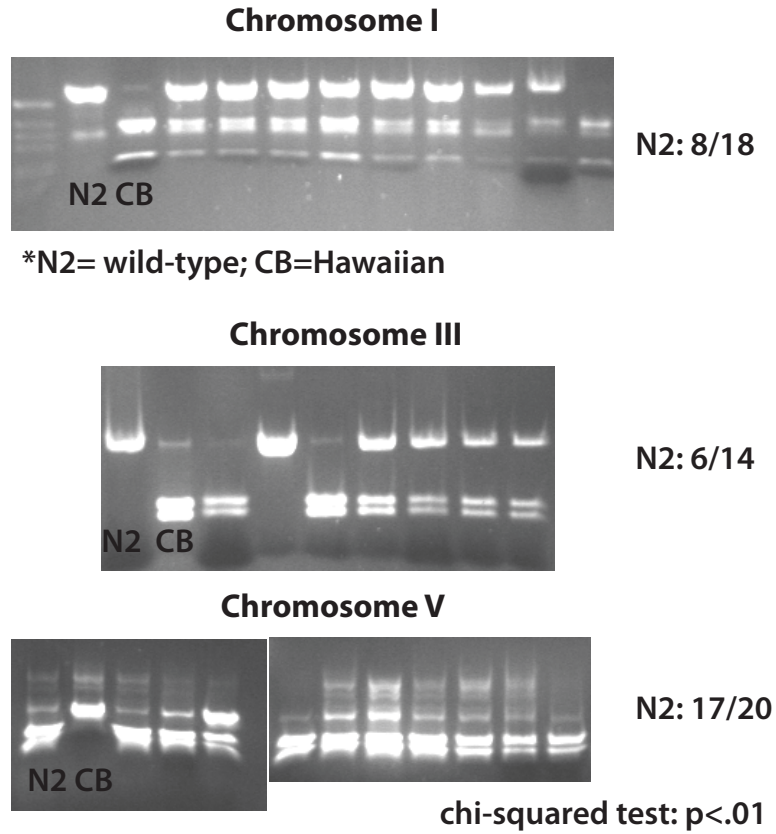
### Step 2: Lyse individual mutants, PCR SNPs and digest



N2 is uncut: TTTCAA  
Hawaiian is cut: TTT AAA

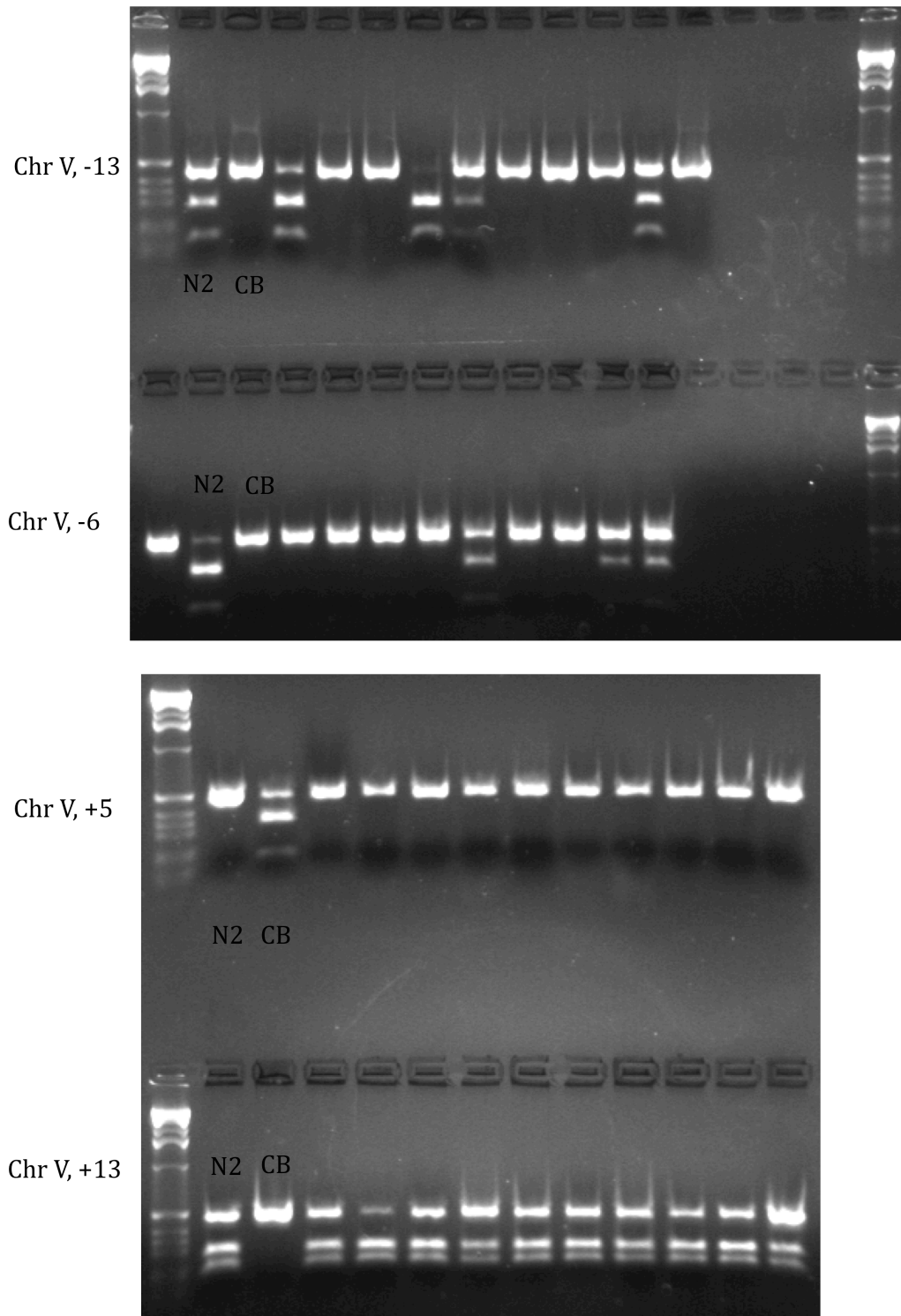
Areas near the mutation will be predominantly N2.

Figure 2.2. Mapping strategy for mapping of *rde-12*.



**Figure 2.3.** *rde-12* maps to Chromosome V.





**Figure 2.4 *rde-12* maps near Chromosome V, +5.** From top to bottom:  
 Chromosome V -13 (N2: 7/20), Chromosome V -6 (N2: 3/20), Chromosome V +5  
 (N2: 20/20), Chromosome V +13 (N2: 20/20).

Locations physically linked to the *rde-12* gene will have predominantly N2 SNPs. Indeed, I found that chromosome V had statistically significant levels of N2 SNPs (Figure 2.3). Further interval mapping revealed that *rde-12* mapped near Chromosome V, +5 (Figure 2.4). To identify the molecular lesion in *rde-12*, I obtained a whole-genome sequence using Illumina sequencing. Analysis of this data showed that there was a nonsense mutation (at Arg694) in the open reading frame F58G11.2 within the region to which I mapped the mutation. Moreover, knock-down of F58G11.2 in N2 wild-type resulted in a decrease in sensitivity to exogenous RNAi (data not shown). Sanger sequencing of five other alleles of *rde-12* revealed that all had nonsense mutations located in F58G11.2. Injection of wild-type genomic F58G11.2 into *qt131* generated partial, but clear rescue of the Rde phenotype (Figure 2.5F). Therefore, we conclude that F58G11.2 encodes RDE-12 (Figure 2.1B).

***Rde-12* is strongly resistant to exogenous dsRNA.** We tested the response of *rde-12* to feeding RNAi of multiple genes in different tissues. We found that *rde-12*(*qt131*) is strongly resistant to RNAi targeting muscle (*unc-22* and *unc-45*), gonad (*fkh-6*), germline (*pos-1*), cuticle (*bli-1*) and intestine-expressed (*act-5*) genes (Figure 2.5A-E; G). These data suggested that mRNA levels remain high despite RNAi targeting that gene. Indeed, we found that *pos-1* mRNA levels remained at levels similar to unexposed worms after exposure to *pos-1* feeding RNAi (Figure 2.5H).

**Rde-12 is a dosage-sensitive RNAi defective.** Two simple possibilities would explain the RNAi defective seen in *rde-12* animals. First, RDE-12 could be important for the transport of silencing cues (Sid, systemic RNAi defective).

Alternatively, RDE-12 might be important in cell-autonomous RNAi (Rde). It is also formally possible that RDE-12 is

Figure 2.5

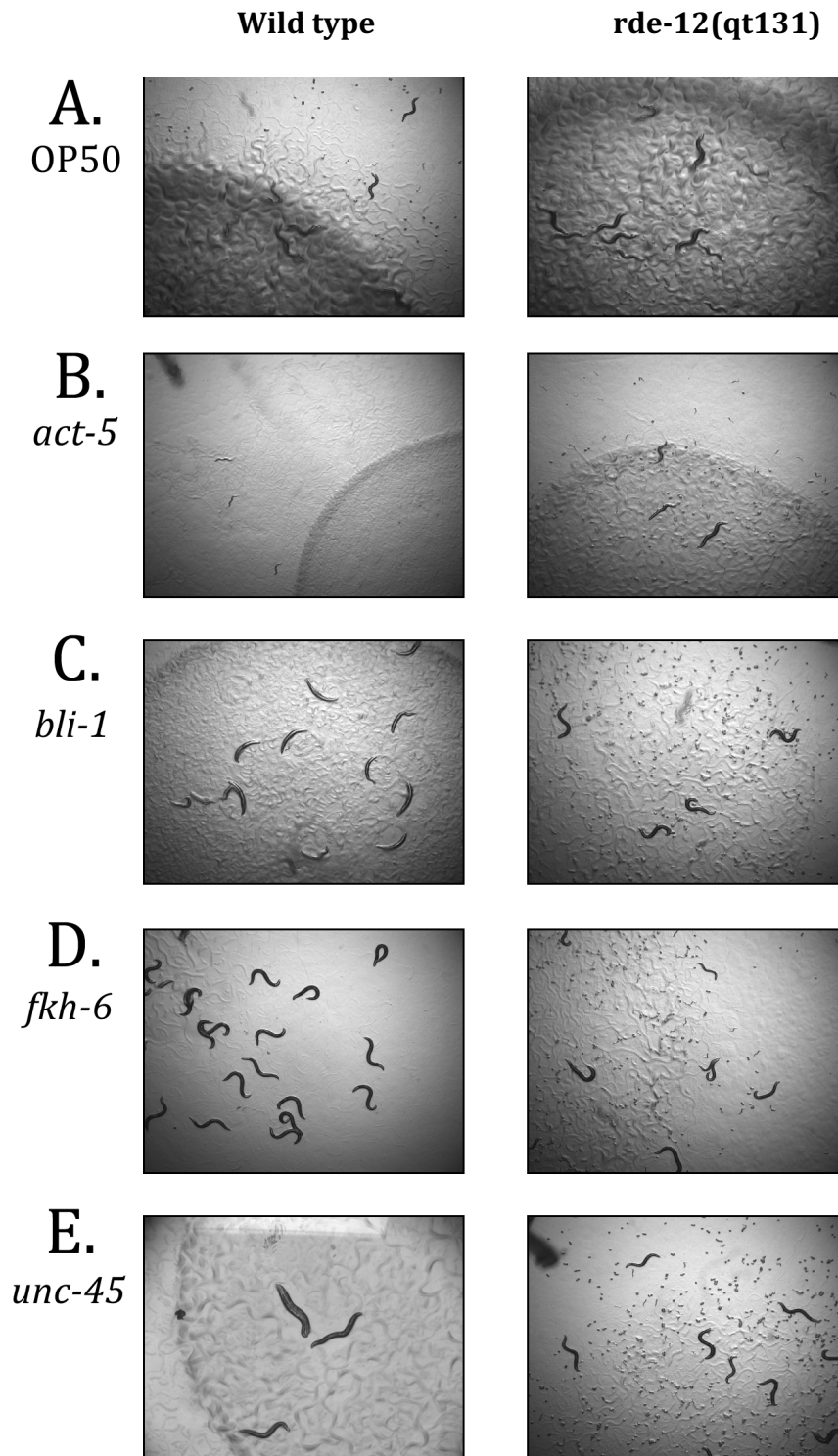
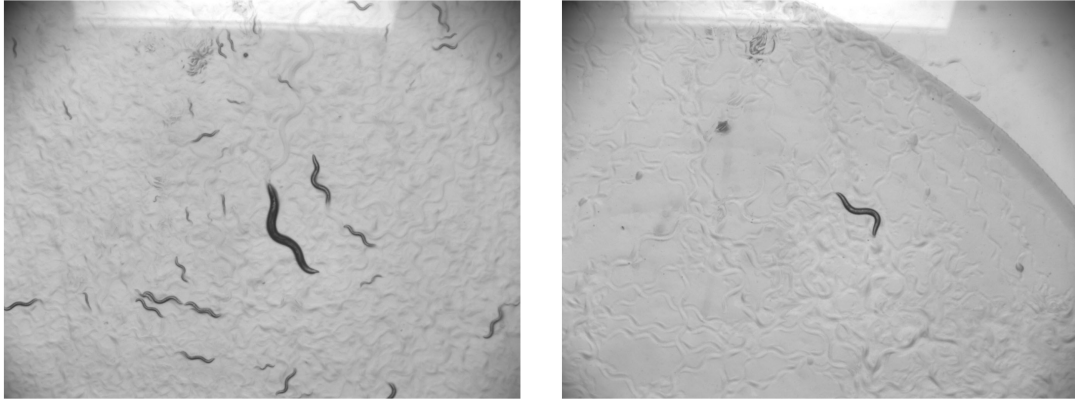


Figure 2.5 (continued)

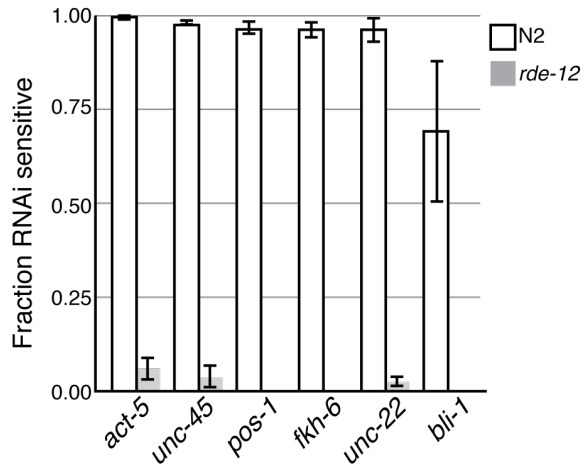
*rde-12(qt131)*

*rde-12(qt131)+rde-12 rescue*

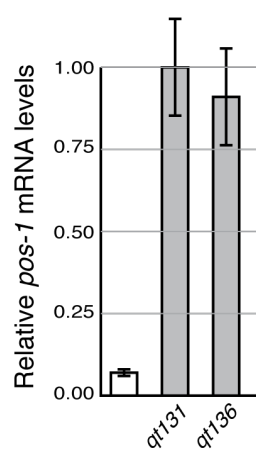
F



G



H



I

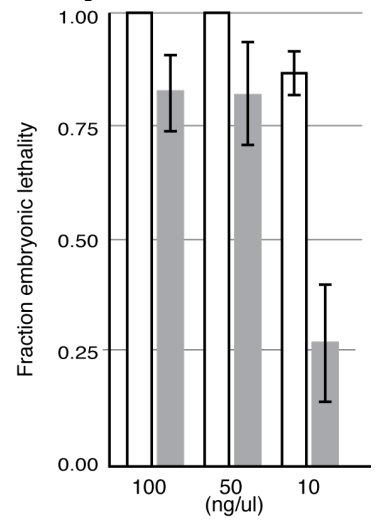


**Figure 2.5 (continued). *rde-12* is a dose-dependent RNAi defective mutant.**

A-E: Wild type or *rde-12* animals on either control (A) or RNAi foods (B-E).

F. Left, *rde-12*(*qt131*) on *fkh-6* RNAi food. Right, *rde-12*(*qt131*)

*PS1Ex[F58G11.2 rescue fragment]* on *fkh-6* RNAi food.

G. *rde-12* animals are broadly resistant to RNAi targeting genes in multiple tissues

H. *pos-1* mRNA levels in response to ingested *pos-1* dsRNA in wild-type and *rde-12* mutants

I. Injection of *pal-1* dsRNA directly into both gonad arms shows that *rde-12* mutants are dose-dependent Rde.

important for both systemic and cell-autonomous RNAi. To determine if *rde-12* is cell-autonomous RNAi defective, we injected double-stranded RNA targeting *pal-1*, a gene essential for embryogenesis, directly into both gonads, bypassing the need for systemic RNAi. *Rde-12* animals were resistant to *pal-1* dsRNA (Figure 2.5I) in a dosage-dependent fashion, indicating that *rde-12* is Rde.

**Rde-12 is not systemic RNAi defective.** Although we determined that *rde-12* was RNAi defective, a possibility remained that *rde-12* was both RNAi defective and systemic RNAi defective. Two lines of evidence suggested that *rde-12* may be defective for an aspect of systemic RNAi (Sid). First, *qt131* worms are partially sensitive to feeding RNAi against *act-5*, an intestinal target, but strongly resistant to every other target tested. This could represent an export defect or, because *act-5* is a very strong food, may reflect only a near complete loss of RNAi capacity. The second line of evidence is that, in an *rde-12* background, GFP dsRNA expressed from the pharynx efficiently silences pharyngeally expressed GFP, but is completely ineffective at silencing body-wall muscle GFP (Figure 2.1A). However, because the *rde-12* reporter is not expressed in the pharynx (Figure 2.8B), RDE-12 may be required for cell autonomous RNAi in non-pharyngeal cells.

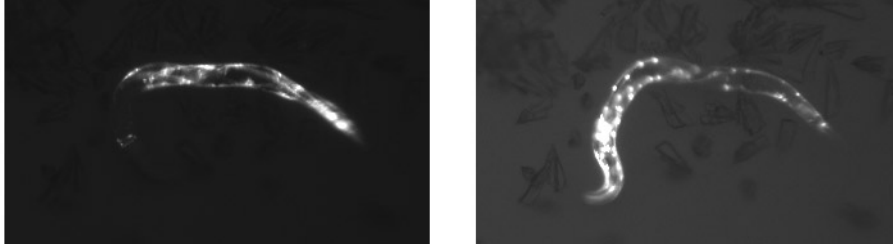
To determine if RDE-12 functions cell-autonomously, we rescued *rde-12(-)* worms that express GFP in the body-wall muscle with body-wall muscle promoter driven *mCherry::rde-12(+)*. On GFP RNAi food, this resulted in strong silencing in the body-wall muscle (Figure 2.6A). Furthermore, mosaic analysis showed that the rescue is cell-autonomous (Figure 2.6B). We therefore concluded that RDE-12 does not play a role in export of dsRNA.

**Figure 2.6**

A.







B.

**Figure 2.6 (continued):** *rde-12(+)* can function cell-autonomously. A. *mCherry::rde-12(+)* was driven by a body-wall muscle specific promoter (*myo-3*) in the HC57 (pharynx and muscle driven GFP, pharynx driven GFP-hairpin) background and fed on GFP RNAi *E. coli*. The worm on the left contains the transgenic *mCherry::rde-12(+)*, whereas the worm on right lacks the array. Neither *rde-12(+)* expressed in pharynx nor mCherry expressed the body-wall muscle could rescue silencing (data not shown). Middle, mCherry expression. Bottom, GFP expression. B. Mosaic expression of *mCherry::rde-12(+)* indicates that *rde-12* can function cell-autonomously. Left panel, mCherry expression. Right panel, GFP expression. Note the presence of bright GFP expression where *rde-12(+)* is absent.

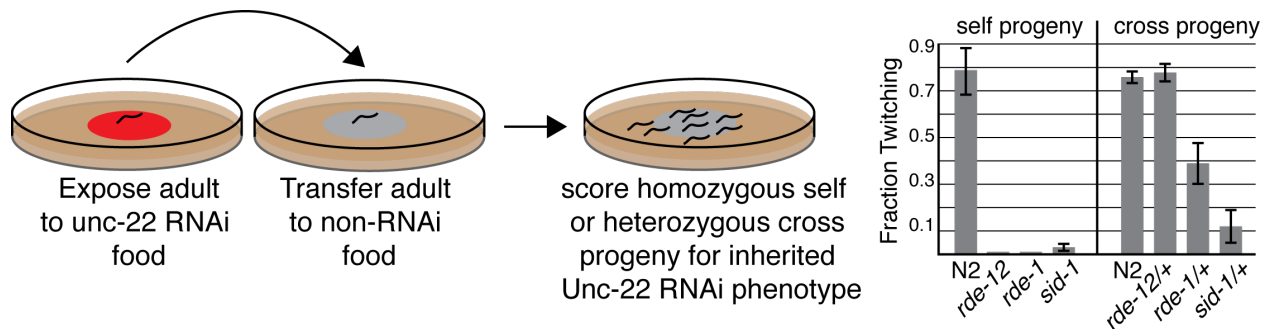


**Figure 2.7. *rde-12* mutants are not Sid.**

Adult animals were exposed to *unc-22* dsRNA expressing bacteria until adulthood and transferred to OP50 where they either produce self-progeny or are crossed to WT males.

Self-progeny wild type (N2) animals twitch showing that they have inherited a silencing signal from their mothers previous exposure to dsRNA food. Self progeny from *rde-12*, *rde-1*, and *sid-1* mutants do not twitch. Cross progeny are wild-type and twitch if they have inherited silencing signals.

To determine if *rde-12* is systemic RNAi defective, we tested whether *rde-12* mutants could transport silencing signals from the intestine to the germline. We placed *rde-12* animals on *unc-22* food. *unc-22* knockdown in the body-wall muscle causes a scoreable twitching phenotype. *rde-12* animals are not strong twitchers when placed on *unc-22* RNAi food. If *rde-12* worms can transport *unc-22* dsRNA from the intestine to the germline, then heterozygous progeny should twitch (Figure 2.7). When crossed to male wild-type worms, the progeny of *rde-12* worms twitched, indicating that *rde-12* is not required for transport of silencing signals to the germline (Figure 2.7).

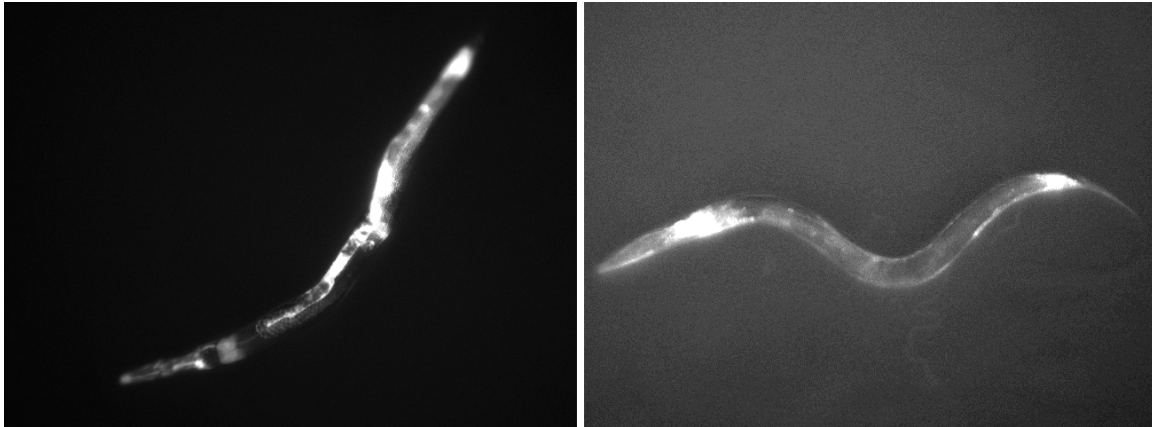
**Expression data.** To determine the tissues that express *rde-12*, we built translational and transcriptional reporters. The *rde-12* promoter drives mCherry expression in a broad range of tissues (Figure 2.8). To determine where RDE-12 localizes, I fused mCherry to the RDE-12 C-terminus. Worms expressing this construct localize mCherry in cytoplasmic puncta, consistent with the hypothesis that RDE-12 localizes to RNA granules.

**Rde-12 is deficient in production of siRNA.** To measure siRNA levels in *rde-12* mutants, we used a novel hybridization-based assay, the Fireplex assay, which was developed to measure miRNA levels. Briefly, short probes anti-sense to target small RNAs are embedded within a hydrogel particle. Target molecules diffuse into this matrix and hybridize to the short probe. Hybridization leads to fluorescence that can be detected by flow cytometry. We choose to examine the five most abundant *pos-1* secondary siRNAs produced (Zhang et al, 2012); of these, four probes were found to be specific.

To validate the Fireplex assay for siRNA detection, we measured *pos-1* siRNA generated in response to feeding on *pos-1* dsRNA expressing bacteria in wild-type and

**Figure 2.8. RDE-12 expression.**

**A.**



**B.**

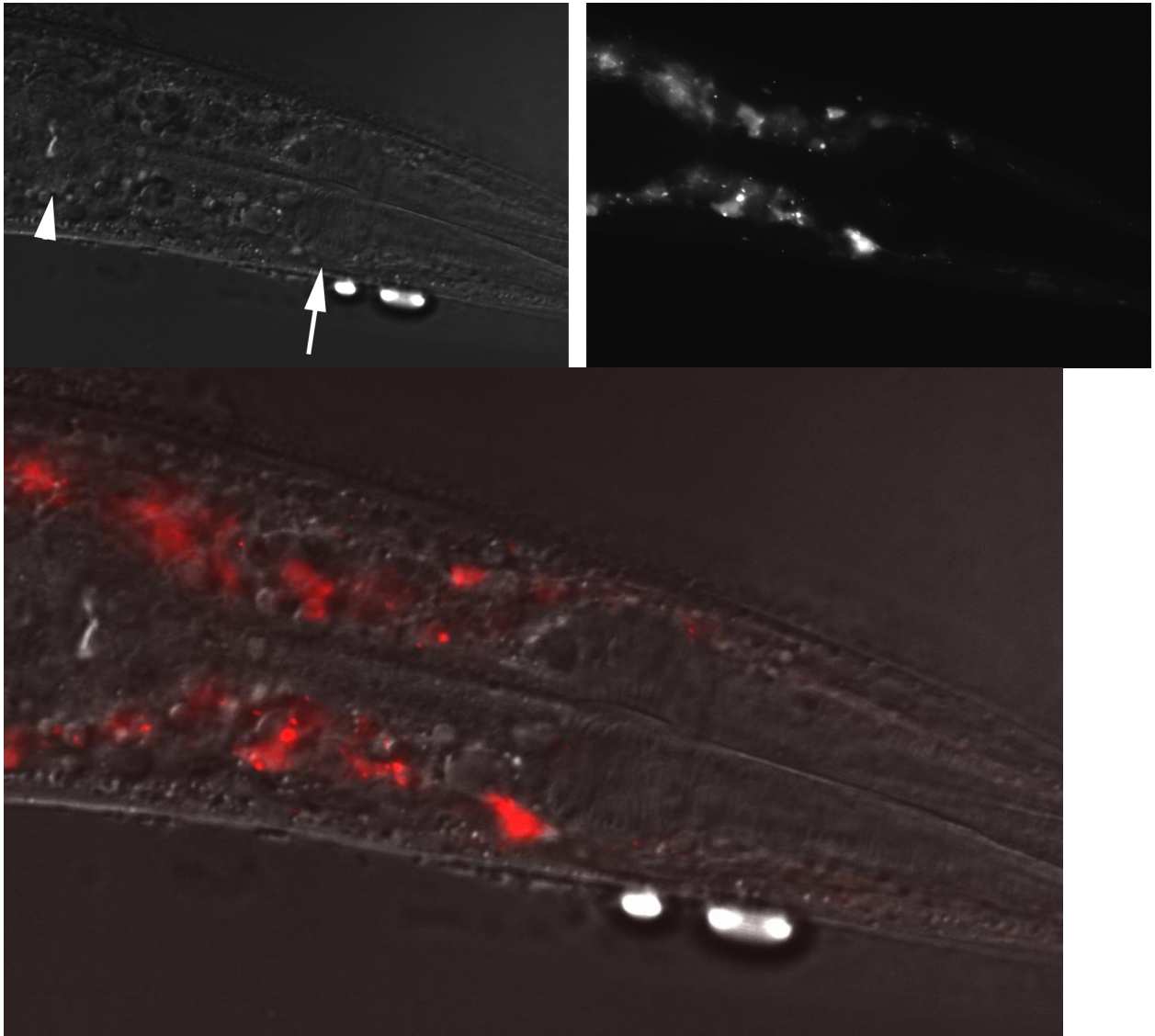


**Figure 2.8 (continued): RDE-12 is broadly expressed throughout the worm. A.** Left, *Rde-12* transcriptional fusion. Right, *Rde-12* translational fusion. Anterior is on the left for both images. **B.** RDE-12 is found in cytoplasmic puncta. Top Left, DIC. For orientation, arrow marks the metacarpus of the pharynx, and an arrowhead marks the terminal bulb. Top Right, mCherry expression of the RDE-12::mCherry translational fusion. Bottom, composite. RDE-12::mCherry translational fusions is in red. DIC is in gray.

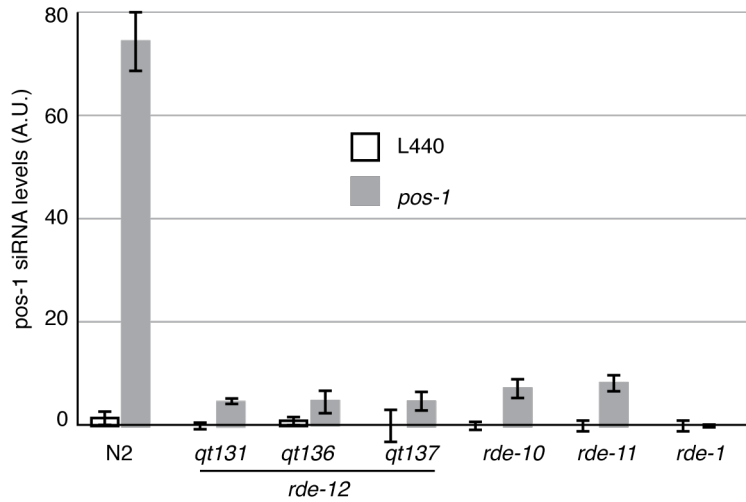


**Figure 2.9. *rde-12* worms are defective for accumulation of *pos-1* secondary siRNAs.** Animals were placed on bacteria expressing *pos-1* dsRNA. *Pos-1* siRNA levels were then assayed by the Fireplex assay. This is data from probe 1 (GATCACCGTATGAGCATGCCT); the other three probes had similar response. Error bars are standard error.

RNAi defective mutants known to affect secondary siRNA levels. It is known that *rde-1* mutants do not produce any secondary siRNAs, whereas *rde-10* and *rde-11* mutants are strongly defective for production of secondary siRNAs. Our control data was consistent with previous results, indicating that the Firefly assay can accurately quantify siRNA levels. Three *rde-12* alleles were tested; all were defective for accumulation of *pos-1* siRNAs, with siRNA levels comparable to that of *rde-10* and *rde-11* (Figure 2.9). Therefore, we conclude that *rde-12* is deficient in accumulation of siRNA. Our data is consistent with the hypothesis, that like *rde-10* and *rde-11*, *rde-12* is defective for the production or accumulation of secondary siRNAs.

**Structure-function analysis:** RDE-12 is a putative DEAD-box RNA helicase. To determine if residues essential for activity in other DEAD-box helicases are essential for RDE-12 activity, we developed a rescue assay. When wild-type worms are placed in the cholinergic agonist levamisole, they hypercontract and paralyze. However, after *unc-22* knock-down, worms have a characteristic twitching phenotype. *rde-12* mutants are resistant to the *unc-22* knock-down induced twitching (Figure 2.5G). However, when we expressed wild-type *rde-12* in the body-wall muscle in *rde-12(qt131)*, we found that this rescued the twitching phenotype. We then attempted to rescue the twitching phenotype with *rde-12* that has a mutation motif I, which is essential for ATP binding (Pause and Sonenberg, 1992; Corbin et al, 2006). We found that this residue, essential for activity in other functional RNA helicases, is essential for RDE-12 activity (Table 1).



**siRNAs are not necessary for silencing of pharynx.** Our original screen was designed to find systemic RNAi mutants, but exclude cell-autonomous RNAi defective mutants. We hypothesized that cell-autonomous RNAi defective mutants would have

| <b>Strain</b>                        | <b>Twitching phenotype</b> |
|--------------------------------------|----------------------------|
| Wild-type                            | +++                        |
| <i>rde-12</i>                        | -                          |
| <i>rde-12</i> Wild-type rescue       | ++                         |
| <i>rde-12</i> A424V rescue (motif I) | -                          |

**Table 2.1.** A conserved motif essential for DEAD-box helicase activity is essential for RDE-12 activity. Rde-12 was rescued with either wild-type or mutated *rde-12*.

**Figure 2.10.**

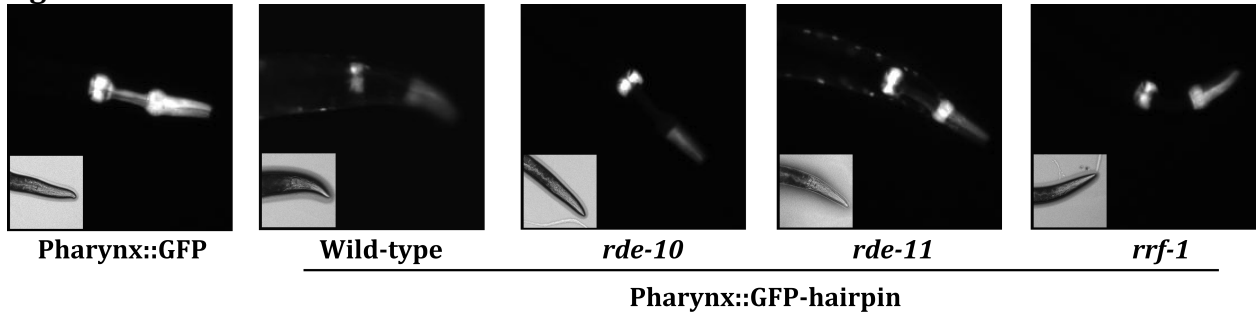


**Figure 2.10. RNAi silencing by primary siRNA in the pharynx.**

Myo-2p::gfp expression is silenced by myo-2p::gfp-pfg hairpin dsRNA in wild-type (N2) and secondary siRNA mutants but not *rde-1* mutants (see Figure 2.10).

unsilenced (i.e., bright green) pharynxes, despite the presence of the *myo-2* driven GFP-hairpin. Indeed, an *rde-1* mutant has a bright green pharynx (Winston, Molodowitch and Hunter, 2002, Figure 2.1). However, *rde-12* has a silenced pharynx but bright body-wall muscle (Figure 2.1).

We hypothesized that in the presence of large amounts of primary siRNA, secondary siRNAs are not required for pharyngeal silencing. To test this hypothesis, we built strains containing expressing both GFP and a GFP-hairpin in the pharynx and either *rrf-1*, which is fully defective for somatic secondary siRNA production or *rde-10*, which has approximately 10% of secondary siRNAs as wild-type (Figure 2.9 and Yang et al., 2012). Both of these strains were able to silence GFP in the pharynx (Figure 2.10). Moreover, we sequenced *rde-10* and *rde-11* in unknown strains identified in a genetic screen for novel systemic RNAi mutants. We isolated a single nonsense allele of *rde-11* (Figure 2.10). Since *rrf-1*, *rde-10* and *rde-11* strains, which can produce primary but cannot efficiently produce secondary siRNAs, can result in pharyngeal silencing, we conclude that secondary siRNAs are not necessary for silencing of the pharynx in the presence of large amounts of silencing signal.

**Discussion:** We have shown that *rde-12* is broadly resistant to exogenous dsRNA. It is not a systemic RNAi mutant, rather, it acts cell-autonomously. RDE-12 activity is required for efficient accumulation of secondary siRNAs, and requires an intact ATPase domain. Finally, it is a dosage-sensitive Rde. Although *rde-12* is initially resistant to *act-5* dsRNA, *rde-12* worms do form a bag-of-worms phenotype (data not shown). Additionally, when a GFP-hairpin is strongly expressed in the

pharynx, secondary siRNAs are not required for silencing. These two data explain why *rde-12* was found in our screen for systemic RNAi export mutants.

To examine RDE-12 more closely, we collaborated with the Mak lab. The Mak lab previously identified RDE-10 and RDE-11, two proteins also required for secondary siRNA accumulation. These proteins both bind mRNA, and are required for secondary siRNA production and mRNA degradation (Yang et al., 2012, Zhang et al., 2012). Our collaborators in the Mak lab found that RDE-12 localizes to cytoplasmic processing bodies (P bodies), cytoplasmic foci where mRNA processing and degradation occur. They also found that RDE-12 binds target mRNA, and this binding requires primary siRNA. While RDE-12 binding to mRNA was dependent on RDE-1, RDE-10 mRNA binding is dependent on RDE-12 (Yang et al., 2014). Additionally, small RNA-sequencing revealed that RDE-12 is essential for accumulation of ERGO-1 siRNAs, a class of endo-siRNAs. Together, our data suggest that RDE-12 binds mRNA in particular foci and facilitates the amplification of secondary siRNAs.

Given its role in the efficient accumulation of secondary siRNAs, and the requirement for an intact ATPase domain (Yang et al., 2014), we hypothesize four different possibilities RDE-12 may play in secondary siRNA accumulation: (1) it may serve as a clamp or scaffold for other proteins to bind to the mRNA being amplified, (2) it may clear away secondary structure of the mRNA being amplified, (3) it may remove siRNA from the mRNA or (4) it may remove proteins (e.g., RRF-1) from the mRNA, making the process more processive. Therefore, further experiments will be necessary to determine the potential substrates of RDE-12. If RDE-12 indeed acts as

a scaffold for other proteins to bind the mRNA, as we hypothesize in Yang et al., 2014, then directly tethering the mRNA to RDE-12, using for example the boxB/N-peptide system, may be sufficient to trigger *rde-1* independent silencing.

## Methods

### Genetic Screen Details

HC57 worms, which express GFP in the pharyngeal muscle and body-wall muscle, as well as a GFP-hairpin in the pharyngeal muscle, were mutagenized with ethyl methane sulfonate. Gravid F1 hermaphrodites were bleached, and F2s were placed onto *unc-45* or *bli-1* feeding RNAi plates. Animals that were alive, (i.e., did not blister) were collected. F3s were then placed onto *E. coli* that express *act-5*, an intestinal target, to enrich for export mutants.

A total of 60,000 genomes were screened, and 116 mutants were found to be resistant to dsRNA targeting *bli-1*. 76 of these mutants were sterile. 35 of the 40 viable strains were confirmed as resistant to *bli-1*, while 5 were found to be sensitive in the second round of *bli-1* dsRNA exposure.

**SNP-Snip Mapping** Mapping was performed as described in Davis et al., 2005.

Briefly, *rde-12 (qt131)* worms were crossed to CB4856 worms. F1 progeny were allowed to self-fertilize, then F2 progeny were singled to *act-5* RNAi plates. Resistant F2 worms were selected and moved individually to new plates and allowed to self fertilized. DNA from F3 and F4 worms was extracted.

### DNA Digestion

Worms were dissolved in worm lysis buffer:

500 uL 1 M KCl

100 uL 1 M Tris pH 8.2 (or 50/50 pH 8, 8.5)

20 uL 1 M MgCl<sub>2</sub>

90 uL Tween-20

100 uL 1% Gelatin

9.1 mL H<sub>2</sub>O

4 uL of proteinase K was added to .5 mL worm lysis buffer. 40 uL of this solution was added to small PCR tubes, then 10-12 worms were added to each tube. This was frozen in liquid nitrogen to break open cuticles, then incubated at 60C for 1 hour, followed by 85C for 5 minutes.

### **PCR**

The following polymerase chain reaction conditions were used:

5 uL Taq Buffer

1 uL R primer

1 uL F primer

5 uL Template (lysed worm in SWL)

1 uL dNTP

1 uL Deb's Taq

36 uL dH<sub>2</sub>O

Cycling conditions:

92 for 2 minutes

34 times:

94C for 15 seconds; 60C for 45 seconds; 72C for 1:00

Then 72C for 10 minutes, and 10C forever.

### **DraI digestion:**

Each digestion was performed as follows:

14.15 uL PCR Product



1.6 uL Cutsmart Buffer

.25 uL DraI

for a volume of 16 uL.

Cut for 2-3 hours at 37C.

### **F58G11.2 Rescue**

F58G11.2 genomic DNA was amplified with the following primers: F58G11.2 F

CCTAATCCTCAATGGCTGAAGTGTG and F58G11.2 R

CGCTGTTCTTGTACTCCCTAGTTG. The resulting 4.9 kb PCR product was injected

along with 10 ng/ul pCFJ104, which expresses myo-3::mCherry, which expresses mCherry in the body-wall muscle.

### **Whole genome sequencing**

**DNA Extraction:** Worms were grown on multiple 6cm NGM plates. To minimize *E. coli* contamination, these plates were allowed to starve out. Worms were washed 2 times with M9 buffer, then incubated at 20C, with shaking, for 30 minutes to clear worm intestines of ingested *E. coli*.

Worms were the lysed in lysis buffer: 200mM NaCl, 100mM Tris-HCl pH 8.5, 50mM EDTA, 0.5% SDS. Proteinase K to 0.1mg/mL.

5 volumes lysis buffer was added to worms; ~500 uL lysis buffer to 100 uL worms. Worms were frozen for 1 hour at -80C, then lysed for 2-3 hours at 60 C. Lysis solution was extracted in 2 volumes phenol/chloroform/isoamyl alcohol (25:24:1). The aqueous solution was removed, and to this 0.1 volume 3M sodium acetate and >2 volumes 100% ethanol was added. DNA was pellet by centrifugation

at 14000rpm for 5min. The supernatant was removed and the pellet was washed with 70% ethanol. The pellet was air dried, then resuspended in TE.

RNA was removed using Riboshredder RNase blend. 1 uL RiboShredder was added per 130 ug nucleic acids and incubated at 37C for 10 minutes.

Phenol/Chloroform extraction followed by ethanol precipitation removed the Riboshredder.

To generate 200 nt fragments, the Covaris S220 sonicator was used. 1 ug total DNA was loaded into 130 uL. We followed the provided 200 base-pair peak guidelines: 10% Duty Factor, 175 Peak Incident Power (W), 200 cycles per burst, 180 total seconds.

To prepare this fragmented DNA for illumina sequencing, we used the NEBNext DNA sequencing kit from New England Biolabs. Briefly, this kit repairs DNA ends, then adaptors are ligated to these ends. Ligated fragments are size selected and cleaned. Then adaptor-ligated DNA is PCR enriched.

**Feeding RNAi.** For GFP RNAi, *E. coli* expressing either dsRNA targeting GFP or control dsRNA (L4440) was fed to L1 animals on agar plates containing 1 mM isopropyl  $\beta$ -D-1-thiogalactopyranoside (Timmons and Fire, 1998).

For *act-5* RNAi, embryos were placed on *E. coli* expressing *act-5* dsRNA, then 3 days later, the fraction of animals reaching adulthood was scored. For GFP RNAi, worms were placed on *E. coli* expressing *GFP* dsRNA, then 3 days later, animals were imaged then blindly scored for silencing. All feeding RNAi experiments were performed at 20° C. Bacteria engineered to express *gfp* dsRNA were prepared as

described previously (Winston et al., 2003). All other bacteria expressing dsRNA were from the Ahringer library (Kamath and Ahringer, 2003).

**Statistics.** P-values were calculated using the Student's t-test.

**Live Microscopy.** Worms were immobilized for imaging by placing plates on ice for 15-30 minutes. Images being compared in each Figure were taken using the same nonsaturating exposure conditions and processed identically using Adobe Illustrator for display. 8-bit images were taken at 10x magnification at 8-bit using an Olympus SZX2 microscope, a Hamamatsu C8484 camera and HCI Imaging Software.

#### **Pos-1 reverse transcription and qPCR**

RNA was purified and reverse transcribed using random hexamers and Thermoscript RT (Invitrogen). 2 uL of the resulting cDNA (diluted 1:10 in water) was used in a 25 uL QuantiTect SYBR Green (Qiagen) reaction: 25 uL PCR Master Mix, 1.5 uL F Primer (10 uM), 1.5 uL R Primer, 1 uL Template cDNA, 21 uL RNase-free water. The qPCR was performed using an Eppendorf Mastercycler Realplex4 and Noiseband quantification with the following PCR cycle: 15 minutes 95° C, 15 seconds 94° C, 30 seconds 52° C, 30 seconds 72° C, read, cycle to step 2 for 40 cycles. Analysis was performed using the  $\Delta\Delta$ CT method.

Pos-1 qPCR F: CCTCCCATCATCACTAGTTTCTC

Pos-1 qPCR R: GGGACTGCACCAGGTATT

#### **Rde vs Sid assays:**

Adults were placed onto *unc-22* RNAi food, for 24 hours, then moved to OP50, where they either self-fertilized or were crossed to wild-type males, that were not exposed to *unc-22* RNAi. After allowing worms to mate for 24 hours, hermaphrodites were

singled to new plates, and the fraction of self progeny or cross-progeny displaying twitching on 1 mM levamisole was scored.

### **Fireplex Assay**

Here, we introduce and describe the use of the FirePlex assay for the quantification of siRNAs in *C. elegans*. Although the FirePlex assay was originally commercialized for miRNAs, we have found that it can robustly quantify siRNA levels as well. The FirePlex platform utilizes encoded hydrogel particles to perform multiplexed detection of up to 68 targets in each well of a standard 96-well filter plate. Particles bear unique barcodes that correspond to a single target detected on each. The assay is performed in three steps – hybridization, labeling and reporting, with rinses between each step (Fig. 1). During hybridization, targets bind to siRNA-specific DNA probes embedded in the hydrogel particles. Labeling is accomplished via ligation of a biotinylated universal adaptor using the probe as a template. In the final step, a streptavidin-conjugated fluorescent reporter is added to visualize the hybridization event. The assay provides quantitative results, with the level of fluorescence on each particle corresponding to the amount of siRNA target present in the sample. The encoded particles are then scanned in a standard flow cytometer.

We used the FirePlex assay with purified total RNA as the input, though the system may also be applied to crude cell and tissue digests. Samples can be analyzed on-site with a FirePlex kit and a conventional flow cytometer, or alternatively, sent directly to Firefly BioWorks for custom analysis with additional costs. Although the FirePlex assay is considerably simpler than conventional siRNA sequencing, it has important limitations. First, the assay is not a discovery tool – target sequences

must be known and specified. Furthermore, while the FirePlex assay allows examination of up to 68 targets per well, short RNA sequencing provides a comprehensive analysis of all siRNAs in the sample. And last, the FirePlex platform has limited sensitivity; we have been able to detect sequences found at a comparable rate of 150 reads/million in a previously published siRNA sequencing dataset (Table 1) [18]. However, our previous results suggest that the FirePlex assay is likely an order of magnitude more sensitive. Despite these disadvantages, the simplicity and throughput of the FirePlex assay should make it a very attractive tool for researchers. We imagine that the FirePlex assay can be used to quickly screen through various mutants or conditions, with interesting results being followed-up with siRNA sequencing, if necessary.

**Materials required for RNA Extraction and FirePlex Assay:**

1. 1.5 ml Phase-Lock Gel tubes, heavy (Eppendorf)
2. TRIzol Reagent (Life Technologies)
3. PTFE (Polytetrafluoroethylene) Tissue Grinder Douncer, 2 mL, glass vessel and serrated plunger (VWR)
4. Chloroform
5. 5M NaCl: dissolve 29.22 g of NaCl in 80ml of water and fill up to 100 ml. Sterilize by autoclaving or sterile filter. Also available from commercial sources.
6. 20 mg/ml glycogen as a carrier for RNA precipitation. Available form commercial sources.
7. Isopropanol
8. FirePlex kit (Firefly BioWorks, Inc., Cambridge, MA, USA)

9. A standard flow cytometer (established settings exist for Millipore Guava easyCyte 8HT, BD Accuri C6, Millipore Guava easyCyte 6HT, BD LSRFortessa and Life Technologies Attune)

10. Vacuum Manifold for 96-well filter plates (one optimized for FirePlex is available from Firefly BioWorks)

### **RNA Extraction Protocol**

1. Wash several (2-5) 10-centimeter plates of animals into a 15 ml conical centrifuge tube using water (see Note 2). Centrifuge at 11,000 $\times$ g, 1 minute.
2. Wash 3 times with 15 ml water.
3. Discard the final wash. Using a Pasteur pipette, transfer 200-350  $\mu$ l of worms into a 1.5 ml microfuge tube. Freeze at -80°C for one hour.
4. Prepare phase-lock tubes by centrifugation at 11,000 $\times$ g for 1 minute.
5. Add 400  $\mu$ l Trizol to each sample.
6. Vortex samples at room-temperature until the Trizol-worm mixture is a slurry.
7. Transfer the solution into a douncer on ice using a RNase-free glass pasteur pipette.
8. Dounce slurry with a twisting motion 20 times on ice. Between samples clean with RNase-Out and DEPC-treated water or use a new douncer (see Note 3).
9. Transfer the lysed worms to a phase-lock tube.
10. Add 80  $\mu$ l chloroform, mix by inversion for 1 minute and incubate at room-temperature for 5 minutes.

11. Centrifuge at 15,000 x *g* for 15 minutes at 4°C.
12. Transfer the top aqueous layer to a siliconized 1.5 mL microfuge tube.
13. Add, in this order, 50 µl of 5M NaCl, 2.5 µl of 20 mg/ml glycogen and 800 µl of isopropanol to each tube.
14. Mix by inversion for 1 minute and place at -80°C for 1 hour.
15. Centrifuge at 11,000 x *g* for 15 minutes at 4°C.
16. Remove the supernatant with a pipette.
17. Wash with 500 µl of ice-cold 100% ethanol.
18. Spin at 11,000 x *g* at 4°C for 1 minute.
19. Remove the supernatant and let remaining ethanol evaporate for about 5 minutes at room temperature. Do not allow the pellet to dry out completely.
20. Dissolve the RNA pellet in 80 µl of water by vortexing at room temperature.
21. Quantitate the RNA concentration using a Nanodrop or an equivalent spectrophotometer.

At this point, samples can be sent directly to Firefly Bio for commercial analysis.

Alternatively, samples can be processed in house using a standard flow-cytometer.

### **3.2 FirePlex Assay Protocol**

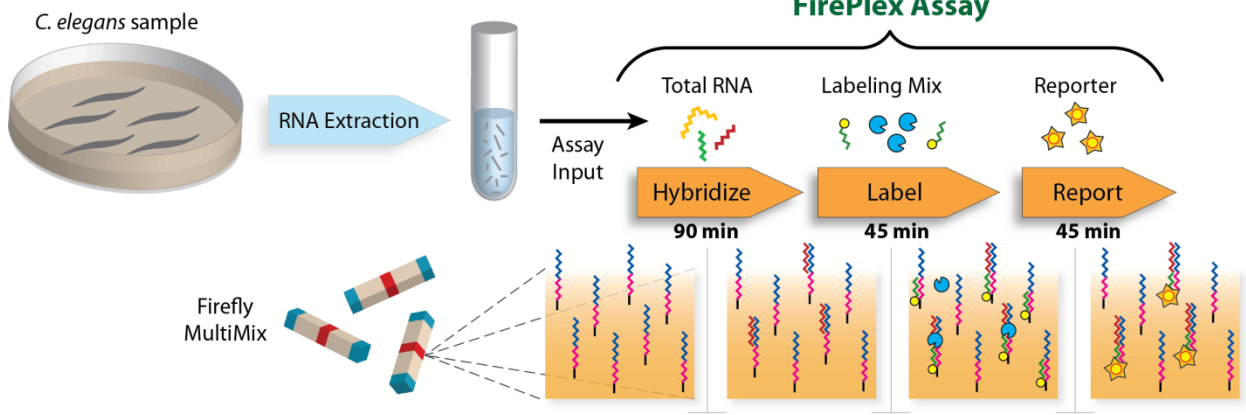
1. Cut the plate seal to expose assay wells on the filter plate required for the experiment (provided in the assay kit- see Note 4).
2. Dilute sample to twice the final concentration, in our hands this would routinely be 200ng/µl (see Note 5).
3. Invert, then vortex MultiMix (provided with the assay) for 3 seconds. Add 35 µl of MultiMix to each well. Mix by pipetting up and down (see Note 6).

4. Vacuum filter the plate, wipe the bottom dry (see Notes 7, 8 and 9).
5. Add 25  $\mu$ l of hybridization buffer to each well, followed by 25  $\mu$ l of sample.
6. Hybridize the plate for 90 minutes at 37 °C shaking at 750 rpm (see Note 10).
7. Near the end of the hybridization step, prepare 1 x rinse buffer by mixing 0.2 ml of 10x Rinse Buffer with 1.8ml of water per assay well. Prepare the Labeling Mix by mixing 78  $\mu$ l of water, 1.6  $\mu$ l of 50 x labeling buffer, and 0.4  $\mu$ l of labeling enzyme per assay well.
8. After hybridization, add 200  $\mu$ l 1 x Rinse Buffer to each well, and vacuum filter the plate.
9. Repeat step 8. Blot dry the bottom rside of the plate.
10. Add 75  $\mu$ l of Labeling Mix to each well and shake at room temperature at 750 rpm for 45 minutes.
11. Prepare the Reporter Mix by mixing 64  $\mu$ l of water with 16  $\mu$ l of 5 x Reporter Solution per each assay well.
12. After Labeling, add 200  $\mu$ l 1 x Rinse Buffer to each well, and vacuum filter the plate.
13. Repeat step 13. Blot dry the bottom side of the plate.
14. Add 75  $\mu$ L Reporter Mix to each well. Shake at room temperature at 750 rpm for 45 minutes. After the incubation, add 200  $\mu$ l 1 x Rinse Buffer to each well and vacuum filter the plate.
15. Repeat step 17. Blot dry the bottom side of the plate.
16. Add 175  $\mu$ l Run Buffer to each well.



17. Apply the correct scan settings for the specific flow-cytometer used  
(provided at <http://www.fireflybio.com/productsupport>).
18. Scan at least 100  $\mu$ l of sample for each well.
19. Save the FCS file for analysis using the FireCode software  
(<http://www.fireflybio.com/productsupport>).

**Figure 2.11**



A schematic of the FirePlex Assay. See text.

## References:

- [1] Guang S, Bochner AF, Pavelec DM, Burkhardt KB, Harding S, Lachowiec J, et al. An Argonaute transports siRNAs from the cytoplasm to the nucleus. *Science* 2008;321:537–41. doi:10.1126/science.1157647.
- [2] McEwan DL, Weisman AS, Hunter CP. Uptake of Extracellular Double-Stranded RNA by SID-2. *Mol Cell* 2012;47:746–54. doi:10.1016/j.molcel.2012.07.014.
- [3] Pak J, Fire A. Distinct populations of primary and secondary effectors during RNAi in *C. elegans*. *Science* 2007;315:241–4. doi:10.1126/science.1132839.
- [4] Shiu PK, Zhuang JJ, Hunter CP. *Animal Endo-SiRNAs* 2014;1173:71–87. doi:10.1007/978-1-4939-0931-5.
- [5] Tabara H, Yigit E, Siomi H, Mello CC. The dsRNA binding protein RDE-4 interacts with RDE-1, DCR-1, and a DExH-Box helicase to direct RNAi in *C. elegans*. *Cell* 2002;109:861–71. doi:10.1016/S0092-8674(02)00793-6.
- [6] Winston WM, Molodowitch C, Hunter CP. Systemic RNAi in *C. elegans* requires the putative transmembrane protein SID-1. *Science* (80- ) 2002;295:2456–9. doi:10.1126/science.1068836 1068836 [pii].
- [7] Winston WM, Sutherlin M, Wright AJ, Feinberg EH, Hunter CP. *Caenorhabditis elegans* SID-2 is required for environmental RNA interference. *Proc Natl Acad Sci U S A* 2007;104:10565–70. doi:0611282104 [pii] 10.1073/pnas.0611282104.
- [8] Yang H, Vallandingham J, Shiu P, Li H, Hunter CP, Mak HY. The DEAD box helicase RDE-12 promotes amplification of RNAi in cytoplasmic foci in *C. Elegans*. *Curr Biol* 2014;24:832–8.
- [9] Yang H, Zhang Y, Vallandingham J, Li H, Li H, Florens L, et al. The RDE-10/RDE-11 complex triggers RNAi-induced mRNA degradation by association with target mRNA in *C. elegans*. *Genes Dev* 2012;26:846–56. doi:10.1101/gad.180679.111.
- [10] Yigit E, Batista PJ, Bei Y, Pang KM, Chen CCG, Tolia NH, et al. Analysis of the *C. elegans* Argonaute Family Reveals that Distinct Argonautes Act Sequentially during RNAi. *Cell* 2006;127:747–57. doi:10.1016/j.cell.2006.09.033.
- [11] Zhang C, Montgomery TA, Fischer SEJ, Garcia SMDA, Riedel CG, Fahlgren N, et al. The *Caenorhabditis elegans* RDE-10/RDE-11 complex regulates RNAi by promoting secondary siRNA amplification. *Curr Biol* 2012;22:881–90. doi:10.1016/j.cub.2012.04.011.

- [12] Zhuang JJ, Hunter CP. RNA interference in *Caenorhabditis elegans*: uptake, mechanism, and regulation. *Parasitology* 2012;139:560–73.

### **Chapter 3: Early developmental exposure to dsRNA is critical for initiating efficient nuclear RNAi in *C. elegans***

#### **Summary**

RNA interference (RNAi) has enabled researchers to study the function of many genes. However, it is not understood why some RNAi experiments succeed, while others do not. Here, we show in *C. elegans* that pharyngeal muscle is resistant to RNAi when initially exposed to dsRNA by feeding, but sensitive to RNAi in the next generation. Investigating this observation, we find that pharyngeal muscle cells as well as vulval muscle cells require nuclear rather than cytoplasmic RNAi. Further, we find in both these cell types that nuclear RNAi silencing is most efficiently triggered during early development, defining a critical period for initiating nuclear RNAi.

## Introduction

RNA interference (RNAi) is a phenomenon in which double-stranded RNA (dsRNA) triggers silencing of cognate genes (Fire et al., 1998). RNAi is a particularly powerful research tool for studying the nematode *C. elegans* because simply feeding worms bacteria engineered to express gene-specific dsRNA can trigger RNAi, a process known as environmental RNAi (eRNAi) (Timmons and Fire, 1998). In *C. elegans*, RNAi silencing is associated with both cytoplasmic and nuclear RNAi pathways (Yigit et al., 2006, Guang et al., 2008).

Cytoplasmic and nuclear silencing processes share upstream dsRNA processing activities, but use divergent silencing effectors. In the common steps, cytoplasmic dsRNA is cleaved by the Dicer complex into short (~22 nucleotide) interfering RNA (siRNA) that bind to the Argonaute (Ago) protein RDE-1, which removes the passenger strand, resulting in a single-stranded primary siRNA that guides the RDE-1 complex to a complementary mRNA (Tabara et al., 1999, Tabara et al., 2002, Parrish and Fire, 2001, Steiner et al., 2009). The mRNA bound RDE-1 complex recruits an RNA-dependent RNA polymerase (e.g., RRF-1) which uses the mRNA as a template to synthesize abundant anti-sense secondary siRNAs (Sijen et al., 2001). In cytoplasmic RNAi silencing, these secondary siRNAs then bind to numerous secondary Argonautes that act redundantly to degrade siRNA targeted mRNA. Quadrupal mutation of the cytoplasmic argonautes *sago-1*, *sago-2*, *ppw-1* and *wago-4* causes strong defects in exogenous RNAi (Yigit et al., 2006). In nuclear RNAi silencing, secondary siRNAs bind the non-redundant Argonautes NRDE-3 and HRDE-1, which act, respectively in the soma and germline. NRDE-3 shuttles

secondary siRNA into the nucleus where it complexes with other nuclear RNAi components, including NRDE-2 (Guang et al., 2008). This siRNA complex binds to nascent transcripts complementary to the siRNA to impede RNA polymerase elongation, and subsequently recruits histone methyltransferases to the silenced locus (Tabara et al., 1999). It is assumed that the cytoplasmic (PTGS) and nuclear (TGS) pathways function in parallel to efficiently repress gene expression.

Interestingly, nuclear RNAi is considerably more potent in the F1 progeny than in the P0 worms that were initially exposed to dsRNA (Burton et al., 2011, Zhuang et al., 2013). For example, the phenotype of *dpy-11* RNAi is much stronger in the F1 progeny than in the P0 generation, and deposition of H3K9 methylation at the *dpy-11* locus is also much higher in the F1 generation than the P0 generation (Burton et al., 2011). However, why nuclear RNAi is more potent in the second-generation remains unknown. One explanation is that germline transmission of silencing signals potentiates silencing ability. For example, it has been proposed that germline transmission might “mark” the locus to be silenced or that a particular siRNA silencing species may be created as a result of germline transmission (Burton et al., 2011).

In addition to the differences in RNAi efficiency between the germline and the soma, particular somatic tissues have different sensitivities to exogenous dsRNA. For example, neurons are generally resistant to RNAi, possibly because they lack the dsRNA uptake channel, SID-1 (Calixto et al., 2010). Indeed, overexpressing SID-1 in neurons enhances neuronal RNAi. Additional tissue-specific enhanced RNAi (Eri) phenotypes in response to particular Eri mutants (e.g., *rrf-3* vs. *eri-1*) have been

described, indicating that differing activity levels of endogenous small RNA metabolism genes compete to varying degrees with exogenous RNAi (Zhuang and Hunter, 2011). Finally, some groups have reported strikingly different silencing results for the same gene in the same tissue. For example, multiple groups have reported that the pharynx is resistant to RNAi (Kumsta and Hansen, 2012, Ashe et al., 2015), while others report success in knocking down gene expression in the pharynx (Horner et al., 1998, Winston et al., 2002). Understanding the differences in RNAi efficiency between different RNAi protocols and between different tissues in *C. elegans* may eventually shed light on the endogenous role of RNAi in *C. elegans*. Furthermore, understanding the differences in RNAi efficiency between tissues is essential for *C. elegans* researchers using RNAi as an experimental tool.

In this chapter, I examined the sensitivity of pharyngeal muscle cells to exogenous RNAi. I found that feeding RNAi fails to silence GFP expression in pharyngeal muscle of worms in the P0 generation but efficiently silences GFP expression in their progeny. The silencing in the progeny requires nuclear RNAi, but contrary to expectations, maternal RNAi activity is not required for silencing. Specifically, I used a heat-shock inducible promoter to express dsRNA at particular developmental time points, identifying a critical early developmental period for nuclear RNAi: earlier exposure to dsRNA results in stronger silencing in pharyngeal muscle cells. Furthermore, I found that vulval muscle cells are also dependent on nuclear RNAi for silencing and this silencing also has a critical period.

## **Results**

### **Pharyngeal muscle is resistant to exogenous dsRNA by feeding**



It has been reported that the pharynx is strongly resistant to eRNAi (Kumsta and Hansen, 2012, Ashe et al., 2015, Devanapally et al., 2015). To confirm these observations, we exposed worms expressing GFP in the pharyngeal and body-wall muscle to feeding RNAi targeting GFP. We found that pharyngeal muscle cells are indeed resistant to eRNAi (Figure 3.1A, 1B). Embryos hatched and grown to adulthood on GFP RNAi food displayed dim body-wall muscle, indicating that eRNAi was effective (Figure 3.1A, middle panel), but bright pharyngeal muscle, confirming that pharyngeal muscle cells are not responsive to eRNAi.

Although our results are consistent with previous reports that pharyngeal muscle is resistant to RNAi, other researchers have reported effective RNAi in the pharynx (Horner et al., 1998, Winston et al., 2002). Interestingly, when we examined the F1 progeny of worms fed bacteria expressing GFP dsRNA, these worms had dim pharyngeal muscle (Figure 3.1A, 1C). To avoid confusion with the term “heritable RNAi”, which is increasingly associated with *hrde-1*-dependent silencing, in this chapter I term this “second-generation RNAi.” Worms initially exposed to ingested dsRNA are worms exposed to “first-generation RNAi.” Thus, pharyngeal muscle cells are sensitive to second-generation RNAi, but not to first-generation RNAi. The pharyngeal muscle’s particular resistance to first-generation RNAi might arise if the pharyngeal muscle is competent at particular aspects of the RNAi pathway but not others.

**Figure 3.1**

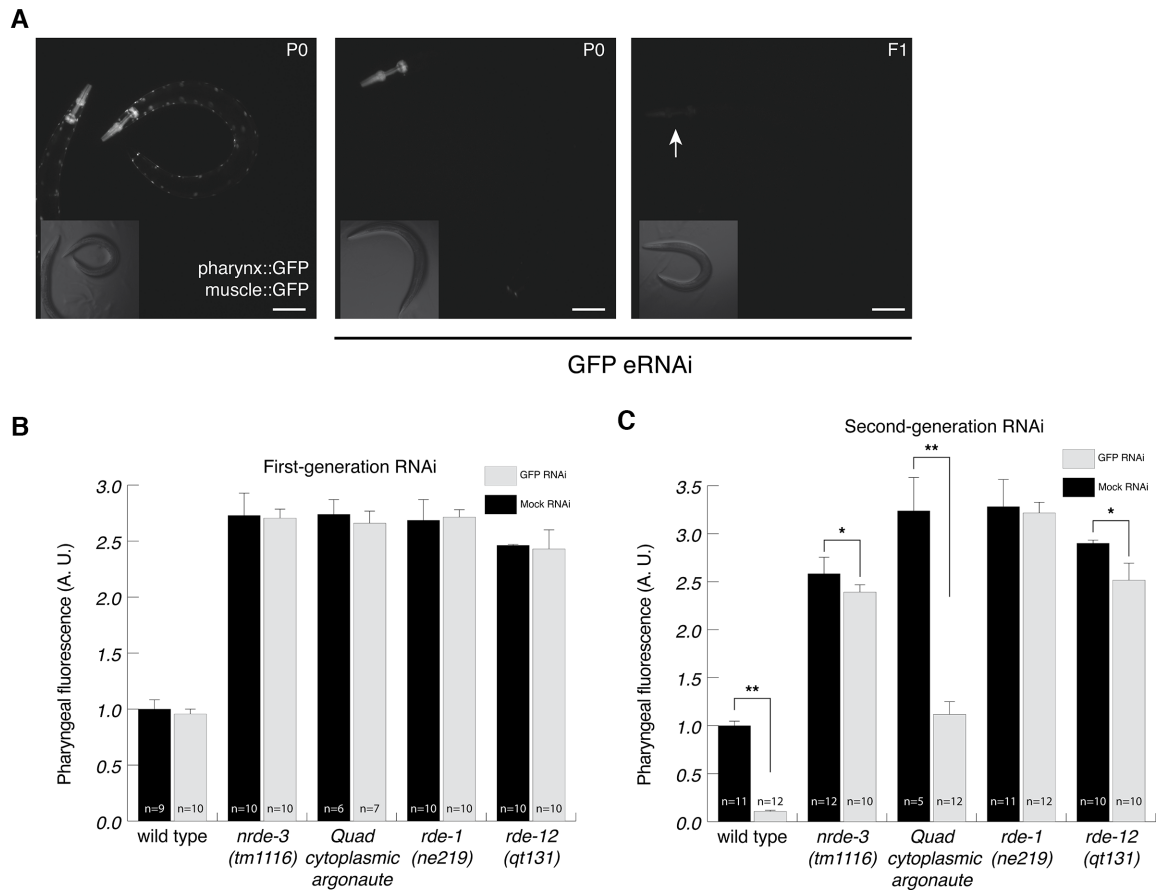


**Figure 3.1. Pharyngeal muscle cells are sensitive to second-generation RNAi and require nuclear RNAi.** (A) The pharyngeal muscle is defective for first-generation RNAi, but competent for second-generation RNAi. Representative photos of worms not exposed to dsRNA (left), an adult grown on GFP RNAi from hatching (first-generation RNAi, middle), and the F1 progeny of worms grown on GFP RNAi (second-generation RNAi, right). Scale bars represent 10  $\mu$ m. (B and C) Quantified fluorescence intensity of pharyngeal muscle following first-generation (B) or second-generation (C) feeding RNAi. Wild type on mock RNAi is defined as 1 arbitrary unit (A. U.). Error bars show standard deviation, n= number of animals scored (\* $p < .05$ , \*\*  $p < .01$ ).

## **Nuclear RNAi is required for second-generation pharyngeal silencing**

Distinct genes act in diverse RNAi pathways. To test the role of specific RNAi components in first- and second-generation silencing of the pharyngeal muscle, we crossed pharyngeal and body-wall muscle GFP reporters into several RNAi mutants and then placed them onto bacteria expressing GFP dsRNA for one or two generations.

Consistent with the known role of these four genes in transgene silencing (Yigit et al., 2006, Grishok et al., 2005, Fischer et al., 2013, Yang et al., 2014, Shirayama et al., 2014, Shiu et al., 2014), expression of the GFP reporter was significantly enhanced in all four mutants, but in no mutant was significant pharyngeal silencing in the first-generation observed (Figure 3.1B). RDE-1, an Argonaute essential for primary siRNA maturation (Steiner et al., 2009, Sijen et al., 2001), is required for second-generation pharyngeal muscle silencing (Figure 3.1C). Likewise, RDE-12, which acts downstream of primary siRNA production, and is required for secondary siRNA amplification (Yang et al., 2014, Shirayama et al., 2014, Shiu et al., 2014), is required for strong second-generation pharyngeal muscle silencing. However, consistent with our previous report that *rde-12* is dosage-sensitive (Yang et al., 2014), there was some statistically significant *rde-12*-independent silencing (Fig 3.1C).

Downstream of primary and secondary siRNA production are two parallel silencing pathways: nuclear and cytoplasmic RNAi. Cytoplasmic RNAi, which acts in parallel to nuclear RNAi, uses multiple redundant worm-specific Ago proteins to silence gene expression. Although a quadruple cytoplasmic Ago mutant [*sago-1*

(*tm1195*), *sago-2 (tm894)*, *ppw-1(tm914)*, *wago-4(tm1019)*] was, as expected, completely resistant to strong RNAi foods targeting *act-5* (Figure 3.2) and *unc-22* (Yigit et al., 2006), we found that it was sensitive to second-generation RNAi in the pharyngeal muscle (Figure 3.1C). However, as reported previously (Yigit et al., 2006), this strain is not fully resistant to eRNAi, as GFP is silenced in body-wall muscle cells (Table 3.1). This RNAi sensitivity likely represents either other muscle-expressed cytoplasmic Ago proteins and or compensating nuclear RNAi. Nuclear RNAi requires NRDE-3, an Ago protein that shuttles siRNA into the nucleus. We found that, although *nrde-3* is not required for second-generation RNAi in body-wall muscle cells (Table 3.1), it is required for second-generation RNAi in the pharyngeal muscle (Figure 3.1C). Similar to *rde-12*, there was some statistically significant *nrde-3* independent silencing (Fig 3.1C). These observations suggest that, in the absence of compensating cytoplasmic silencing, nuclear silencing is required for pharyngeal RNAi. Further, it is likely that the requirement for second-generation RNAi to effectively silence gene expression in pharyngeal muscle cells reflects this dependence on nuclear RNAi.

**Table 3.1**

| Genotype                           | First-generation RNAi |                            |                     | Second-generation RNAi |                            |
|------------------------------------|-----------------------|----------------------------|---------------------|------------------------|----------------------------|
|                                    | <b>pha-4 RNAi</b>     | <b>pharyngeal GFP RNAi</b> | <b>BWM GFP RNAi</b> | <b>pha-4 RNAi</b>      | <b>pharyngeal GFP RNAi</b> |
| N2                                 | -                     | -                          | +                   | ++                     | +                          |
| <i>sid-1</i>                       | -                     | -                          | -                   | -                      | -                          |
| <i>rde-1</i>                       | -                     | -                          | -                   | -                      | -                          |
| <i>rrf-1</i>                       | -                     | -                          | NT                  | ++                     | -                          |
| <i>rde-12</i>                      | -                     | -                          | +/-                 | -                      | -                          |
| MAGO (four cytoplasmic argonautes) | -                     | -                          | +                   | -                      | +                          |
| <i>hrde-1</i>                      | -                     | NT                         | NT                  | ++                     | NT                         |
| <i>nrde-2</i>                      | -                     | NT                         | NT                  | -                      | NT                         |
| <i>nrde-3</i>                      | -                     | -                          | +*                  | -                      | -                          |
| <i>rrf-3</i>                       | +/-                   | NT                         | NT                  | ++                     | NT                         |
| <i>eri-1</i>                       | -                     | +/-                        | NT                  | ++                     | +                          |
| <i>lin-15ab</i>                    | +                     | +                          | NT                  | ++                     | +                          |
| <i>lin-35</i>                      | +                     | NT                         | NT                  | ++                     | NT                         |
| <i>lin-35, nrde-2</i>              | -                     | NT                         | NT                  | -                      | NT                         |
| Maternal <i>sid-1(-)</i>           | NA                    | NA                         | NA                  | NT                     | -                          |

**Table 3.1. Summary of sensitivity of various RNAi mutants to feeding RNAi.**

Embryos were placed on *E. coli* expressing either *pha-4* or *GFP* dsRNA. For *pha-4* RNAi, worms were scored as ++ if arrested prior to L2, + if arrested prior to L4, and +/- if only a fraction of worms arrested prior to L4. See Figures 1 and 5. For body-wall muscle RNAi, +/- represents that worms were only partially silenced. +\* represents that vulval muscle were not silenced, see Figure 4. For maternal *sid-1* tests, *sid-1(qt78)* young adult hermaphrodites were fed GFP dsRNA expressing bacteria and crossed to male wild-type worms with the *myo-2::GFP* array. The cross progeny were reared on OP50 and scored for silencing. NT: Not tested. NA: Not applicable.

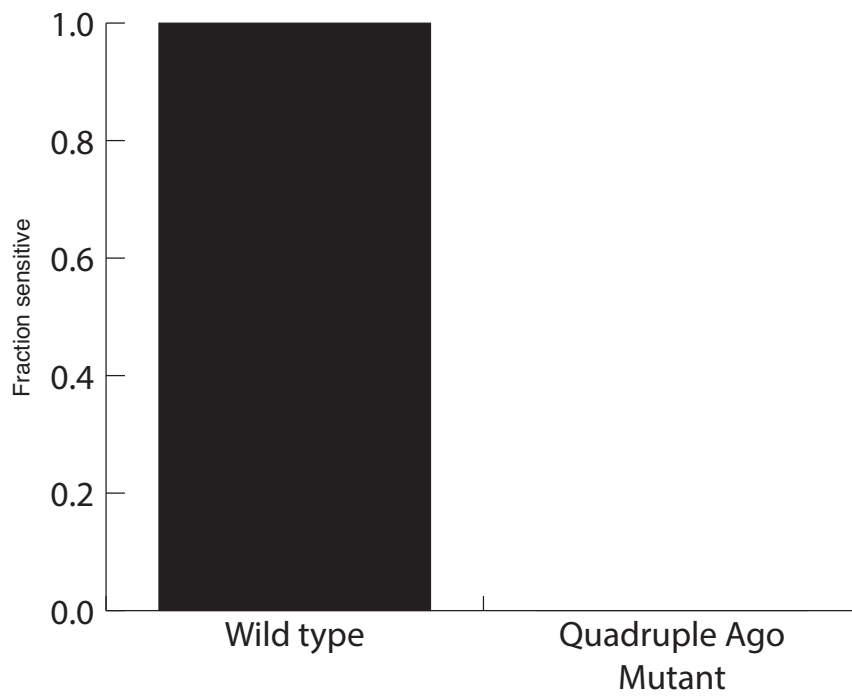


**Figure 3.2. Cytoplasmic argonautes are required for RNAi.** HC1054 [*sago-1(tm1195)*, *sago-2(tm894)*, *ppw-1(tm914)*, *wago-4(tm1019)*] quadruple mutant is resistant to *act-5* feeding RNAi. N=10.



### **Maternal RNAi is not required for second-generation silencing**

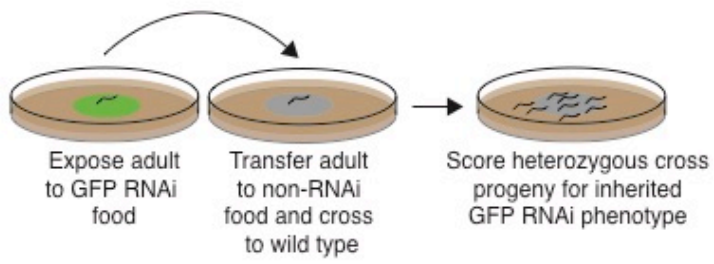
It has been proposed that germline transmission of silencing signals may promote nuclear RNAi [14]. To test this, we exposed mutant or wild-type worms to GFP RNAi food, then crossed these worms to wild-type worms expressing GFP in their pharynx (Figures 3.2, 3.3A). *rde-1(ne219)/+* heterozygous cross progeny had silenced pharynxes, indicating that first-generation RNAi is not required for second-generation RNAi silencing (Figure 3.3B). However, the cross progeny of wild-type worms had more strongly silenced pharynxes. Because abundant secondary siRNA production requires an mRNA template and the GFP transgene is absent from the maternal genome, this *rde-1*-dependent inherited silencing factor cannot be secondary siRNAs. Thus, it is possible that inherited primary siRNA, which may be mobile [8], or maternal *rde-1* gene products, may promote more efficient silencing in progeny (Figure 3B). In contrast to the cross progeny of *rde-1* mutants, the heterozygous cross progeny of *sid-1 (qt78)* worms have bright pharynxes (Figure 3B). *Sid-1* mutants are unable to import dsRNA into the germline [5], thus a requirement for second-generation silencing is maternal deposition of dsRNA to progeny.

### **A critical period for nuclear RNAi**

These results suggest that nuclear RNAi may not require maternal RNAi activity. One difference between first-generation RNAi and second-generation RNAi is that in second-generation RNAi, dsRNA passes through the germline and into the progeny. It has been proposed that this germline transmission of silencing signals may promote nuclear RNAi (Burton et al., 2011), and may possibly even be required for

**Figure 3.3**

A



B

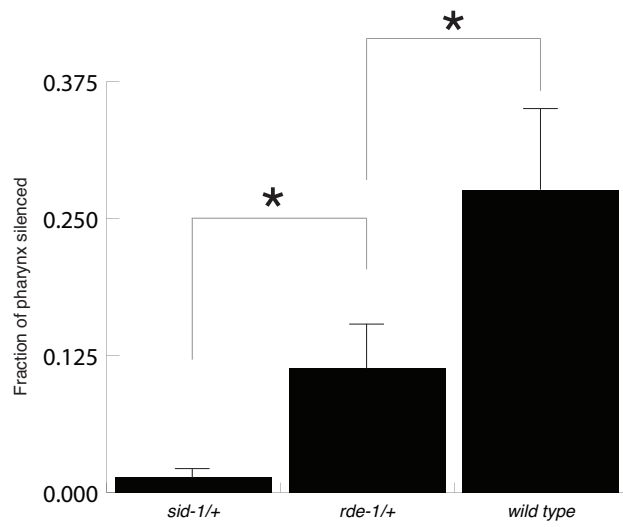


**Figure 3.3 (continued).** Maternal RNAi is not required for pharyngeal RNAi in their progeny. (A) Schematic of the experiment. (B) Mutant or wild-type embryos were placed on bacteria expressing GFP dsRNA, transferred at adulthood to control bacteria and crossed to *myo-2::GFP* males. Cross progeny were scored for pharyngeal GFP silencing as adults. (\*P<.05). Bars show SEM (N=14 to 26).

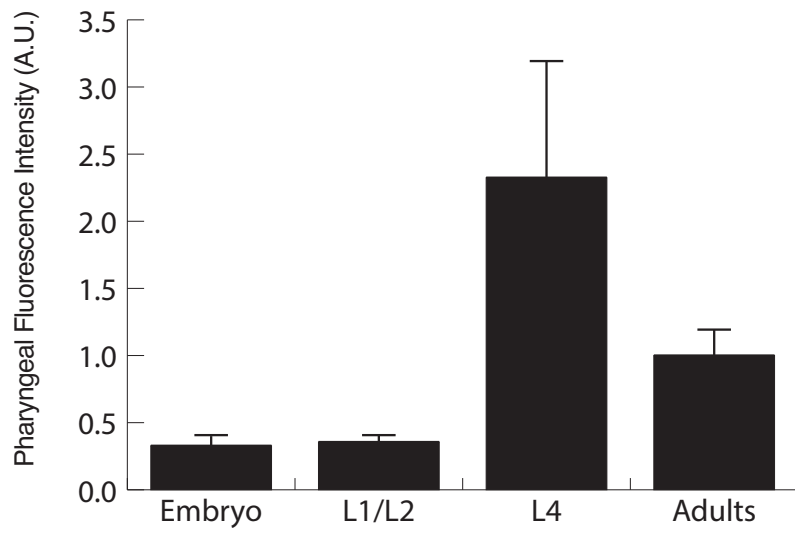
silencing. Alternatively, it is possible that because we cannot feed embryos dsRNA before they hatch, that nuclear RNAi may simply require early, pre-hatching, exposure to dsRNA and/or siRNAs to establish silencing. To distinguish between these possibilities, we used a heat-shock inducible promoter, *hsp-16.2*, to induce GFP dsRNA at different developmental time-points. The *hsp-16.2* promoter is active in a variety of tissues, including the pharynx (Stringham et al., 1992, Fire et al., 1990).

To test the suitability of using the *hsp-16.2* promoter to drive GFP-hairpin expression at successive developmental times, we first measured pharyngeal muscle GFP fluorescence intensity from a *hsp-16.2::GFP* construct 24 hours after heat-shock. We found that the promoter is activated at all tested developmental time points, but more GFP fluorescence is detected in the pharynx and in non-pharyngeal tissues of late larvae and adults than in young larvae (Figure 3.4A; and data not shown). Although it is difficult to compare promoter activity between young larvae and adult worms, because of changes in volume and/or translation efficiency, we note that the significantly higher pharyngeal fluorescence intensity in older worms suggests that it is very unlikely that the *hsp-16.2* promoter is more active in young worms than L4 larvae or adults.

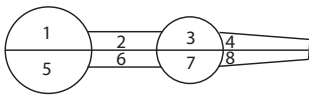
We first obtained synchronized populations of *hsp-16.2p::gfp-hp; myo-2p::gfp* worms at successive developmental time points, then heat-shocked these worms. These worms were then returned to 20C for two days and then scored for GFP silencing by counting the fraction of their pharyngeal muscle that lacked GFP expression (Figure 3.4C).

**Figure 3.4**

**A**



**B**



**C**

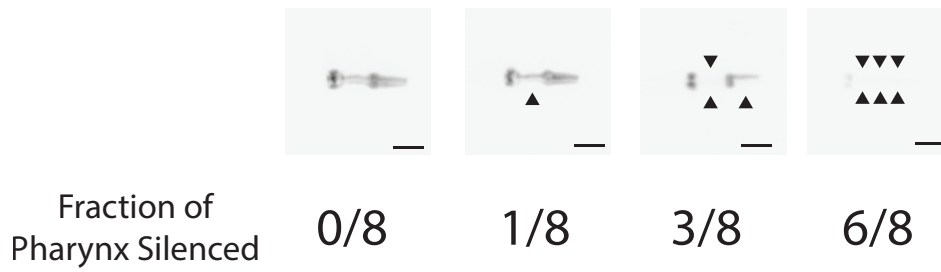


**Figure 3.4 (continued). Heat-shock promoter expression in the pharynx and scoring GFP silencing in the pharynx.** A) The hsp-16.2 promoter is not more strongly expressed in the pharynx of young worms. Pharyngeal GFP fluorescence intensity 24 hours post heat-shock in *hsp-16.2::GFP* worms at different stages. Error bars represent standard deviation; n=19-22 animals per developmental stage. B) To score pharyngeal silencing, the pharynx was divided into eight sections. C) The number of strongly silenced sections, out of eight, was determined. Arrowheads point to silenced sections. Scoring was done blind to the identity of the worm. Scale bars represent 5  $\mu$ m.

If maternally produced and deposited silencing signals are strictly required for pharyngeal muscle silencing, then we expect no silencing, since we are examining heat-shocked worms themselves, rather than their progeny. In contrast, the critical period hypothesis posits that earlier exposure to dsRNA should lead to stronger silencing than later silencing. Our data is consistent with the hypothesis that there is an early critical period for nuclear RNAi. Heat-shock induced GFP dsRNA expression in embryos, directly after they were laid, generated the strongest silencing (Figure 3.5A). The response to heat-shock induced GFP dsRNA expression decreased as the worms aged; the older the worms were at the time of heat shock-induced GFP dsRNA expression, the less the pharyngeal muscle was silenced. Indeed, induction of GFP dsRNA expression after the L3 stage caused virtually no silencing (Figure 3.5A). Additionally, this data confirms that a maternal contribution is not required for pharyngeal silencing.

An alternate explanation for the above result is that GFP protein is unusually stable in the adult pharyngeal muscle. Therefore, we used reverse transcription quantitative PCR to directly measure GFP mRNA levels following heat-shock induced GFP dsRNA expression. We compared GFP mRNA levels between heat-shocked worms with and without the *hsp-16.2p::GFP* dsRNA array 48 hours post-heat shock. We note that presence of the GFP dsRNA array, similar to RNAi mutants, caused de-silencing of *myo-2::GFP*, possibly due to titration of silencing factors. We found that GFP mRNA levels were strongly reduced by heat-shock induced GFP dsRNA expression in embryos (Figure 3.6). However, consistent with measured GFP fluorescent intensity, inducing GFP dsRNA expression in L4 worms did not result in

**Figure 3.5**

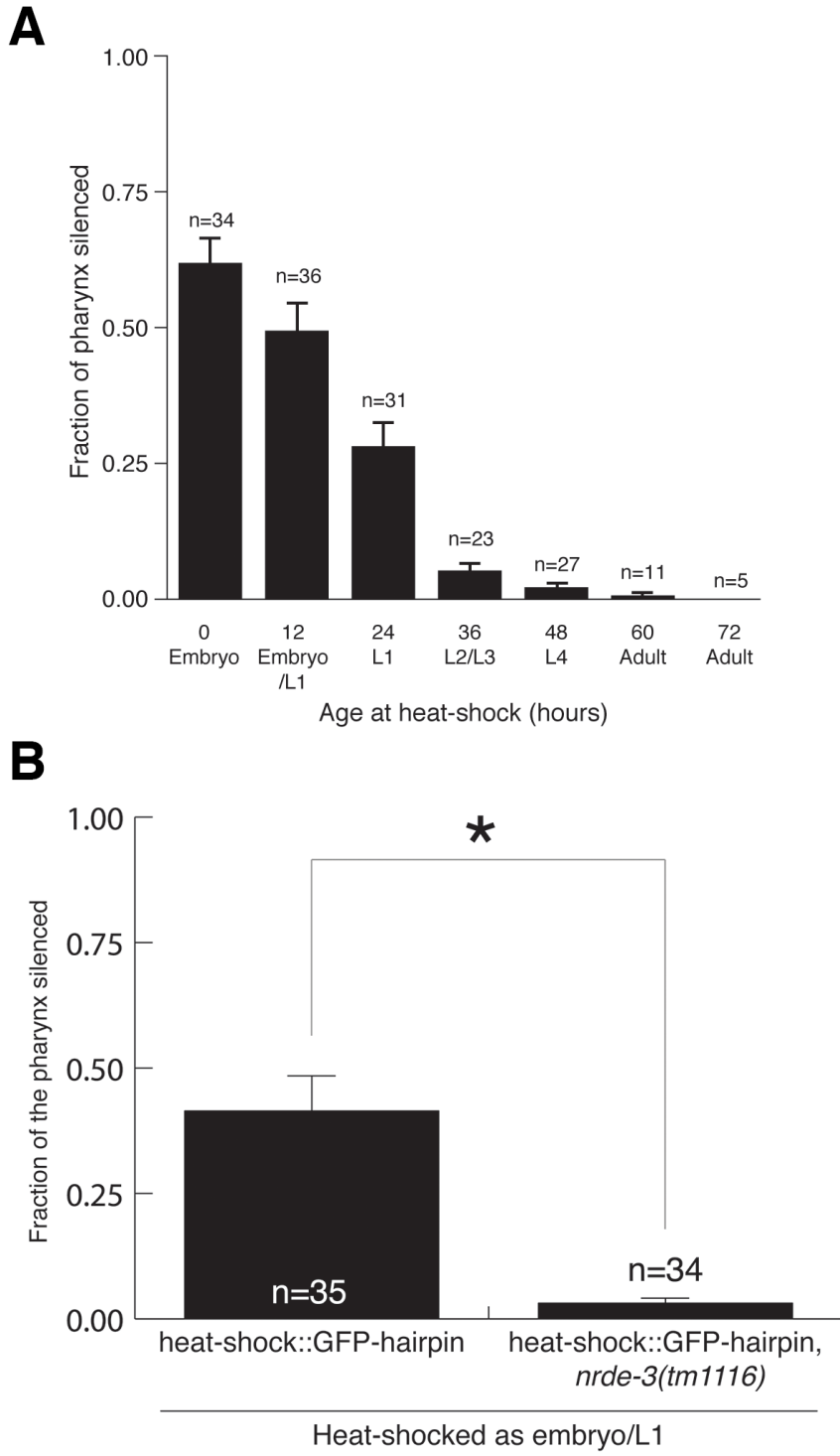




**Figure 3.5 (continued). A critical period for nuclear RNAi.** (A) Earlier dsRNA exposure results in stronger pharyngeal silencing. Bars show SEM, n = number of animals scored. (B) Pharyngeal RNAi by heat-shock-induced GFP dsRNA requires *nrde-3*-dependent nuclear RNAi. Bars show SEM from three trials ( $P < .05$ ). (A and B) Silencing of individual sections of the pharyngeal muscle was scored.

**Figure 3.6**

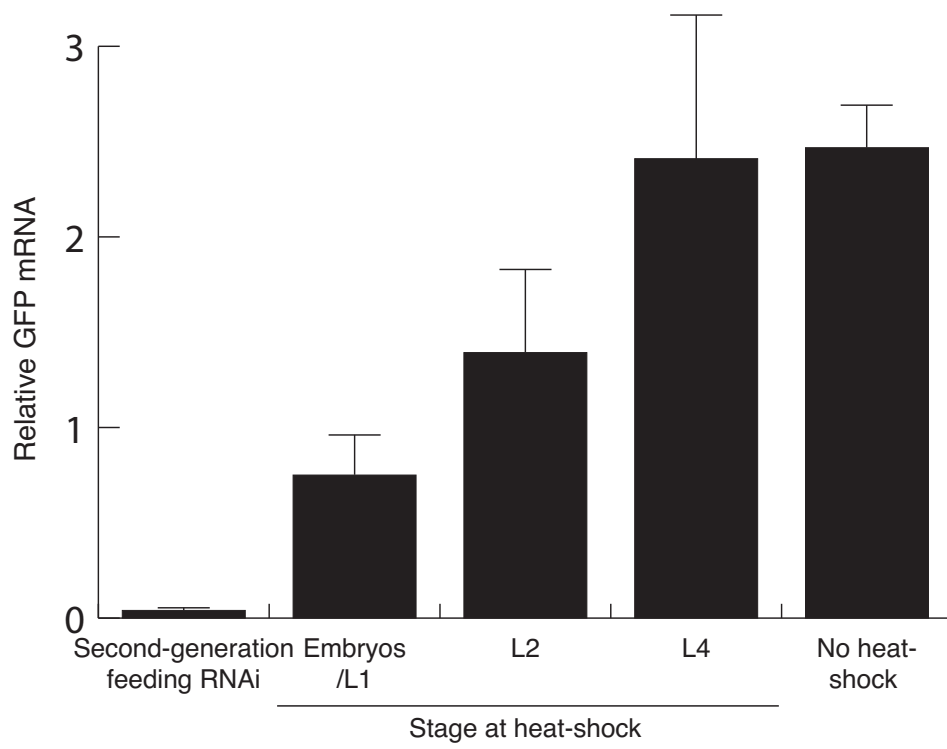
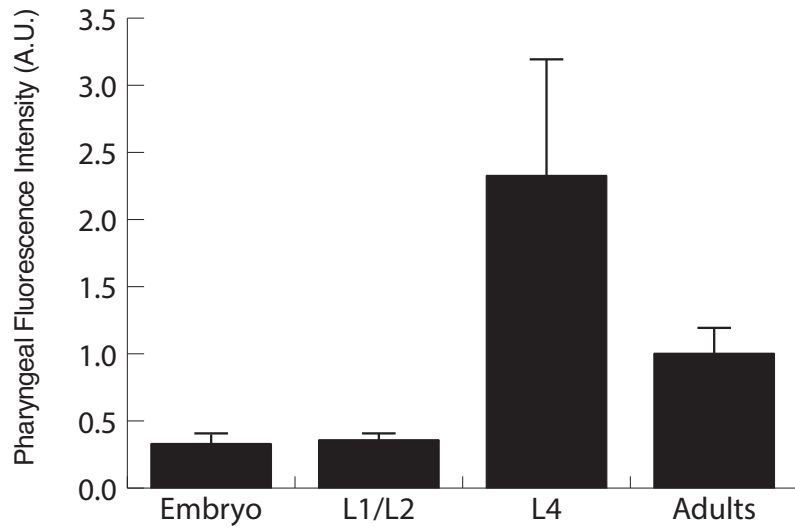


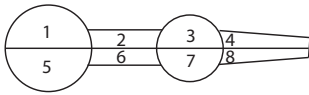
**Figure 3.6 GFP mRNA is reduced when embryos are induced to express GFP dsRNA, but not when older worms are.** Worms were either fed GFP dsRNA for two generations, or heat-shocked at the indicated times. For feeding RNAi, worms were normalized to animals treated with mock RNAi, while the heat-shock experiments, heat-shocked animals with the *hsp-16.2::GFP* dsRNA array were normalized to worms lacking the array. RNA levels were measured 48 hours after GFP dsRNA induction. N=5-11. Bars represent SEM.

**Figure 3.7**

A



B



C

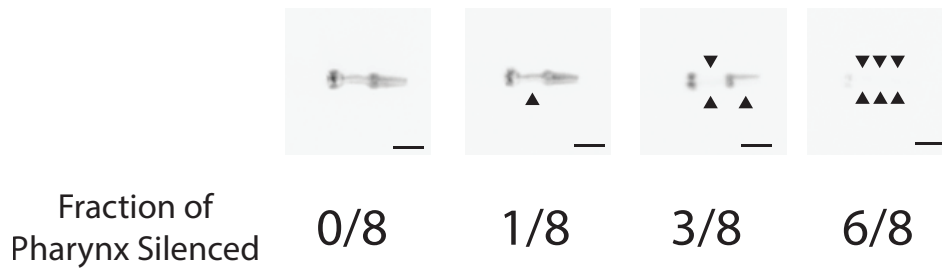


**Figure 3.7 (continued). Heat-shock promoter expression in the pharynx and scoring GFP silencing in the pharynx.** A) The *hsp-16.2* promoter is not more strongly expressed in the pharynx of young worms. Pharyngeal GFP fluorescence intensity 24 hours post heat-shock in *hsp-16.2::GFP* worms at different stages. Error bars represent standard deviation; n=19-22 animals per developmental stage. B) To score pharyngeal silencing, the pharynx was divided into eight sections. C) The number of strongly silenced sections, out of eight, was determined. Arrowheads point to silenced sections. Scoring was done blind to the identity of the worm. Scale bars represent 5  $\mu$ m.

a decrease in GFP mRNA (Figure 3.6). Thus, the observed critical window is the result of differences in stage-specific RNAi efficiency, not GFP stability. Finally, the reduced silencing observed at later developmental times is not due to poor *hsp-16.2* promoter activity at these times; this promoter is actually more active within the pharynx and other tissues in older worms than young worms (Figure 3.7). Together, these results support the hypothesis that early exposure to dsRNA more readily initiates RNAi than later exposure to dsRNA.

Nuclear RNAi is required to silence pharyngeal GFP in response to second-generation feeding RNAi. To determine whether nuclear RNAi is also required for pharyngeal silencing from heat-shock induced GFP dsRNA, we tested *nrde-3(tm1116)* worms in this assay. In contrast to wild type, induction of GFP dsRNA via heat-shock did not result in pharyngeal silencing in *nrde-3(tm1116)* embryos and L1 larvae (Figure 3.6B). Thus, we propose that for effective nuclear RNAi in the pharyngeal muscle, dsRNA must be delivered before or during a critical period, corresponding to embryonic and early larval development.

We initially examined pharyngeal muscle expression from an integrated transgenic array, *mIs11[myo-2p::GFP + pes-10p::GFP + F22B7.9p::GFP]*. Complex transgenic arrays are often silenced by RNAi (e.g., Figure 3.1B). To determine if our results held for non-array transgenes, we repeated our experiments with a single-copy integrated *myo-2::GFP* transgene (Norris et al., 2015, and see experimental procedures). We found that, like the multi-copy array, the single-copy insertion is resistant to first-generation silencing, sensitive to second-generation silencing, and that this silencing depends, at least in part, on *nrde-3* (Figure 3.8A). Furthermore,

**Figure 3.8**

**A.**

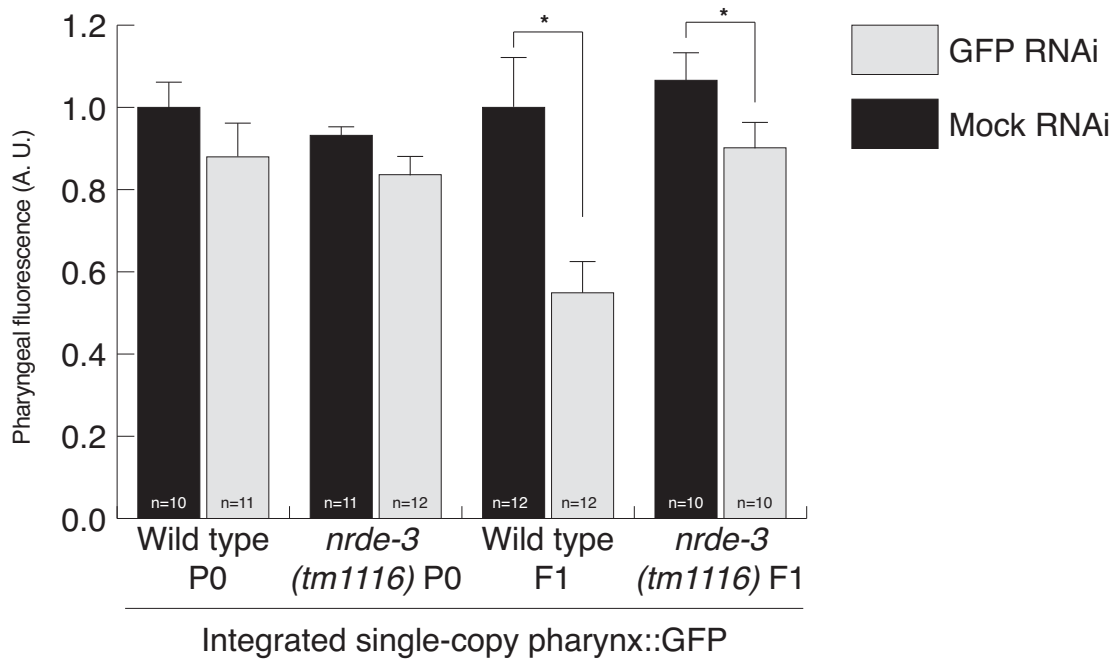
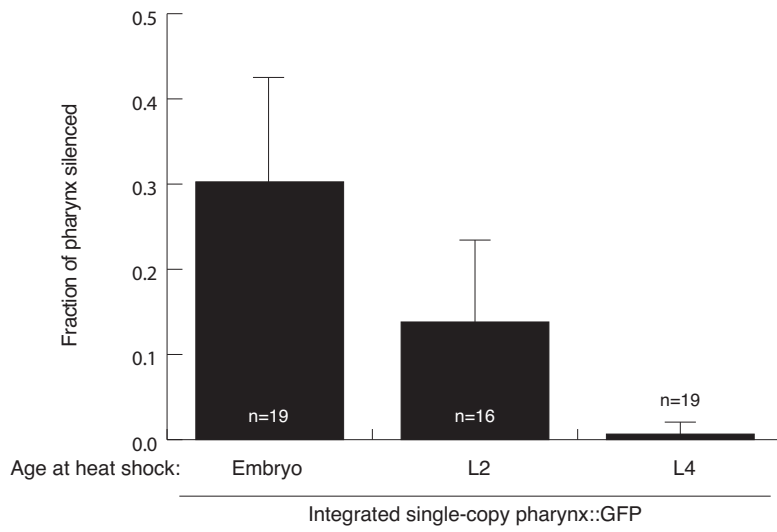


**Figure 3.8, continued**  
**B.**



**C.**

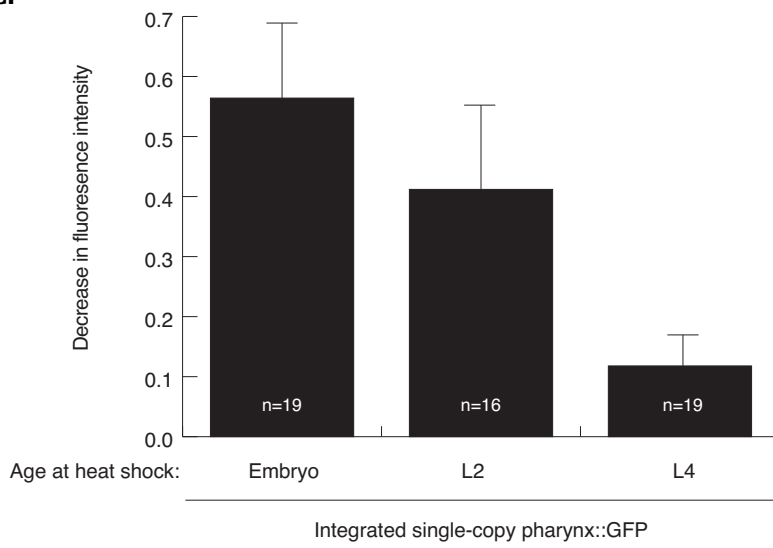




**Figure 3.8. Silencing of a single-copy *myo-2::GFP* insertion is also *nrde-3* dependent and has a critical period.** A) Silencing of a single-copy *myo-2::GFP* insertion by feeding RNAi either in the first or second generation, normalized to wild type fluorescence intensity on mock RNAi. B) Fraction of pharyngeal muscle silenced, as scored in figure S2C. C) Decrease in fluorescence intensity, compared to an age-matched, heat-shocked worm lacking the GFP-hairpin. Error bars represent s.d., n = animals scored.

we found that early exposure to dsRNA by heat-shock generates stronger silencing than late exposure (Figure 3.8B and 3.8C). These results eliminate complications arising from the structure or nature of the complex multi-copy array as being responsible for the critical period and dependence on *nrde-3*.

### **A critical period in vulval muscle silencing**

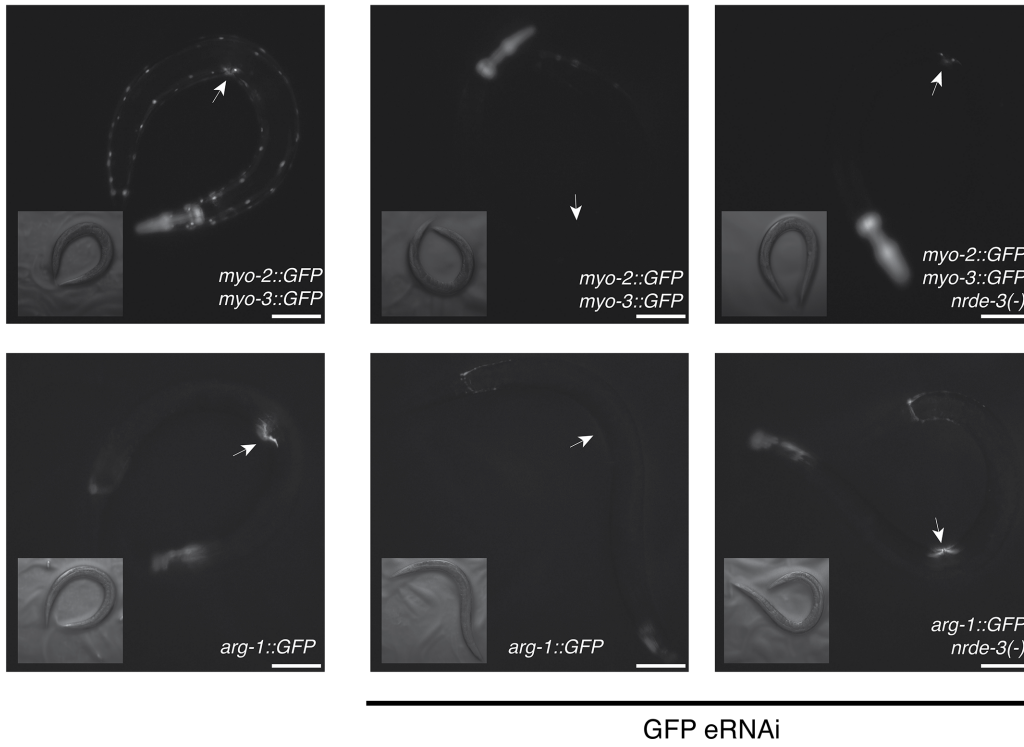
While examining the efficiency of GFP silencing in the body-wall muscle using a *myo-3::GFP* transgene, we noticed that strong silencing in the vulval muscle was dependent on *nrde-3* (Table 3.1, Figure 3.9A, B). When exposed to first-generation GFP feeding RNAi 90% of wild-type animals had silenced vulval muscle cells, while no *nrde-3 (tm1116)* animals had silenced vulval muscle cells (Figure 3.9B). To study this further, we examined a second GFP transgene, *arg-1::GFP*, which expresses GFP in the vm1 and vm2 vulval muscle cells as well as the head mesodermal cell and four enteric muscles (Kostas and Fire, 2002). We found that silencing of this *arg-1::GFP* transgene in vulval muscle cells also was dependent on *nrde-3* (Figure 3.9A, B).

Although these two transgenes could be silenced in the vulval muscle cells in the first-generation, because their silencing is dependent on *nrde-3* we wondered whether vulval muscle silencing might also have a critical period. To test this, we fed early- and late-staged worms bacteria expressing GFP dsRNA for three days and examined silencing in the vulval muscle. Indeed, consistent with the critical period hypothesis, feeding RNAi initiated after the L4 larval stage resulted in little to no silencing (Figure 3.9B, C). In the *myo-3::GFP* array, we used the two body-wall muscle cells directly anterior to the vulval muscle as a convenient internal control

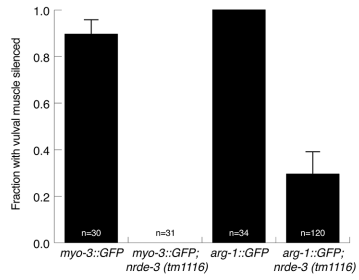
(Figure 3.9B), demonstrating that this defect in silencing is particular to the vulval muscle cells, which specifically require *nrde-3* for silencing.

**Figure 3.9**

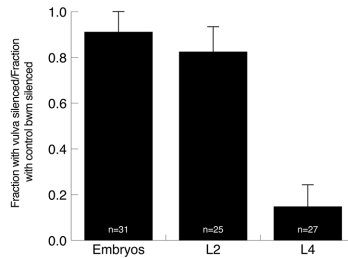
**A**



**B**



**C**



**D**

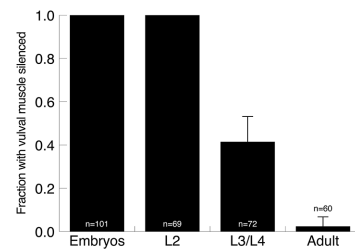


**Figure 3.9 (continued).** Vulval muscle cell silencing requires nuclear RNAi and has a critical period. (A) *myo-3::GFP* (top) and *arg-1::GFP* (bottom) are expressed in vulval muscle cells (left panels), are silenced by first-generation feeding RNAi (middle panels), which requires nuclear RNAi (right panels). Arrow points to the vulva. Scale bars represent 10  $\mu\text{m}$ . (B) Vulval muscle cell silencing requires nuclear RNAi. (C and D) A critical period for vulval muscle cell silencing. In (C), two body-wall muscle cells directly anterior to the vulval muscle cells were used as an internal control for RNAi efficiency. (B-D) n = number of animals scored, bars show standard deviation.

## Discussion

### Pharyngeal RNAi

We hypothesize that for most tissues, cytoplasmic and nuclear RNAi work in parallel and redundantly, enabling efficient RNAi. For example, *rde-1*-dependent body wall muscle cell silencing can occur in the absence of either the cytoplasmic or nuclear pathways (Figure 3.2). In contrast, we found that RNAi silencing in the pharyngeal muscle is dependent on *nrde-3*-dependent nuclear RNAi and may be independent of cytoplasmic Ago-dependent processes (Figure 3.1C). Therefore, one hypothesis to explain the *nrde-3*-dependence of pharyngeal silencing is a lack of redundant cytoplasmic silencing factors in the pharyngeal muscle. Blazie et al. recently performed tissue-specific RNA-Seq in mixed-staged worms comparing gene expression between the pharyngeal muscle, body-wall muscle and intestine (Blazie et al., 2015). When we examined their data, we found that cytoplasmic argonaute mRNAs (*sago-1*, *sago-2*, and *ppw-1*) were detected in the body-wall muscle and intestine samples, but were not detected in the pharyngeal muscle (Table 3.2) (Blazie et al., 2015). The lack of these three cytoplasmic argonautes is known to confer strong resistance to RNAi targeting the body wall muscle expressed *unc-22* gene (Yigit et al., 2006). If the pharyngeal muscle is resistant to eRNAi because it lacks these three cytoplasmic argonautes, then restoring their expression in pharyngeal muscle cells should restore sensitivity to first-generation RNAi. However, co-expressing *sago-1*, *sago-2* and *ppw-1* under the pharyngeal-specific *myo-2* promoter did not enable first generation eRNAi (data not shown), possibly because other cytoplasmic RNAi factors are also not expressed in the pharyngeal muscle.

|                                      | RNA Abundance (FKPM) |                  |                   |
|--------------------------------------|----------------------|------------------|-------------------|
|                                      | Intestine            | Body-wall Muscle | Pharyngeal Muscle |
| <b>Cytoplasmic Argonautes</b>        |                      |                  |                   |
| <i>C04F12.1/vrsa-1</i>               | 0.94                 | 0.23             | 0.06              |
| <i>wago-4</i>                        | 0.09                 | 1.86             | 0.16              |
| <i>ppw-1</i>                         | 3.33                 | 3.15             | <b>0</b>          |
| <i>ppw-2</i>                         | 0.27                 | 0.99             | 0.11              |
| <i>sago-1</i>                        | 6.83                 | 0.36             | <b>0</b>          |
| <i>sago-2</i>                        | 1.8                  | 0.26             | <b>0</b>          |
| <b>Systemic RNAi genes</b>           |                      |                  |                   |
| <i>sid-1</i>                         | 2.09                 | 0.82             | 0.96              |
| <i>sid-2</i>                         | 3.96                 | 0                | 0                 |
| <b>Primary siRNA processing</b>      |                      |                  |                   |
| <i>dcr-1</i>                         | 0.81                 | 0.82             | 0.55              |
| <i>rde-1</i>                         | 1.9                  | 0.94             | 0.39              |
| <b>Secondary siRNA amplification</b> |                      |                  |                   |
| <i>rde-10</i>                        | 0.57                 | 0.62             | 0.54              |
| <i>rde-11</i>                        | 1.77                 | 0.94             | 0.31              |
| <i>rde-12</i>                        | 1.72                 | 1.47             | 0.94              |
| <i>rrf-1</i>                         | 1.15                 | 0.52             | 0.14              |
| <b>Nuclear RNAi pathway</b>          |                      |                  |                   |
| <i>nrde-1</i>                        | 1.08                 | 0.35             | 0.43              |
| <i>nrde-2</i>                        | 1.77                 | 1.39             | 0.88              |
| <i>nrde-3</i>                        | 1.52                 | 0.26             | 0.37              |
| <i>nrde-4</i>                        | 2.79                 | 0.52             | 0.86              |

**Table 3.2. RNA abundance levels of various RNAi-related genes, in FKPM, in the intestine, body-wall muscle and pharynx.** Data is from Blazie et al., 2015.

### **A critical period for nuclear RNAi**

We note that there is a graded temporal response to nuclear RNAi, with early exposure to dsRNA triggering stronger nuclear RNAi. Eventually, exposure to dsRNA is insufficient to trigger efficient silencing, defining a critical period for nuclear RNAi. The observation that nuclear RNAi must be initiated during an early critical period likely explains the lack of first-generation pharyngeal silencing. In first-generation eRNAi exposure of cells to ingested dsRNA is delayed, as the consumed dsRNA must be transported into the intestine, exported from the intestine, and finally imported into the recipient cells. By the time sufficient dsRNA accumulates in the pharyngeal muscle, the critical period has passed. The observation that second-generation eRNAi requires SID-1 activity in the mother (Table 3.1) suggest that maternally acquired dsRNA may be deposited in the embryo. Consequently, silencing can be initiated before the embryo hatches and begins consuming dsRNA itself. Similarly, heat-shock induced dsRNA expression in embryos and early larvae promotes immediate expression and accumulation of abundant dsRNA directly in the pharyngeal muscle cells. The abundance of heat-shocked induced dsRNA may explain the first generation post-embryonic silencing observed in some larvae.

It has been observed that progeny of worms exposed to dsRNA have greater quantities of H3K9 trimethylation marks within the silenced gene than the worms initially exposed to dsRNA (Burton et al., 2011). This suggested that there might be a requirement for germline transmission for efficient nuclear RNAi. Our heat-shock data demonstrates that there is no strict requirement for germline transmission of



silencing signals for efficient nuclear RNAi, however, we cannot rule out the possibility that germline transmission might potentiate silencing. We propose that a critical period determines the strength of nuclear RNAi. By depositing dsRNA and perhaps abundant secondary siRNAs directly in the fertilized embryo, germline transmission of dsRNA allows for early initiation, and therefore, more potent nuclear RNAi.

### **Development, gene silencing and cancer**

Why might nuclear RNAi have a critical period? Nuclear RNAi promotes histone H3K9 and histone H3K27 trimethylation, resulting in transcriptional silencing (Burton et al., 2011, Mao et al., 2015). One possibility is that cell division or development is coupled to nuclear RNAi. As embryos develop, developmental plasticity decreases (Mango, 2009, Meister et al., 2011). The critical period of nuclear RNAi may be related to this phenomenon; limiting histone methylation past a particular time may be useful in maintaining a particular developmental fate.

Consistent with the possibility that development and the critical period are linked is the fact that the critical period for vulval muscle extends later than the critical period for pharyngeal muscle. Although the pharyngeal muscle is resistant to first generation silencing, vulval muscle cells are not. However, by L4 and adulthood, feeding RNAi fails to silence GFP expressed in the vulval muscle cells. Interestingly, the vulval muscle cells are not generated until the L4 stage (Sternberg, 2005), thus, they and their precursors likely must remain developmentally plastic until at least this stage. By contrast, pharyngeal muscle cells are born during

embryogenesis. Thus, we propose that the nuclear RNAi critical period and developmental plasticity may be functionally linked.

### **Tissue-specificity in RNAi**

One remaining question is why particular tissues are more or less sensitive to exogenous dsRNA. It is known that neurons are refractory to eRNAi unless *sid-1* is experimentally overexpressed in them (Calixto et al., 2010). Thus far, the only known role for exogenous RNAi is for defense against viral infection (Schott et al., 2005, Felix et al., 2011). The only virus known to infect *C. elegans* is restricted to infecting the intestine (Franz et al., 2014). Therefore, it is possible that there is no selective pressure to maintain strong exogenous RNAi in the pharyngeal muscle, vulval muscle cells, or in neurons. There may be other roles for eRNAi (Sarkies and Miska, 2013). Identifying the natural substrates of eRNAi may inform an understanding about why particular tissues are differentially sensitive to dsRNA, while an understanding of these sensitivities may help guide that search.

## **Experimental Procedures**

**Feeding RNAi.** For GFP RNAi, *E. coli* expressing either dsRNA targeting GFP or control dsRNA (L4440) was fed to L1 animals on agar plates containing 1 mM isopropyl  $\beta$ -D-1-thiogalactopyranoside (Timmons and Fire, 1998).

For *act-5* RNAi, embryos were placed on *E. coli* expressing *act-5* dsRNA, then 3 days later, the fraction of animals reaching adulthood was scored. For GFP RNAi, worms were placed on *E. coli* expressing *GFP* dsRNA, then 3 days later, animals were imaged then blindly scored for silencing. All feeding RNAi experiments were performed at 20° C. Bacteria engineered to express *gfp* dsRNA were prepared as described previously (Winston et al., 2003). All other bacteria expressing dsRNA were from the Ahringer library (Kamath and Ahringer, 2003).

**Heat-shock.** Adult worms were placed on seeded plates and allowed to lay embryos for approximately 6 or 12 hour time windows and then removed. The collected embryos developed for the specified time at 20C and were then heat-shocked on the growth plates at 34° C for two-hours in an air incubator. Two days post heat-shock, the pharynxes were scored as below for silencing.

**Statistics.** P-values were calculated using the Student's t-test.

**Live Microscopy.** Worms were immobilized for imaging by placing plates on ice for 15-30 minutes. Images being compared in each figure were taken using the same nonsaturating exposure conditions and processed identically using Adobe

Illustrator for display. 8-bit images were taken at 10x magnification at 8-bit using an Olympus SZX2 microscope, a Hamamatsu C8484 camera and HCI Imaging Software.

**Quantification of pharyngeal fluorescence.** The pharyngeal fluorescence was quantified in one of two complementary methods, whole pharynx fluorescence quantification or scoring of individual pharynx sections. In both methods, worms were imaged as above and *mls11* or the single-copy *myo-2::GFP* transgene was the only GFP transgene. In the first method, the fluorescence of the entire pharynx was quantified. Worm images were analyzed with Fiji (an ImageJ distribution) by first tracing the pharynx, measuring the average fluorescence intensity and subtracting the background as performed in Gavet and Pines, 2010.

Because silencing in the pharyngeal muscle is often partial and incremental, we also analyzed silencing of individual sections of the pharyngeal muscle, in which we divided the pharynx into eight sections (Fig 3.4C). Although the pharynx has three-fold rotational symmetry, for convenience of scoring, we divided the pharynx in half corresponding to half of each of the procorpus, metacarpus, isthmus and terminal bulb of the pharynx. The number of each of these sections were scored for strong silencing (Figure 3.4). The genotype of each worm was blinded from the scorer. We note that these two methods result in similar results (Figures 3.8B, 3.8C), while qPCR and scoring of individual sections also are consistent (Figures 3.2A and 3.8).

**Single-copy *myo-2::GFP* transgene.** This single-copy insertion *myo-2::GFP* transgene (Norris et al., 2015) was generated by CRISPR/Cas9 genome editing, and

is inserted at, and disrupts the function of, *F32B4.4*, which encodes a putative RNA binding protein. There is no evidence that *F32B4.4* plays a role in RNAi (Figure 3.8A) and data not shown.

**qPCR.** RNA, collected as in Ly et al., 2005, was treated with Dnase I (Roche) (30° C 20 minutes), heat inactivated (75° C for 10 minutes) and reverse transcribed using random hexamers and Thermoscript RT (Invitrogen). 2 uL of the resulting cDNA (diluted 1:10 in water) was used in a 50 uL QuantiTect SYBR Green (Qiagen) reaction: 25 uL PCR Master Mix, 1.5 uL F Primer (10 uM), 1.5 uL R Primer, 1 uL Template cDNA, 21 uL RNase-free water. The qPCR was performed using an Eppendorf Mastercycler Realplex4 and Noiseband quantification with the following PCR cycle: 15 minutes 95° C, 15 seconds 94° C, 30 seconds 56° C, 35 seconds 72° C, read, cycle to step 2 for 40 cycles. Analysis was performed using the  $\Delta\Delta CT$  method. Primers specific to GFP mRNA, and not the GFP-hairpin were used. GFP mRNA levels was normalized to *act-1* mRNA levels. To calculate the decrease in GFP, heat-shocked worms were normalized to heat-shocked worms lacking the array.

**DNA constructs.** We used pCFJ104 to express mCherry in the body-wall muscle and pCFJ910 to express NeoR, which confers G418 resistance to worms (Frokjaer-Jensen et al., 2014).

To create the *hsp-16.2p::GFP-hairpin* plasmid pHC236, the GFP hairpin was cut out of pPD126.25 using NotI and AgeI. This fragment was inserted into pPD118.26, which had been digested with NotI and BspEI.

**Primers:**

act-1 qPCR F : ACGCCAACACTGTTCTTTCC

act-1 qPCR R: GATGATCTTGATCTTCATGGTTGA

Myo-2 GFP qPCR F: AGCTCCCGAGATCCTATCG

Myo-2 GFP qPCR R: ATTGGGACAACTCCAGTGAAA

## Strains used in this study

| Strain name | Genotype   | Reference             |
|-------------|--|-----------------------|
| N2 Bristol  | Wild type  | Brenner, 1974         |
| HC57        | <i>mIs3[Pmyo2:: gfp-hp RNA]; mIs11[myo-2p::GFP + pes-10p::GFP + gut-promoter::GFP]; ccls4251[(pSAK2) myo-3p::GFP::LacZ::NLS + (pSAK4) myo-3p::mitochondrial GFP + dpy-20(+)]</i> | Winston et al., 2002  |
| HC1050      | <i>mIs11, ccls4251</i>   | This study            |
| HC1051      | <i>rde-1 (ne219); mIs11; ccls4251</i>  | This study            |
| HC1052      | <i>rde-12(qt131); mIs11; ccls4251</i>  | This study            |
| HC1053      | <i>nrde-3 (tm1116); mIs11; ccls4251</i>  | This study            |
| HC1054      | <i>sago-1 (tm1195); sago-2 (tm894); ppw-1(tm914); wago-4(tm1019); mIs11; ccls4251,</i>   | This study            |
| HC1077      | <i>rde-1 (ne219); mIs11;</i>   | This study            |
| HC1078      | <i>rde-12 (qt131); mIs11;</i>  | This study            |
| HC1079      | <i>nrde-3 (tm1116); mIs11;</i>   | This study            |
| HC1095      | <i>sago-1 (tm1195); sago-2 (tm894); ppw-1(tm914); wago-4(tm1019); mIs11;</i>   | This study            |
| HC1055      | <i>qtEx197[hsp-16.2::GFP dsRNA, myo-3::mCherry, NeoR]; mIs11</i>   | This study            |
| HC1056      | <i>qtEx198[hsp-16.2::GFP dsRNA, myo-3::mCherry, NeoR]; mIs11, nrde-3(tm1116)</i>   | This study            |
| HC1057      | <i>qtEx198, mIs11</i>  | This study            |
| PD4443      | <i>ccls4443 [arg-1::GFP + dpy-20(+)]</i>   | Kostas and Fire, 2002 |
| HC1082      | <i>ccls4443; nrde-3(tm1116)</i>  | This study            |
| HC1065      | <i>eri-1 (mg366); qtEx197; mIs11</i>   | This study            |
| HC1066      | <i>lin-15ab (n765), qtEx197, mIs11</i>   | This study            |
| HC1062      | <i>eri-1 (mg366), mIs11, ccls4251</i>  | This study            |
| HC1063      | <i>lin-15ab (n765) mIs11, ccls4251,</i>  | This study            |
| GR1373      | <i>eri-1 (mg366)</i>   | Kennedy et al., 2004  |
| MT8189      | <i>lin-15ab (n765)</i>   | Wang et al., 2005     |
| MT10430     | <i>lin-35 (n745)</i>   | Lu and Horvitz, 1998  |
| HC1068      | <i>lin-35 (n745), nrde-2 (gg91)</i>  | This study            |
| NL2099      | <i>rrf-3(pk1426)</i>   | Simmer et al., 2002   |
| TJ375       | <i>gpIs1[hsp-16.2p::GFP]</i>   | Rea et al., 2005      |
| HC1073      | <i>f32b4.4(-), myo-2p::GFP</i>   | This study            |
| HC1094      | <i>f32b4.4(-), myo-2p::GFP, nrde-3 (tm1116)</i>  | This study            |
| WM27        | <i>rde-1 (ne219)</i>   | Tabara et al., 1999   |
| HC445       | <i>sid-1(qt9)</i>  | Winston et al., 2002  |
| NL2098      | <i>rrf-1(pk1417)</i>   | Sijen et al., 2001    |
| HC820       | <i>rde-12(qt131)</i>   | Yang et al., 2014     |
| FX1200      | <i>hrde-1(tm1200)</i>  | Buckley et al., 2012  |

|       |                             |                    |
|-------|-----------------------------|--------------------|
| YY186 | <hr/> <i>nrde-2(gg91)</i>   | Guang et al., 2010 |
| WM156 | <hr/> <i>nrde-3(tm1116)</i> | Gu et al., 2009    |



## References

- [1] Ashe A, Sarkies P, Le Pen J, Tanguy M, Miska EA. Antiviral RNAi against Orsay virus is neither systemic nor transgenerational in *Caenorhabditis elegans*. *J Virol* 2015;JVI.03664-14. doi:10.1128/JVI.03664-14.
- [2] Blazie SM, Babb C, Wilky H, Rawls A, Park JG, Mangone M. Comparative RNA-Seq analysis reveals pervasive tissue-specific alternative polyadenylation in *Caenorhabditis elegans* intestine and muscles. *BMC Biol* 2015;13. doi:10.1186/s12915-015-0116-6.
- [3] Brenner S. The genetics of *Caenorhabditis elegans*. *Genetics* 1974;77:71–94.
- [4] Buckley B a., Burkhart KB, Gu SG, Spracklin G, Kershner A, Fritz H, et al. A nuclear Argonaute promotes multigenerational epigenetic inheritance and germline immortality. *Nature* 2012;489:447–51. doi:10.1038/nature11352.
- [5] Burton NO, Burkhart KB, Kennedy S. Nuclear RNAi maintains heritable gene silencing in *Caenorhabditis elegans*. *Proc Natl Acad Sci* 2011;108:19683–8. doi:10.1073/pnas.1113310108.
- [6] Calixto A, Chelur D, Topalidou I, Chen X, Chalfie M. Enhanced neuronal RNAi in *C. elegans* using SID-1. *Nat Methods* 2010;7:554–9. doi:10.1038/nmeth.1463.
- [7] Felix MA, Ashe A, Piffaretti J, Wu G, Nuez I, Belicard T, et al. Natural and experimental infection of *Caenorhabditis* nematodes by novel viruses related to nodaviruses. *PLoS Biol* 2011;9:e1000586. doi:10.1371/journal.pbio.1000586.
- [8] Fire A, Harrison SW, Dixon D. A modular set of lacZ fusion vectors for studying gene expression in *Caenorhabditis elegans*. *Gene* 1990;93:189–98.
- [9] Franz CJ, Renshaw H, Frezal L, Jiang Y, Félix M-A, Wang D. Orsay, Santeuil and Le Blanc viruses primarily infect intestinal cells in *Caenorhabditis* nematodes. *Virology* 2014;448:255–64. doi:10.1016/j.virol.2013.09.024.
- [10] Frokjaer-Jensen C, Davis MW, Sarov M, Taylor J, Flibotte S, LaBella M, et al. Random and targeted transgene insertion in *C. elegans* using a modified Mos1 transposon. *Nat Methods* 2014;11:529–34. doi:10.1038/nmeth.2889.Random.
- [11] Guang S, Bochner AF, Pavelec DM, Burkhart KB, Harding S, Lachowiec J, et al. An Argonaute transports siRNAs from the cytoplasm to the nucleus. *Science* 2008;321:537–41. doi:10.1126/science.1157647.

- [12] Jose AM, Garcia GA, Hunter CP. Two classes of silencing RNAs move between *Caenorhabditis elegans* tissues. *Nat Struct Mol Biol* 2011;18:1184–8. doi:10.1038/nsmb.2134.
- [13] Kennedy S, Wang D, Ruvkun G. A conserved siRNA-degrading RNase negatively regulates RNA interference in *C. elegans*. *Nature* 2004;427:645–9. doi:10.1038/nature02302.
- [14] Kostas SA, Fire A. The T-box factor MLS-1 acts as a molecular switch during specification of nonstriated muscle in *C. elegans*. *Genes Dev* 2002;16:257–69. doi:10.1101/gad.923102.
- [15] Kumsta C, Hansen M. *C. elegans* rrf-1 Mutations Maintain RNAi Efficiency in the Soma in Addition to the Germline. *PLoS One* 2012;7:e35428. doi:10.1371/journal.pone.0035428.
- [16] Ly K, Reid SJ, Snell RG. Rapid RNA analysis of individual *Caenorhabditis elegans*. *MethodsX* 2015;2:59–63. doi:10.1016/j.mex.2015.02.002.
- [17] Mao H, Zhu C, Zong D, Weng C, Yang X, Huang H, et al. The Nrde Pathway Mediates Small-RNA-Directed Histone H3 Lysine 27 Trimethylation in *Caenorhabditis elegans*. *Curr Biol* 2015;25:2398–403. doi:10.1016/j.cub.2015.07.051.
- [18] Norris AD, Kim HM, Colaiácovo MP, Calarco JA. Efficient genome editing in *caenorhabditis elegans* with a toolkit of dual-marker selection cassettes. *Genetics* 2015;201:449–58. doi:10.1534/genetics.115.180679.
- [19] Rea SL, Wu D, Cypser JR, Vaupel JW, Johnson TE. A stress-sensitive reporter predicts longevity in isogenic populations of *Caenorhabditis elegans*. *Nat Genet* 2005;37:894–8. doi:10.1038/ng1608.
- [20] Sarkies P, Miska E a. Is there social RNA? *Science* (80- ) 2013;341:467–8. doi:10.1126/science.1243175.
- [21] Schott DH, Cureton DK, Whelan SP, Hunter CP. An antiviral role for the RNA interference machinery in *Caenorhabditis elegans*. *Proc Natl Acad Sci U S A* 2005;102:18420–4. doi:0507123102 [pii] 10.1073/pnas.0507123102.
- [22] Shirayama M, Stanney W, Gu W, Seth M, Mello CC. The Vasa homolog RDE-12 engages target mRNA and multiple argonaute proteins to promote RNAi in *C. elegans*. *Curr Biol* 2014;24:845–51. doi:10.1016/j.cub.2014.03.008.
- [23] Sijen T, Fleenor J, Simmer F, Thijssen KL, Parrish S, Timmons L, et al. On the role of RNA amplification in dsRNA-triggered gene silencing. *Cell* 2001;107:465–76. doi:10.1016/S0092-8674(01)00576-1.

- [24] Stringham EG, Dixon DK, Jones D, Candido EP. Temporal and spatial expression patterns of the small heat shock (hsp16) genes in transgenic *Caenorhabditis elegans*. *Mol Biol Cell* 1992;3:221–33. doi:10.1016/0169-328X(92)90206-Q.
- [25] Tabara H, Sarkissian M, Kelly WG, Fleenor J, Grishok A, Timmons L, et al. The *rde-1* gene, RNA interference, and transposon silencing in *C. elegans*. *Cell* 1999;99:123–32. doi:10.1016/S0092-8674(00)81644-X.
- [26] Tabara H, Yigit E, Siomi H, Mello CC. The dsRNA binding protein RDE-4 interacts with RDE-1, DCR-1, and a DExH-Box helicase to direct RNAi in *C. elegans*. *Cell* 2002;109:861–71. doi:10.1016/S0092-8674(02)00793-6.
- [27] Timmons L, Fire a. Specific interference by ingested dsRNA. *Nature* 1998;395:854. doi:10.1038/27579.
- [28] Winston WM, Molodowitch C, Hunter CP. Systemic RNAi in *C. elegans* requires the putative transmembrane protein SID-1. *Science* (80- ) 2002;295:2456–9. doi:10.1126/science.1068836 1068836 [pii].
- [29] Yang H, Vallandingham J, Shiu P, Li H, Hunter CP, Mak HY. The DEAD box helicase RDE-12 promotes amplification of RNAi in cytoplasmic foci in *C. Elegans*. *Curr Biol* 2014;24:832–8.
- [30] Yigit E, Batista PJ, Bei Y, Pang KM, Chen CCG, Tolia NH, et al. Analysis of the *C. elegans* Argonaute Family Reveals that Distinct Argonautes Act Sequentially during RNAi. *Cell* 2006;127:747–57. doi:10.1016/j.cell.2006.09.033.
- [31] Zhang C, Montgomery T a., Fischer SEJ, Garcia SMD a, Riedel CG, Fahlgren N, et al. The *Caenorhabditis elegans* RDE-10/RDE-11 complex regulates RNAi by promoting secondary siRNA amplification. *Curr Biol* 2012;22:881–90. doi:10.1016/j.cub.2012.04.011.
- [32] Zhuang JJ, Banse S a., Hunter CP. The nuclear Argonaute NRDE-3 contributes to transitive RNAi in *Caenorhabditis elegans*. *Genetics* 2013;194:117–31. doi:10.1534/genetics.113.149765.

## Chapter 4: SynMuv B Enhanced RNAi requires nuclear RNAi

### Abstract

Loss of the Rb homolog *lin-35*, along with other proteins in the synthetic multivulvae Class B (SynMuv B) pathway, causes enhanced RNAi. However, the mechanism of this enhanced RNAi is not known. One model posits that in synMuv B mutants, RNAi germline enriched genes are misexpressed in the soma, causing the Eri phenotype. In contrast to this model, we show that identified misexpressed germline genes are dispensable for *lin-35* enhanced RNAi. We also show that loss of Rb pathway genes lengthens the critical period for nuclear RNAi silencing and that the Eri phenotype of Rb pathway mutants depends on nuclear RNAi. Finally, we demonstrate that local chromatin may play a role in nuclear RNAi silencing efficiency. We propose that loss of Rb pathway genes may enhance RNAi by lengthening the critical period through a mechanism that may involve changes to local chromatin.

## Introduction

Although RNAi in *C. elegans* is highly efficient, compared to other species, loss of several classes of genes can make exogenous RNAi even more effective. Many enhanced RNAi (Eri) genes encode proteins required for endogenous siRNA production, suggesting that that endogenous siRNA biogenesis competes with exogenous siRNA biogenesis (Simmer et al., 2002, Kennedy et al., 2004, Duchaine et al., 2006, Zhuang et al., 2013). For example, loss of *eri-1* or *rrf-3* results in depletion of a particular class of endo-siRNAs, and enhanced sensitivity to exogenous RNAi.

In contrast to these mutants that have a clear role in endogenous siRNA production is the Rb pathway class of enhanced RNAi mutants. These genes code for transcriptional regulators and chromatin modifying enzymes with no obvious role in endogenous siRNA production. For example, *lin-35* is the worm homolog of the tumor suppressor Rb. Rb is a “pocket protein” transcriptional repressor with many functions, the best characterized of which is its role in promoting cell-cycle exit by inhibiting E2F transcription factors and repression of expression of other cell-cycle genes (Dick and Rubin, 2013).

Other genes in the synthetic multivulvae Class B genes display enhanced RNAi. These genes were originally found in screens for genes that cause a multivulva phenotype in combination with mutations in SynMuv Class A genes. SynMuv B genes that cause enhanced RNAi include *lin-15b*, a DNA binding protein, and *hpl-2*, a gene encoding a HP-1 (heterochromatin protein) homolog that binds H3K9 and H3K27 trimethylated histones (Wang et al., 2005).

One hypothesis for the Eri phenotype of Rb pathway mutants postulates that the Eri phenotype arises due to a transformation of the soma into germline (Wang et al., 2005). In *lin-15b* and other synMuv B mutants, germline genes are misexpressed in the soma. Interestingly, RNAi in the germline is thought to be significantly more potent than RNAi in the soma; for example, transgenes are often silenced by RNAi dependent silencing factors in the germline, but expressed in the soma. In *lin-15b* mutants transgenes are also silenced in the soma. In particular, Wu et al examined microarray analysis of *lin-35* mutants and hypothesized that misexpression of three germline RNAi genes, C04F12.1/*vsra-1* (which encodes a cytoplasmic Argonaute), *sago-2* (which encodes a cytoplasmic argonaute), *rrf-2* (encoding a RNA-dependent RNA polymerase) may account for the enhanced RNAi phenotype of *lin-35* mutants.

In contrast to the model of Wu et al., we show that these three genes are dispensable for *lin-35* enhanced RNAi. Here we show that Eri mutants, including those in the synMuv B class, extend the critical period for pharyngeal muscle silencing. Additionally, we show that synMuv B enhanced RNAi depends on nuclear RNAi. Furthermore, we find that different insertions of a single copy of *myo-2::GFP* are silenced to varying degrees, indicating that local chromatin may affect nuclear RNAi silencing efficiency. Because nuclear RNAi is most efficient early in development, and different loci are differentially sensitive to nuclear RNAi, our results suggest the possibility of an unexpected link between development, chromatin and nuclear RNAi in *C. elegans*.

## Results

### **Enhanced RNAi in *lin-35* mutants does not depend on *sago-2*, *rrf-2* or *C04F12.1***

Wu et al postulate that the Eri phenotype of SynMuv B class mutants arises due to misexpression of three genes, *sago-2*, *rrf-2* and *C04F12.1*. If this model is correct, than loss of these genes in a *lin-35* mutant should decrease the enhanced RNAi phenotype. However, we find that loss of these three genes does not decrease the fraction of worms sensitive to *lir-1* RNAi (Figure 4.1). Thus, we conclude that misexpression model of Wu et al does not fully explain the Eri phenotype of SynMuv B mutants.

### **Enhanced RNAi mutants extend the pharyngeal critical period**

Enhanced RNAi (Eri) mutants are thought to reflect greater sensitivity to low dsRNA concentrations. However, given the temporal constraints revealed by our discovery of a critical period to induce nuclear RNAi silencing in pharyngeal muscle cells, we hypothesized that Eri mutants may also act to broaden the critical period. To test this hypothesis, we crossed our *hsp::GFP dsRNA* construct, described in chapter 3, into *eri-1* and *lin-15ab* mutants. ERI-1 is required to produce endogenous primary siRNAs that act in the Ergo and Ago-3/4 RNAi pathways (Duchaine et al., 2006, Gabel and Ruvkun 2008, Han et al., 2009). The resulting secondary siRNAs are thought to compete with exogenous secondary siRNAs for limiting RNAi machinery, including secondary cytoplasmic and nuclear Argonautes (Gabel and Ruvkun, 2008). In contrast, loss of *lin-15b* or *lin-35*, and other members of the

**Figure 4.1**

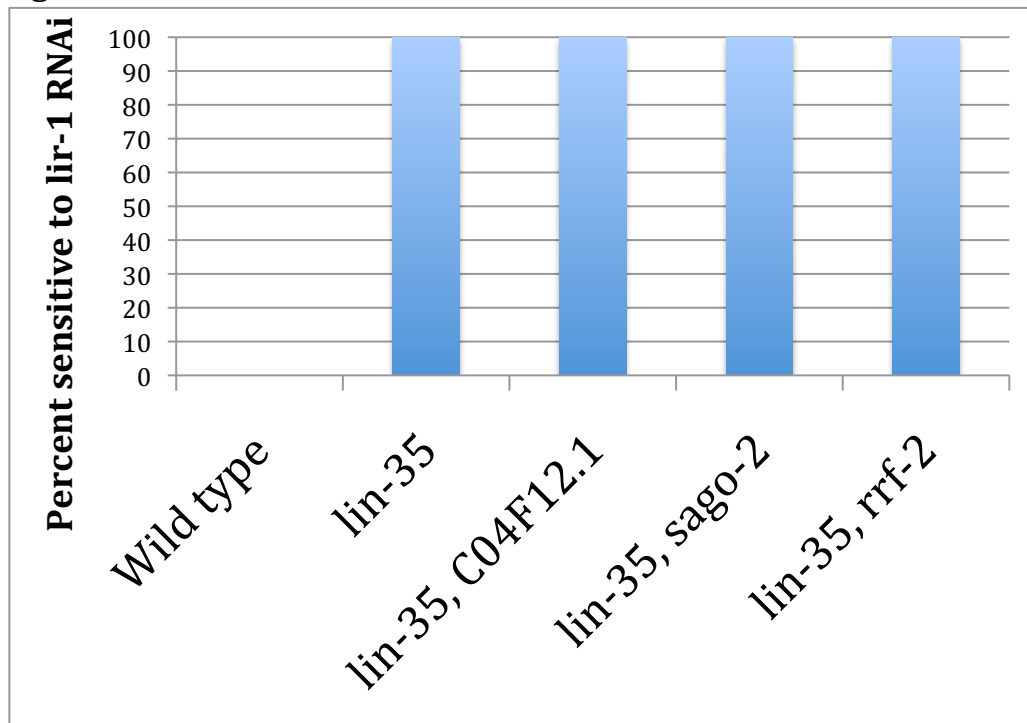


**Figure 4.1** Enhanced RNAi in *lin-35* mutants does not depend on *sago-2*, *rrf-2* or *C04F12.1* The fraction of worms sensitive to *lir-1* RNAi is plotted. n>30 for each strain.



synthetic Multivulva class B genes, results in a soma-to-germline transformation (Wu et al., 2012).

We found *eri-1* and *lin-15ab* mutants extend the detected pharyngeal muscle critical period (Figure 4.2A). When a population of L2 and L3 worms were heat-shocked, the pharynxes of *eri-1* and *lin-15ab* animals were significantly more silenced than those of wild type. *lin-15ab* mutants also enhanced the proportion of silenced pharyngeal muscle in the earliest time, suggesting that in addition to expanding the critical period, they increased RNAi sensitivity. However, when animals were heat-shocked as L4s and young adults *eri-1* and wild-type animals showed a similar minimal silencing, while *lin-15ab* mutants showed significantly more silencing (Figure 4.2A). This indicates that the effect of *eri-1* mutants to extend the critical period may be limited to enhanced sensitivity to dsRNA, while *lin-15ab* mutants also extend the boundary of the critical period into later development. Because *eri-1* and *lin-15ab* mutants both extend the sensitivity and/or breadth of the critical period, we hypothesized that these mutants might be sensitive to first-generation feeding RNAi. Indeed, while first-generation feeding RNAi failed to silence pharyngeal GFP in wild-type animals both *eri-1* and *lin-15ab* mutants displayed strong first-generation RNAi pharyngeal silencing (Figure 4.2B).

Figure 4.2

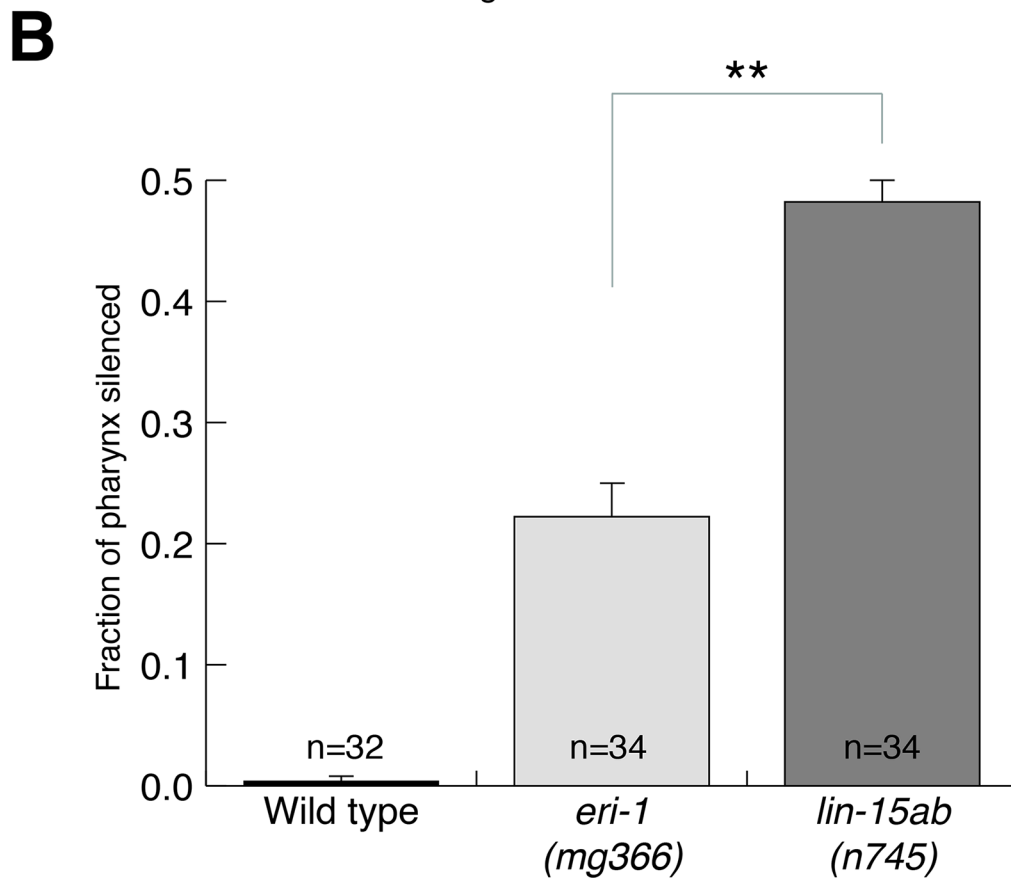
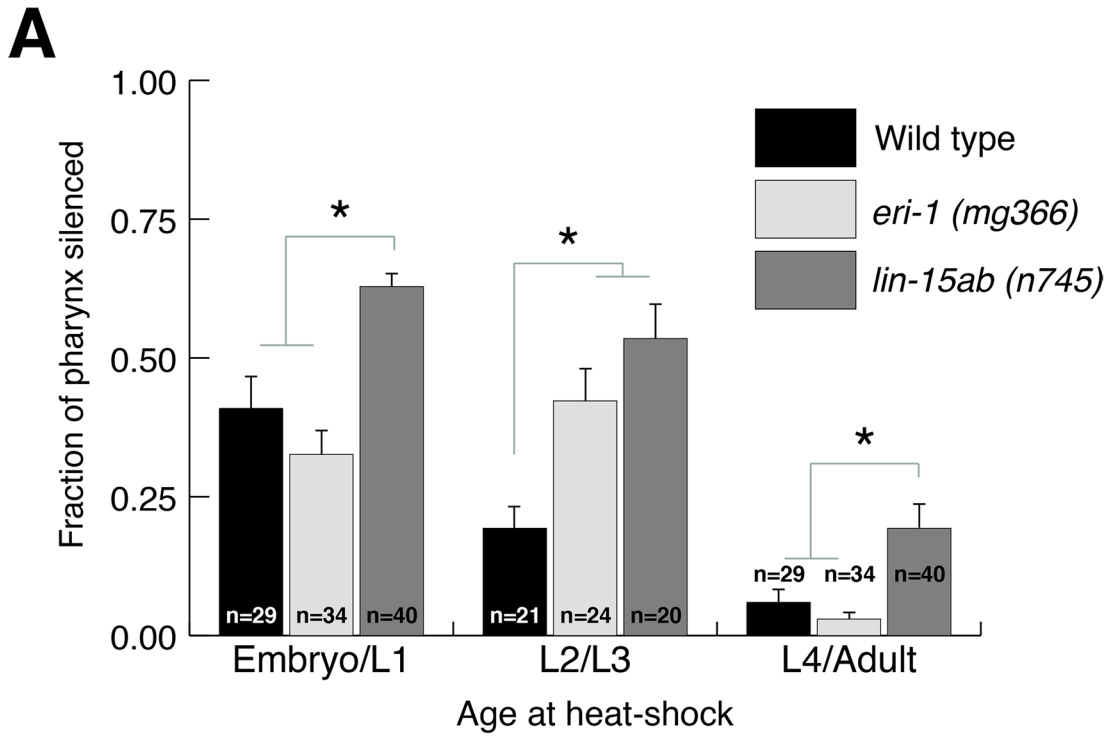


**Figure 4.2 (continued).** Enhanced RNAi mutants extend the critical period. (A) Pharyngeal silencing of the mIs11 integrated array in control and Eri mutants (B) Eri mutants are sensitive to feeding RNAi in the first generation. (A and B) Silencing of individual sections of the pharyngeal muscle was scored. Bars show SEM from three trials, n= number of animals scored ( $P<.01$ ).

### **The enhanced RNAi phenotype of synMuv Class B mutants depends on nuclear RNAi**

The Eri phenotypes of *eri-1* and *rrf-3* is known to depend on nuclear RNAi (Guang et al., 2008, Zhuang et al., 2013). Although pharyngeal silencing in wild type is dependent on nuclear RNAi (Chapter 3), the synMuv B Eri phenotype could result from either or both enhanced nuclear RNAi or re-activated cytoplasmic RNAi. Therefore, we asked whether the Eri phenotype of a *lin-35* mutant depends on nuclear RNAi. *Nrde-3* is thought to function exclusively in the soma (Guang et al., 2008, Burton et al., 2011). To test both germline and somatic RNAi targets, we used *nrde-2* mutants for these tests. We exposed wild-type or mutant worms to first-generation RNAi against a panel of targets known to require enhanced RNAi. Indeed, we found that the Eri phenotype of *lin-35* was strongly dependent on *nrde-2* (Figure 4.3 A-F). For example, first-generation *cel-1* RNAi in *lin-35* worms caused these worms to become sterile, but *lin-35; nrde-2* worms had significantly lower levels of sterility (Figure 4.3A). Furthermore, first-generation *his-14* RNAi caused *lin-35* worms to arrest prior to the L3 stage, but *lin-35; nrde-2* worms did not arrest (Figure 4.3B). Interestingly, *his-14* RNAi exposed *lin-35; nrde-2* worms were sterile (Figure 4.3C), suggesting that loss of synMuv B genes may also enhance cytoplasmic RNAi.

**Figure 4.3**

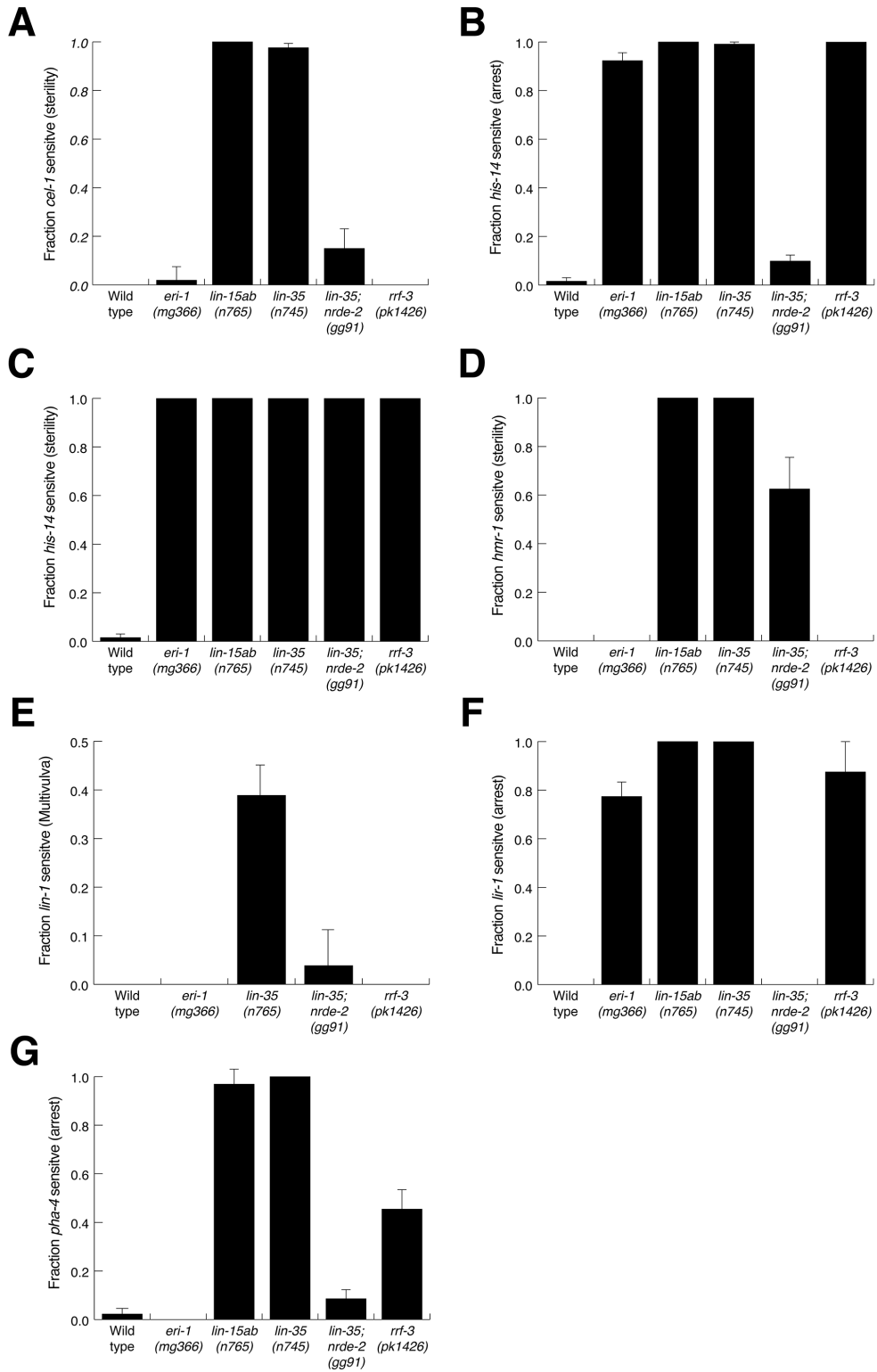


**Figure 4.3 (continued).** *nrde-2* dependent single-generation RNAi in synMuv B class mutants. (A-G) The fraction of single and double-mutants that displayed the indicated phenotypes when placed as embryos on *E. coli* expressing the listed dsRNA. Bars show SEM from three trials, n>45 animals tested.

### ***Pha-4* RNAi requires nuclear RNAi and is enhanced by synMuv B mutants**

To confirm that the genetic requirements for silencing pharyngeal GFP extend to endogenous genes, we examined the genetics of *pha-4* RNAi silencing. PHA-4 is a FoxA transcription factor that specifies pharyngeal organ identity (Horner et al., 1998, Mango et al., 1994). Although *pha-4* is required embryonically and post-embryonically, wild-type worms exposed to *pha-4* dsRNA from hatching develop to adulthood (Figure 4.3G). However, like pharyngeal GFP RNAi, second-generation *pha-4* RNAi results in a strong phenotype: larvae do not develop past the L2 stage. Furthermore, this second-generation RNAi requires nuclear RNAi (Table 3.1). Additionally, like pharyngeal GFP RNAi, loss of synMuv B genes confers sensitivity to first-generation RNAi (Figure 4.3G, Table 3.1). In contrast to GFP silencing, *pha-4* second-generation RNAi also requires cytoplasmic Argonautes (Table 3.1).

### **Local chromatin may affect silencing efficiency**

Because pharyngeal RNAi requires nuclear RNAi, we hypothesized that local chromatin might affect the efficiency of silencing. To test this, we examined the expression and silencing efficiency of seven different single-copy insertions of a *myo-2::GFP* transgene. These transgenes were initially constructed to study the effects of knock-out each of seven different RNA binding proteins (John Calarco, personal communication). Because these RNA binding proteins might affect RNAi, we first tested these strains for RNAi efficiency and found no changes (data not shown).

Next, we examined the fluorescence intensity of these strains after two generations of exposure to either mock RNAi or GFP RNAi. Remarkably, we found

that there was considerable heterogeneity in silencing efficiency as a result of exposure to GFP dsRNA (Figure 4.4). Heterozygous strains have similar patterns of silencing efficiency, indicating that the genomic location, rather than the gene knock-outs likely cause difference in silencing efficiency (Figure 4.4). Furthermore, crossing strains that silence well to strains that silence poorly results in an intermediate silencing strain, indicating that silencing factors do not act in *trans*. Taken together, our data indicate that local chromatin likely affects efficiency of nuclear RNAi.



**Figure 4.4**

A. Homozygous worms

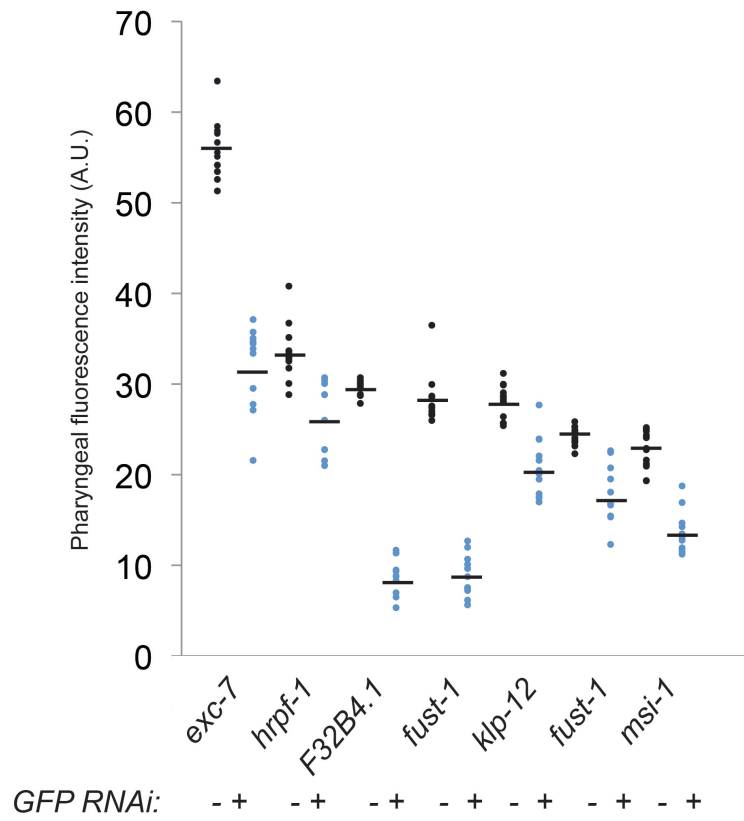


**Figure 4.4 (continued)**

B. Heterozygous worms

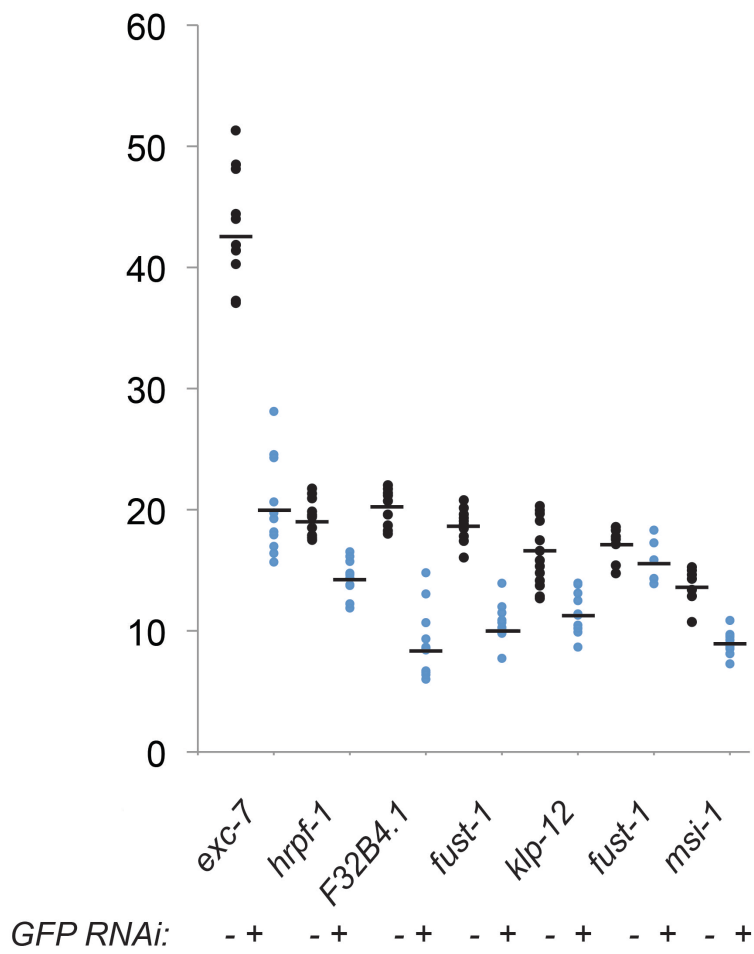


**Figure 4.4C.**

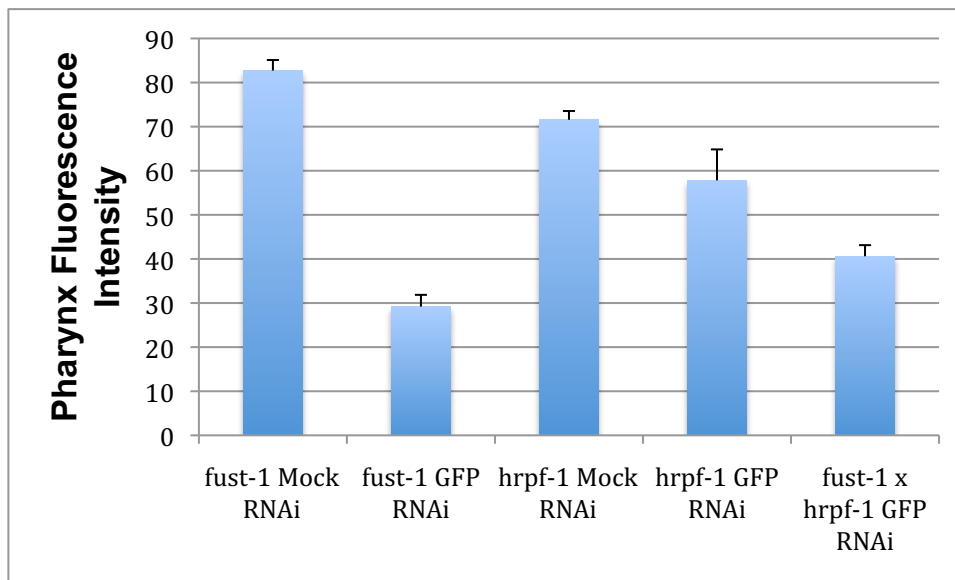


**Figure 4.4 (continued).** Local chromatin affects silencing efficiency. A-B Pharyngeal muscle fluorescence intensity of the indicated insertion location measured after two generations of either mock (black dots) or GFP RNAi (blue dots). C. Silencing does not act in *trans*.

## Discussion

### An alternative model for synMuv B enhanced RNAi

An open question is why loss of synMuv B genes causes an Eri phenotype. SynMuv B genes, such as *lin-15b* and *lin-35*, are chromatin factors that function to repress gene expression, including germline gene expression. It has been postulated that transcriptional misregulation in *lin-35* or *lin-15b* mutants result in their Eri phenotype (Wu et al., 2012). Four RNAi genes in particular, *C04F12.1/vsra-1* (which encodes a cytoplasmic Argonaute), *sago-2* (which encodes a cytoplasmic argonaute), *rrf-2* (encoding a RNA-dependent RNA polymerase) and *hrde-1* (encoding a nuclear RNAi argonaute expressed in the germline), are upregulated in the soma of synMuv B mutants. Curiously, *hrde-1* mutants are weakly enhanced for RNAi, and this RNAi enhancement, like the *eri-1* phenotype, is additive with synMuv B mutations (Wu et al., 2012). Thus, it is likely that, similar to *eri-1* and *rrf-3*, *hrde-1* dependent processes compete with exogenous RNAi pathways. Single loss of any of the other factors, *C04F12.1/vsra-1*, *sago-2* and *rrf-2*, in conjunction with *lin-35* or *lin-15b* caused at most a mild reduction in RNAi efficiency (Figure 4.1 and Wu et al., 2012). Furthermore, overexpression of any of these four factors in the soma did not confer an Eri phenotype. Thus, transcriptional misregulation of these four factors likely does not fully explain the Eri phenotype of synMuv B mutants.

We speculate that the synMuv B Eri phenotype might be a direct result of soma-to-germline transformation, rather than any transcriptional misregulation. During development, chromatin and/or the factors that modify chromatin become less plastic. Because transcriptional gene silencing that accompanies nuclear RNAi

may require malleable chromatin, the closing of the nuclear RNAi window may be coupled to developmental process that restrict developmental cell fate plasticity. Further, we hypothesize that in synMuv B mutants, the somatic chromatin and/or the factors that modify it are more germline-like and naïve. We speculate that the same mechanisms that result in closing of developmental plasticity may also play a role in restricting the initiation of nuclear RNAi. Thus, we hypothesize that synMuv B Eri phenotype represents delayed closing of the critical window for initiating nuclear RNAi.

### **Use of enhanced RNAi strains**

In contrast to other reports (Lehner et al., 2006), we previously reported that synMuv B mutants had weaker Eri phenotypes than either *eri-1* or *rrf-3* (Zhuang et al., 2011). In contrast to this, in this paper we find that *lin-35* and *lin-15ab* generally have stronger nuclear RNAi phenotypes than either *eri-1* or *rrf-3* (Figure 4.3). In our previous report, we exposed L3 staged worms to dsRNA and found that *lin-15b* or *lin-35* did not have as robust of an Eri phenotype as either *eri-1* or *rrf-3*. However, by the time worms are at the L3 stage, the critical window for nuclear RNAi may be nearly closed, leaving open only cytoplasmic RNAi silencing. Perhaps this explains why synMuv B worms did not have strong Eri phenotypes in the earlier report. This result highlights how understanding the fundamental aspects of *C. elegans* RNAi can guide its practical use. For experiments involving young worms, we now suggest using either *lin-35* or, since loss of the two is additive, a *lin-35; eri-1* double mutant. Furthermore, using a synMuv B Eri should allow for single-generation feeding RNAi screens.

## **Local chromatin and nuclear RNAi**

Although different *myo-2::GFP* single copy insertions produce similar levels of protein, we were surprised to find that RNAi silences in these strains significantly differently. A variety of different factors differ between these locations, such as position in the chromosome, transcription levels of the knocked-out gene, and likely chromatin marks at that locus. We hypothesize that chromatin marks may be the difference between strongly and weakly silencing loci. Although we examined ModEncode data on these loci, we observed no obvious correlations between silencing efficiency and these data. We have noticed that young worms are more sensitive to nuclear RNAi, while old worms are not (chapter 3). It is possible that the same changes that develop over time may also distinguish between strong and weakly silencing loci. Examining what heterochromatin modifying genes are required for enhanced RNAi or nuclear RNAi may suggest possibilities for what these possible chromatin marks may be.

## **Enhanced RNAi and transcriptional stability**

It is possible that this decreasing ability to silence gene expression by histone methylation might be a general rule for development in animals. If so, why might this be advantageous? Stabilizing transcription would prevent aberrant transcriptional profiles. One extreme example of this is cancer. Loss of Rb, the mammalian homolog of *lin-35*, results in high rates of cancer. We find that loss of *lin-35* or *lin-15ab* results in an abnormal sensitivity to transcriptional silencing late in development. It is possible that Rb, in addition to regulating the cell cycle, may also play a role in regulating gene expression and a critical window for gene silencing. It

may be possible that in cancers with loss of Rb, chromatin may be vulnerable to stochastic gene silencing; if tumor suppressor genes are silenced, then this could lead to further cancer progression.

### **Experimental Procedures**

**Feeding RNAi.** For GFP RNAi, *E. coli* expressing either dsRNA targeting GFP or control dsRNA (L4440) was fed to L1 animals on agar plates containing 1 mM isopropyl  $\beta$ -D-1-thiogalactopyranoside (Timmons and Fire, 1998).

For *act-5* RNAi, embryos were placed on *E. coli* expressing *act-5* dsRNA, then 3 days later, the fraction of animals reaching adulthood was scored. For GFP RNAi, worms were placed on *E. coli* expressing *GFP* dsRNA, then 3 days later, animals were imaged then blindly scored for silencing. All feeding RNAi experiments were performed at 20° C. Bacteria engineered to express *gfp* dsRNA were prepared as described previously (Winston et al., 2003). All other bacteria expressing dsRNA were from the Ahringer library (Kamath and Ahringer, 2003).

**Heat-shock.** Adult worms were placed on seeded plates and allowed to lay embryos for approximately 6 or 12 hour time windows and then removed. The collected embryos developed for the specified time at 20C and were then heat-shocked on the growth plates at 34° C for two-hours in an air incubator. Two days post heat-shock, the pharynxes were scored as below for silencing.

**Statistics.** P-values were calculated using the Student's t-test.

**Live Microscopy.** Worms were immobilized for imaging by placing plates on ice for 15-30 minutes. Images being compared in each figure were taken using the same nonsaturating exposure conditions and processed identically using Adobe Illustrator for display. 8-bit images were taken at 10x magnification at 8-bit using an Olympus SZX2 microscope, a Hamamatsu C8484 camera and HCI Imaging Software.

**Quantification of pharyngeal fluorescence.** The pharyngeal fluorescence was quantified in one of two complementary methods, whole pharynx fluorescence quantification or scoring of individual pharynx sections. In both methods, worms were imaged as above and *mls11* or the single-copy *myo-2::GFP* transgene was the only GFP transgene. In the first method, the fluorescence of the entire pharynx was quantified. Worm images were analyzed with Fiji (an ImageJ distribution) by first tracing the pharynx, measuring the average fluorescence intensity and subtracting the background as performed in Gavet and Pines, 2010.

Because silencing in the pharyngeal muscle is often partial and incremental, we also analyzed silencing of individual sections of the pharyngeal muscle, in which we divided the pharynx into eight sections. Although the pharynx has three-fold rotational symmetry, for convenience of scoring, we divided the pharynx in half corresponding to half of each of the procorpus, metacarpus, isthmus and terminal bulb of the pharynx. The number of each of these sections were scored for strong silencing. The genotype of each worm was blinded from the scorer.



## References

- Ashe A, Sarkies P, Le Pen J, Tanguy M, Miska EA. Antiviral RNAi against Orsay virus is neither systemic nor transgenerational in *Caenorhabditis elegans*. *J Virol* 2015;JVI.03664–14.
- Burton NO, Burkhart KB, Kennedy S. Nuclear RNAi maintains heritable gene silencing in *Caenorhabditis elegans*. *Proc Natl Acad Sci* 2011;108:19683–8. doi:10.1073/pnas.1113310108.
- Calixto A, Chelur D, Topalidou I, Chen X, Chalfie M. Enhanced neuronal RNAi in *C. elegans* using SID-1. *Nat Methods* 2010;7:554–9. doi:10.1038/nmeth.1463.
- Duchaine TF, Wohlschlegel JA, Kennedy S, Bei Y, Conte D, Pang K, et al. Functional proteomics reveals the biochemical niche of *C. elegans* DCR-1 in multiple small-RNA-mediated pathways. *Cell* 2006;124:343–54. doi:10.1016/j.cell.2005.11.036.
- Fire A, Harrison SW, Dixon D. A modular set of lacZ fusion vectors for studying gene expression in *Caenorhabditis elegans*. *Gene* 1990;93:189–98.
- Fire A, Xu S, Montgomery MK, Kostas SA, Driver SE, Mello CC. Potent and specific genetic interference by double-stranded RNA in *Caenorhabditis elegans*. *Nature* 1998;391:806–11. doi:10.1038/35888.
- Fischer SEJ, Pan Q, Breen PC, Qi Y, Shi Z, Zhang C, et al. Multiple small RNA pathways regulate the silencing of repeated and foreign genes in *C. elegans*. *Genes Dev* 2013;27:2678–95. doi:10.1101/gad.233254.113.
- Gabel HW, Ruvkun G. The exonuclease ERI-1 has a conserved dual role in 5.8S rRNA processing and RNAi. *Nat Struct Mol Biol* 2008;15:531–3. doi:10.1038/nsmb.1411.
- Gavet O & Pines J (2010) Progressive activation of CyclinB1-Cdk1 coordinates entry to mitosis. *Dev Cell* 18: 533-543
- Grishok a, Sinskey JL, Sharp P a. Transcriptional silencing by RNAi in the soma of of a transgene *C. elegans*. *Genes Dev* 2005;19:683–96. doi:10.1101/gad.1247705.genes.
- Guang S, Bochner AF, Burkhart KB, Burton N, Pavelec DM, Kennedy S. Small regulatory RNAs inhibit RNA polymerase II during the elongation phase of transcription. *Nature* 2010;465:1097–101. doi:10.1038/nature09095.
- Guang S, Bochner AF, Pavelec DM, Burkhart KB, Harding S, Lachowiec J, et al. An Argonaute transports siRNAs from the cytoplasm to the nucleus. *Science* 2008;321:537–41. doi:10.1126/science.1157647.

Han T, Manoharan AP, Harkins TT, Bouffard P, Fitzpatrick C, Chu DS, et al. 26G endo-siRNAs regulate spermatogenic and zygotic gene expression in *Caenorhabditis elegans*. *Proc Natl Acad Sci U S A* 2009;106:18674–9. doi:10.1073/pnas.0906378106.

Horner MA, Quintin S, Domeier ME, Kimble J, Labouesse M, Mango SE. *pha-4*, an HNF-3 homolog, specifies pharyngeal organ identity in *Caenorhabditis elegans*. *Genes Dev* 1998;12:1947–52.

Kamath RS, Ahringer J. Genome-wide RNAi screening in *Caenorhabditis elegans*. *Methods* 2003;30:313–21. doi:10.1016/S1046-2023(03)00050-1.

Kumsta C, Hansen M. *C. elegans rrf-1* Mutations Maintain RNAi Efficiency in the Soma in Addition to the Germline. *PLoS One* 2012;7:e35428.

Lehner B, Calixto A, Crombie C, Tischler J, Fortunato A, Chalfie M, et al. Loss of LIN-35, the *Caenorhabditis elegans* ortholog of the tumor suppressor p105Rb, results in enhanced RNA interference. *Genome Biol* 2006;7:R4. doi:10.1186/gb-2006-7-1-r4.

Mango SE, Lambie EJ, Kimble J. The *pha-4* gene is required to generate the pharyngeal primordium of *Caenorhabditis elegans*. *Development* 1994;120:3019–31.

Mango SE. The molecular basis of organ formation: insights from the *C. elegans* foregut. *Annu Rev Cell Dev Biol* 2009;25:597–628.

Mao H, Zhu C, Zong D, Weng C, Yang X, Huang H, et al. The Nrde Pathway Mediates Small-RNA-Directed Histone H3 Lysine 27 Trimethylation in *Caenorhabditis elegans*. *Curr Biol* 2015;25:2398–403.

Meister P, Mango SE, Gasser SM. Locking the genome: nuclear organization and cell fate. *Curr Opin Genet Dev* 2011;21:167–74.

Norris AD, Kim HM, Colaiácovo MP, Calarco JA. Efficient genome editing in *Caenorhabditis elegans* with a toolkit of dual-marker selection cassettes. *Genetics* 2015;201:449–58. doi:10.1534/genetics.115.180679.

Parrish S, Fire A. Distinct roles for RDE-1 and RDE-4 during RNA interference in *Caenorhabditis elegans*. *RNA* 2001;7:1397–402.

Sijen T, Fleenor J, Simmer F, Thijssen KL, Parrish S, Timmons L, et al. On the role of RNA amplification in dsRNA-triggered gene silencing. *Cell* 2001;107:465–76. doi:10.1016/S0092-8674(01)00576-1.

Steiner FA, Okihara KL, Hoogstrate SW, Sijen T, Ketting RF. RDE-1 slicer activity is required only for passenger-strand cleavage during RNAi in *Caenorhabditis elegans*. *Nat Struct Mol Biol* 2009;16:207–11. doi:10.1038/nsmb.1541.

Sternberg PW. Vulval development. *WormBook*. 2005:1–28.

Stringham EG, Dixon DK, Jones D, Candido EP. Temporal and spatial expression patterns of the small heat shock (*hsp16*) genes in transgenic *Caenorhabditis elegans*. *Mol Biol Cell* 1992;3:221–33.

Tabara H, Sarkissian M, Kelly WG, Fleenor J, Grishok A, Timmons L, et al. The *rde-1* gene, RNA interference, and transposon silencing in *C. elegans*. *Cell* 1999;99:123–32.

Tabara H, Yigit E, Siomi H, Mello CC. The dsRNA binding protein RDE-4 interacts with RDE-1, DCR-1, and a DExH-Box helicase to direct RNAi in *C. elegans*. *Cell* 2002;109:861–71.

Timmons L, Fire A. Specific interference by ingested dsRNA. *Nature* 1998;395:854. doi:10.1038/27579.

Winston WM, Molodowitch C, Hunter CP. Systemic RNAi in *C. elegans* requires the putative transmembrane protein SID-1. *Science* 2002;295:2456–9.

Wu X, Shi Z, Cui M, Han M, Ruvkun G. Repression of germline RNAi pathways in somatic cells by retinoblastoma pathway chromatin complexes. *PLoS Genet* 2012;8:e1002542. doi:10.1371/journal.pgen.1002542.

Yigit E, Batista PJ, Bei Y, Pang KM, Chen CCG, Tolia NH, et al. Analysis of the *C. elegans* Argonaute Family Reveals that Distinct Argonautes Act Sequentially during RNAi. *Cell* 2006;127:747–57

Zhuang JJ, Banse SA., Hunter CP. The nuclear Argonaute NRDE-3 contributes to transitive RNAi in *Caenorhabditis elegans*. *Genetics* 2013;194:117–31. doi:10.1534/genetics.113.149765.

Zhuang JJ, Hunter CP. Tissue Specificity of *Caenorhabditis elegans* Enhanced RNA Interference Mutants. *Genetics* 2011;188:235–7. doi:10.1895/wormbook.1.138.1

## Chapter 5: Conclusion

In this thesis, I made several contributions to our understanding of RNAi in *C. elegans*. In this concluding chapter, I summarize our findings, explain their significance and potential implications, and suggest research avenues that continue from my research findings.

### Brief summary of my findings

I identified *rde-12*, which encodes a DEAD-box RNA helicase. *rde-12* animals are strongly resistant to exogenous RNAi, because they fail to accumulate secondary siRNAs. Although we recovered *rde-12* mutants in a screen designed to enrich for export mutants, I found that *rde-12* functions cell-autonomously, and is not systemic RNAi defective. A residue essential for DEAD-box helicase activity was required for RDE-12 function, suggesting that RDE-12 may indeed function as a RNA helicase (Yang et al., 2014).

Exploring the role that RDE-12 plays in the pharynx, I found that secondary siRNA accumulation is not required for pharyngeal muscle silencing in the presence of a strong dsRNA trigger. In contrast, I found that the pharyngeal muscle has a particular requirement for nuclear RNAi (Shiu and Hunter, 2017). Although Burton et al. have proposed that there might be a requirement for germline RNAi activity for efficient nuclear RNAi, I show that there is no absolute requirement for germline dsRNA transmission. Instead, I find that there is a critical period for nuclear RNAi. In both the pharyngeal muscle and vulval muscle, silencing is dependent on nuclear RNAi, and beyond a particular developmental time, the efficiency of nuclear RNAi silencing greatly decreases.

We hypothesized that enhanced RNAi mutants might extend the critical period. Indeed, we found that Rb pathway mutants significantly extended the critical period for nuclear RNAi silencing in the pharynx. Although this is not predicted by models that hypothesize that Rb pathway enhanced RNAi arises due to misexpression of three particular cytoplasmic RNAi genes, we found that nuclear RNAi is required for the Eri phenotype of Rb pathway mutants. Finally, we found that particular genomic loci are more sensitive to nuclear RNAi than others. We hypothesize that Rb pathway mutants might extend the critical period by directly affecting local chromatin.

### **Significance**

Little was previously known about how primary siRNA and the secondary siRNA amplification were linked. My research suggests that RDE-12 may serve as a hub joining these two processes, directing secondary siRNA accumulation in P-bodies, a location where mRNA degradation is known to occur (Yang et al., 2014).

We found that there is a critical period for nuclear RNAi. Many, and perhaps most, *C. elegans* feeding RNAi experiments are performed by feeding adult worms dsRNA and examining RNAi phenotypes in the progeny. The observation that this method works most efficiently may arise, at least in part, due to the critical period for nuclear RNAi we have found.

Our findings provide several significant lessons for researchers performing RNAi in *C. elegans*. First, the pharyngeal muscle and vulval muscle have a particular dependence on nuclear RNAi, and therefore, at least for the pharynx, two-generations of feeding RNAi are required for efficient silencing. It is possible that

other tissues may also have this particular dependence on particular pathways of RNAi. Secondly, it is possible that particular genes, due to their particular local chromatin, may be more or less susceptible to nuclear RNAi. Thirdly, when researchers want to start feeding RNAi only in a single generation, the timing of when dsRNA is first encountered may be significant. Using an enhanced RNAi strain like *lin-35* or *lin-15b* may allow for first generation silencing when two-generations of RNAi may not be possible. However, if our hypothesis that Rb pathway mutants have significantly abnormal local chromatin is correct, we note that these experiments may produce unexpected artifacts, if chromatin state might affect the particular experiment.

#### **A critical period for nuclear RNAi**

We hypothesize that the critical period for nuclear RNAi might arise due to the general changes to chromatin over developmental time. As cells undergo differentiation, the number of cell fates they may adopt decreases. It is known that as over the course of development, the ability to turn particular genes on decreases. Here, we hypothesize that the ability to turn genes off may also decrease: changes to chromatin might “lock in” particular patterns of transcription.

Loss of Rb pathway proteins enhances RNAi and enables efficient first-generation RNAi. Interestingly, Petrella and colleagues have found that loss of Rb pathway proteins results in delays in chromatin compaction (personal communication). Loss of *lin-35* causes misexpression of germline genes in the soma and adoption of a mixed somatic and germline fate. These data lead us to

hypothesize that loss of Rb pathway genes causes de-differentiation, which in turn results in enhanced RNAi.

### **A possible new role for Rb in cancer**

Rb was the first gene identified as a tumor suppressor, and is mutated in approximately one-third of all human tumors (Calo et al., 2010). Despite significant interest in the role that Rb plays in cancer progression, exactly how Rb loss promotes cancer progression is not fully known (Dalluri and Dick, 2012). Analysis of Rb is difficult because it has many functions, the best known of which is its role in promoting cell-cycle exit by inhibiting E2F transcription factors and repression of expression of other cell-cycle genes. However, its role as an inhibitor of E2F only is part of its role as tumor suppressor. Other members of the “pocket protein” family of genes, including p107 and p130 also inhibit E2F. However, the number of tumors with Rb mutated greatly outnumber the number of tumors with mutations in p107 and p130. This implies that the non-cell cycle roles of Rb may be critical in cancer progression.

Our model of how Rb loss promotes cancer progression has three main aspects.

- 1.** As development proceeds, epigenetic modifications become progressively more difficult
- 2.** Loss of Rb causes de-differentiation.
- 3.** De-differentiation may make epigenetic modifications more likely, possibly including stochastic epigenetic changes. We discuss each aspect in more detail below:

As development proceeds, **epigenetic modifications may become progressively more difficult**. Measuring how susceptible chromatin is to epigenetic modifications is currently difficult, because we have few tools for directing chromatin modifying enzymes to a particular locus. In my work, I have shown that nuclear RNAi, which directs H3K9 and H3K27 trimethylation, becomes progressively more difficult over developmental time. I note, however, that I never directly measured histone methylation, nor is the exact mechanism of why silencing becomes more difficult known. However, the fact that particular chromatin is more susceptible to nuclear RNAi silencing indicates that differences in local chromatin may indeed affect the rate at which silencing and may occur.

As noted earlier, it is known that over the course of development, cell fate plasticity decreases (Meister et al., 2011). An ectopic pulse of *hlh-1* can induce muscle fate specification early in development, but not late in development (Yuzyuk et al., 2009). This implies that transcription profiles become cemented over time; we hypothesize that the same factors that lock in cell fate may also act to prevent nuclear RNAi late in development.

**Loss of Rb causes de-differentiation.** How loss of Rb causes enhanced RNAi is not well understood. It has been noted that loss of Rb causes expression of germline genes in the soma. Wu et al. have postulated that the Eri phenotype may result from misexpression of germline genes in the soma, in particular the three genes *rrf-2*, *C04F12.1* and *sago-2*. However, individual loss of these genes causes at most a mild reduction in the Eri phenotype in either a *lin-35* or *lin-15b* background (Wu et al., 2012), nor does misexpression of *C04F12.1* and *sago-1*, two cytoplasmic



Ago genes, explain why the *lin-35* Eri phenotype should be nuclear RNAi dependent. Furthermore, overexpression of these genes in the soma does not confer an Eri phenotype (Wu et al., 2012). Finally, this hypothesis does not explain why loss of Rb pathway mutants should enhanced RNAi both in the soma and in the germline (Lehner et al., 2006).

We hypothesize that the Eri phenotype in Rb pathway mutants may be a result of changes to the chromatin that result from the soma-to-germline transition. It has been noted that in Rb pathway mutants, there are delays in chromatin compaction (Lisa Petrella, personal communication). Furthermore, loss of the Rb pathway gene *hpl-2* causes chromatin decompaction in the germline of *C. elegans* (Lleres et al, 2017). If loss of Rb pathway genes does indeed cause chromatin to decompact and “act younger,” than this would explain the enhanced RNAi phenotype.

There is substantial evidence to indicate that loss of Rb causes de-differentiation and multipotency in a variety of different organisms. In the Arabidopsis male germline, for example, loss of the Rb homolog causes delays in cell fate determination (Chen et al., 2009). In mammals, Rb is important in the cell fate decision between bone and brown adipose tissue. Loss of Rb results in multipotency: In tissue-culture, wild-type osteoblasts are capable of undergo osteogenesis, but not adipogenesis. In contrast, Rb mutant osteoblasts could become either bone or fat cells (Calo et al., 2010). Furthermore, loss of Rb in vivo resulted in increases in brown fat and decreases in calcified bone (Calo et al, 2010). In another example of Rb’s control of differentiation in mammals, transient

inactivation of Rb and another tumor suppressor protein, Arf, resulted in dedifferentiation of postmitotic muscle cells (Pajcini et al., 2010). These cells could then be transplanted with significant regenerative capacity.

De-differentiation may **make epigenetic modifications more likely**, possibly including stochastic epigenetic changes. We find that loss of Rb causes enhanced RNAi, and hypothesize that this may result from an increased susceptibility to histone modifications in a Rb pathway mutant.

Cancer is thought to be the result of an accumulation of mutations that promote unchecked proliferation. To examine what genes are mutated in pediatric retinoblastomas, Zhang et al. performed whole-genome sequencing on four primary human retinoblastoma samples, as well as their matched somatic tissue (Zhang et al., 2012). Remarkably, they found no mutations in known oncogenic genes, other than Rb1 itself. One sample had no amino-acid changes in genes other than Rb1. Instead, when they performed RNA-seq, they found significant changes in gene expression, despite the lack of mutations. Thus, they concluded that all of the changes that promote cancer progression must have been epigenetic.

We hypothesize that one role of Rb may be to help promote a stable transcriptome by preventing changes to the epigenome. If this is true, then retinoblastomas may arise due to loss of Rb, followed by stochastic changes to the epigenome that promote carcinogenesis. We note that many epigenetic changes result in positive feedback loops, meaning that small perturbations, if unchecked, may result in significant transcriptional changes. For example, H3K9 methylation is recognized by heterochromatin protein 1, HP1. HP1 can recruit the histone

methyltransferase SUV39H1, which can methylate nearby histones, resulting in a positive feedback loop that results in significant H3K9 methylation and gene repression. Likewise, the polycomb repressive complex, PRC2, may also participate in a positive feedback loop to ensure efficient silencing. Ezh2 is a histone methyltransferase that catalyzes H3K27 methylation. Because the PRC2 complex member Eed binds methylated H3K27, this allows for a positive feedback loop where PRC2 binds H3K27me<sub>3</sub>, but also catalyses its formation, resulting in local accumulation of H3K27me<sub>3</sub> and subsequent heterochromatin formation and gene silencing. We note that RNAi in *C. elegans* is amplified by the production of secondary siRNA, and also promotes H3K9me<sub>3</sub> and H3K27me<sub>3</sub>, repressive marks that can spread. In this system, Rb/*lin-35* may serve as a break to this feedback loop. We hypothesize that Rb might also inhibit excessive silencing in other contexts as well. Thus, by preventing stochastic silencing (and potentially activation), Rb may act to maintain the transcriptome.

### **Implications of the Rb-epigenetics model**

If our speculative model about the role Rb might play in carcinogenesis is correct, then there are several interesting implications. First, a more complete understanding of the role of Rb in cancer may provide potential therapeutic avenues. Understanding how Rb affects the sensitivity of chromatin to modifications will be critical in this effort. For example, screens for suppressors of easy epigenetic modifications in an Rb background may reveal promising drug candidates.

Currently, there are significant efforts to sequence cancer samples to understand why mutations drive cancer. These efforts are part of a vision of “personalized medicine,” where the DNA sequence of cancer samples may suggest particular drugs or strategies to use to fight it. If Rb does indeed allow for epigenetic changes, then cancers with Rb will not only have to have their genome sequenced, but also their transcriptional profile and/or epigenome sequenced as well.

A further implication of our model is that, if researchers or clinicians wish to easily perturb transcription or gene expression, then transient knock-down of Rb may facilitate these changes. As mentioned earlier, transient inactivation of Rb and another tumor suppressor protein, Arf, promoted dedifferentiation of muscle cells. Finally, in settings where researchers want to easily manipulate histone modifications to examine their function, performing these experiments in a Rb mutant or Rb knock-down background, may facilitate the efficiency of the experiments.

### **Testing the model**

Thus far, our model relies on data from *C. elegans* and supporting evidence from a variety of different contexts. Of course, it is necessary to directly show that Rb loss eases epigenetic modifications. One way to do this is to direct histone methylation or other modifications to a particular location using guide-RNA directed dCas9 coupled to a histone modifying enzyme. If the efficiency of directed histone modifications is higher in a Rb mutant than wild type, this will be good evidence for our model.

We hypothesize that Rb pathway mutants have changes to chromatin, for example, chromatin decompaction and potentially other changes to chromatin. It will be interesting to examine chromatin compaction in *C. elegans*, for example by using the FRET-FLIM model used by Lleres et al. Additionally, determining what the differences are between “easy to silence” and “hard to silence” *myo-2::GFP* insertions will greatly increase our understanding of why particular chromatin is easy or hard to silence. This could be performed by performing ChIP at these locations for various chromatin marks, or by performing EMS or RNAi screens to identify what genes are required to maintain either “easy to silence” and “hard to silence” chromatin. Finally, screens to identify genes specifically required for *lin-35* enhanced RNAi may also help to reveal the mechanisms through which *lin-35* loss enhances RNAi.

Our model also predicts that in a Rb mutant, stochastic epigenetic changes will occur that do not otherwise occur in wild type cells. This could be tested in cell culture or *in vivo* by measuring different populations of wild type or Rb cells. Our model predicts that the wild type transcriptome should be relatively robust while similar population of Rb mutant cells should have significantly greater diversity in their transcriptomes, i.e., noisier transcriptomes.

### **Conclusion**

We have found that the DEAD-box helicase RDE-12 is essential for secondary siRNA accumulation in *C. elegans*. Additionally, I found that there is a critical period for nuclear RNAi, and that loss of Rb extends that critical period. We hypothesize Rb

may play a role in stabilizing the epigenome, a hypothesis with potentially significant clinical relevance.

## Literature Cited

- [1] Calo E, Quintero-Estades J a, Danielian PS, Nedelcu S, Berman SD, Lees J a. Rb regulates fate choice and lineage commitment in vivo. *Nature* 2010;466:1110–4. doi:10.1038/nature09264.
- [2] Chen Z, Hafidh S, Poh SH, Twell D, Berger F. Proliferation and cell fate establishment during Arabidopsis male gametogenesis depends on the Retinoblastoma protein. *Proc Natl Acad Sci U S A* 2009;106:7257–62. doi:10.1073/pnas.0810992106.
- [3] Lehner B, Calixto A, Crombie C, Tischler J, Fortunato A, Chalfie M, et al. Loss of LIN-35, the Caenorhabditis elegans ortholog of the tumor suppressor p105Rb, results in enhanced RNA interference. *Genome Biol* 2006;7:R4. doi:10.1186/gb-2006-7-1-r4.
- [4] Llères D, Bailly AP, Perrin A, Norman DG, Xirodimas DP, Feil R. Quantitative FLIM-FRET Microscopy to Monitor Nanoscale Chromatin Compaction In Vivo Reveals Structural Roles of Condensin Complexes. *Cell Rep* 2017;18:1791–803. doi:10.1016/j.celrep.2017.01.043.
- [5] Meister P, Mango SE, Gasser SM. Locking the genome: nuclear organization and cell fate. *Curr Opin Genet Dev* 2011;21:167–74. doi:10.1016/j.gde.2011.01.023.
- [6] Pajcini K V., Corbel SY, Sage J, Pomerantz JH, Blau HM. Transient inactivation of Rb and ARF yields regenerative cells from postmitotic mammalian muscle. *Cell Stem Cell* 2010;7:198–213. doi:10.1016/j.stem.2010.05.022.
- [7] Shiu PK, Hunter CP. Early Developmental Exposure to dsRNA Is Critical for Initiating Efficient Nuclear RNAi in *C. elegans*. *Cell Rep* 2017;18:2969–78. doi:10.1016/j.celrep.2017.03.002.
- [8] Talluri S, Dick FA. Regulation of transcription and chromatin structure by pRB: Here, there and everywhere. *Cell Cycle* 2012;11:3189–98. doi:10.4161/cc.21263.
- [9] Wu X, Shi Z, Cui M, Han M, Ruvkun G. Repression of germline RNAi pathways in somatic cells by retinoblastoma pathway chromatin complexes. *PLoS Genet* 2012;8:e1002542. doi:10.1371/journal.pgen.1002542.
- [10] Yuzyuk T, Fakhouri THI, Kiefer J, Mango SE. The Polycomb Complex Protein mes-2/E(z) Promotes the Transition from Developmental Plasticity to Differentiation in *C. elegans* Embryos. *Dev Cell* 2009;16:699–710. doi:10.1016/j.devcel.2009.03.008.

- [11] Zhang J, Benavente CA, McEvoy J, Flores-Otero J, Ding L, Chen X, et al. A novel retinoblastoma therapy from genomic and epigenetic analyses. *Nature* 2012;481:329–34. doi:10.1038/nature10733.